Studies on cellular host factors involved in the HIV-1 life cycle

Part I. Disassembly of APOBEC3G ribonucleoprotein complexes in mRNA processing bodies does not affect incorporation into HIV-1

Mentor: Tariq Rana, Ph.D.

Part II. Cellular host factor UPF1 is required in an early, post-entry step of the HIV-1 life cycle

Mentor: Heinrich Göttlinger, M.D.

A Dissertation Presented

By

Anna Kristina Pilapil Serquiña

Submitted to the Faculty of the University of Massachusetts Graduate School of Biomedical Sciences Worcester, Massachusetts

in partial fulfillment of the requirements for the degree of

DOCTOR OF PHILOSOPHY

August 8, 2012

Biochemistry and Molecular Pharmacology

Studies on cellular host factors involved in the HIV-1 life cycle

A Dissertation Presented
By
Anna Kristina Pilapil Serquiña

The signatures of the Dissertation Defense Committee signifies completion and approval as to style and content of the Dissertation

Tariq Rana, Ph.D., Thesis Advisor

Heinrich Göttlinger, M.D., Thesis Advisor

Paul Clapham, Ph.D., Member of Committee

Melissa Moore, Ph.D., Member of Committee

Mohan Somasundaran, Ph.D., Member of Committee

Ann Sheehy, Ph.D., Member of Committee (External Examiner)

The signature of the Chair of the Committee signifies that the written dissertation meets the requirements of the Dissertation Committee

Alonzo Ross, Ph.D., Chair of Committee

The signature of the Dean of the Graduate School of Biomedical Sciences signifies that the student has met all graduation requirements of the school

Anthony Carruthers, Ph.D.,
Dean of the Graduate School of Biomedical Sciences

Biochemistry and Molecular Pharmacology

August 8, 2012

Acknowledgements

I would like to extend my heartfelt thanks to:

- Heinrich Göttlinger, for adopting me into your lab and sharing your expertise in HIV-1 and for editing my introductory chapter
- Tariq Rana, for the opportunity to work with you and learn from you, especially regarding how to design experiments
- Alonzo Ross, chairperson of my thesis research advisory committee (TRAC) and dissertation examination committee (DEC), for the encouragement to persist and prevail against temporary roadblocks
- my thesis research advisory committee (TRAC) and dissertation examination committee (DEC) members: Paul Clapham, Melissa Moore, Mohan Somasundaran, Zhuoshang Xu, and to Ann Sheehy, my external examiner. Thank you to my DEC for the encouragement, constructive comments and suggestions in improving this written dissertation.
- Ken Knight, for helping me transition in the middle of graduate school
- our collaborators: Melissa Moore and her team of talented postdocs and students, especially Christian Roy, for the great discussions and the helpful experiments
- Siobhan O'Brien and Chia-ying Chu, for fun times inside and outside the lab
- Michael Wichroski, for the mentoring you provided to this naïve graduate student
- Chih-chung Lu, for helpful discussions and collaborations on APOBEC3G experiments
- my colleagues at the Rana Lab: Hong Cao, Rob Nathans, Akbar Ali, G. Brett Robb, Francois Belanger, Zhonghan Li, Chaoshun Yang, Katsu Nakashima, Jie Su, Josh McCarroll, Huricha Baigude, Pam Swain, and Chris Pruitte (my surrogate aunt in UMass)
- my colleagues at the Göttlinger Lab: Eric Weiss, Naomi Tsurutani, Hikaru Yamanakha, Yoshiko Usami, Sergei Popov, Elena Popova, Michio Inoue
- Mark Sharkey, Maria Zapp, Paul Peters, Thomas Musich, Laura Brandano, Jim Coderre, and Ann Dauphin for helping me get started on crucial assays
- my long-time classmates and compatriots: Jenny Babon (thank you for helping edit this manuscript), Rachel Madera, and Arlene Lim; also my former housemates Judith Alamares and Reina Improgo; Freidrich Cruz, Lucy Chao, Abby Guce, Rafa and Ene Carandang
- my parents, Gil and Gina Serquiña, and my brothers Joachim, Dominic, and Michael, for their encouragement and support while living 12 time zones away

Most especially, I would like to express my gratitude to my spouse, Cliff Lounsbury III, for your patient, loving support and for believing I could do it.

Abstract

Human Immunodeficiency Virus Type 1 (HIV-1) is the causative agent of Acquired Immunodeficiency Syndrome (AIDS), currently the leading cause of death from infectious diseases. Since HIV-1 co-opts the host cellular machinery, the study of cellular factors involved is a rational approach in discovering novel therapeutic targets for AIDS drug development. In this thesis, we present studies on two such proteins.

APOBEC3G is from the family of cytidine deaminases known to keep endogenous retroviruses and retrotransposons at bay to maintain stability of the human genome. APOBEC3G targets Vif-deficient HIV-1 particles and renders them non-infectious, partially through deaminase-dependent hypermutation of the provirus during reverse transcription. APOBEC3G largely localizes in mRNA processing (P) bodies, cytoplasmic structures involved in RNA metabolism. Here we explore the significance of APOBEC3G localization in P bodies. We found that disrupting P bodies does not affect virion incorporation of endogenous APOBEC3G, implying that the APOBEC3G fraction in P bodies is not directly involved in the production of nascent, non-infectious particles.

We also study UPF1, another host protein encapsidated by HIV-1. It is an essential protein mainly studied for its role in nonsense-mediated decay (NMD) pathway and belongs to the same helicase superfamily as MOV10, a recently identified antiviral factor. We found that UPF1 is incorporated in HIV-1 virions in a nucleocapsid-dependent manner and is required for single-cycle infectivity at an early, post-entry step of the viral life cycle. This novel function of UPF1 most likely does not involve NMD since depletion of UPF2 does not affect viral infectivity.

Table of Contents

Title Page …… i
Signature Page……..…… ii
Acknowledgements ……..…… iii
Abstract ……...…… iv
Table of Contents …… v
List of Figures ……..…… viii
List of Tables ……..…… ix
List of Abbreviations …….. x
Chapter I: Introduction
A. HIV-1/AIDS: Looking back
i. An epidemic at the turn of the century …….. 3
ii. HIV-1 is the causative agent of AIDS …… 4
B. HIV-1/AIDs: Looking forward
i. HIV/AIDS still world's top infectious killer ……..…..… 5
ii. More accessible testing for HIV-1 ……..… 5
iii. Improved prognosis for patients ...……...… 6
iv. Vaccine trials and prophylaxis regimens ……...…….…… 6
v. A patient is cured……. 9
C. HIV-1/AIDS Life Cycle
i. Overview ……..…..……... 9
ii. Binding to receptors and viral entry……. 10
iii. Uncoating and reverse transcription ……... 15
iv. Nuclear import and integration ……... 20
v. Transcription of provirus and export of viral RNA……. 22
vi. Translation of viral proteins and assembly of viral particles.…..…. 23
D. Cellular host factors 25
i. Partners ……...…….…..……... 28
ii. Assassins ……..…..……... 28
iii. Hostages ……..……..…..……... 29
iv. Bystanders..…….. 29
E. Host factors affecting HIV-1
i. APOBEC3G: from the Old Guard of antivirals ……..……..… 30
ii. Tetherin: thwarting the viral escape …… 32
iii. TRIM5α: intruder sensor alert ..……. 35
iv. TSG101: a partner for cell break out …….. 36
Chapter II : Materials and Methods
A. APOBEC3G Study
i. Cell culture and cell lines …… 39
ii. Plasmids and transfections ……..…… 39
iii. Virion production …… 40
iv. Immunostaining and confocal microscopy …..…… 41
v. siRNA and shRNA knockdown ……..……..… 41

vi. H9 infection and RNA extraction for miRNA microarray study … 42
B. UPF1 Study
i. Transfection of proviral constructs and expression vectors …… 43
ii. siRNA experiments ……..…… 43
iii. Infectivity assays ……..…… 43
iv. Immunoblotting …….. 43
v. Analysis of viral particles ……... 44
vi. Analysis of virion-associated genomic RNA ……..… 44
vii. Analysis of viral fusion ……..……..… 44
viii. Analysis of post-entry events ……..……..… 45
Chapter III: Disassembly of APOBEC3G ribonucleoprotein complexes in mRNA processing bodies does not affect incorporation into HIV-1
Mentor: Tariq, Rana, Ph.D.
A. Abstract ……...…… 49
B. Background and rationale for study
i. Discovery of APOBECs …..…… 50
ii. Vif-mediated degradation of APOBEC3G ……...…….. 53
iii. Vif sensitivity …..…… 54
iv. APOBEC3G structure …..……...…… 54
v. Dissecting APOBEC3G antiviral activity ……...…… 55
vi. APOBEC3G complexes in the cell ……...…….. 56
C. Hypothesis ……..……..… 57
D. Results
i. APOBEC3G is a dynamic component of P bodies …….…… 57
ii. Point mutations in APOBEC3G cytidine deaminase motif 1 and some residues on linker region 1 result in lower protein expression but still exhibit P body localization ……..…… 63
iii. P body depletion does not affect virion packaging of endogenous or exogenous APOBEC3G ……..…… 75
iv. Vif inhibitor RN-18 increases total APOBEC3G protein levels that localize to P bodies ……..…….……...… 84
E. Discussion
i. APOBEC3G and AIDS progression ……... 87
ii. An independent study on APOBEC3G and P bodies ……. 88
iii. Small molecules enhance APOBEC3G expression …… 89
iv. Proposed model for APOBEC3G compartments in the cell …...… 90
Appendix for Chapter III
A3.1 Endogenous APOBEC3G expression and localization in resting and activated primary CD4+ T cells……. 95
A3.2 APOBEC3G expression and subcellular localization in transiently transfected 293T cells ……..… 97-99
A3.3 P body protein DCP2 interacts with APOBEC3G wild-type and mutant proteins……..… 101
A3.4 H9 cell viability after Amaxa nucleofection …….. 103

A3.5 Effect of depletion of P body components on HIV-1 production and single cycle infectivity …… 105
A3.6 Effect of miR29a on HIV-1……..... 107
A3.7 Effect of miR138 on APOBEC3G protein levels …….. 109
Chapter IV. Cellular host factor UPF1 is required in an early, post-entry step of the HIV-1 life cycle
Mentor: Heinrich Göttlinger, M.D.
A. Abstract ……... 113
B. Background and rationale of the study
i. Effect of MOV10 on HIV-1…...…….. 114
ii. Discovery of MOV10 ……..…. 114
iii. MOV10 and UPF1 belong to same subfamily of SF1 helicases …. 115
iv. UPF1 effect on HIV-1 Gag mRNA ……. 115
v. Discovery of UPF1 …….. 116
vi. UPF1 in Nonsense-mediated decay (NMD) ……... 116
vii. UPF1 in Staufen1-mediated decay (SMD) ……. 122
viii. UPF1 in degradation of histone mRNA ……..… 122
ix. UPF1 in regulation of telomere-repeat containing RNA (TERRA) …… 123
x. UPF1 binds to RISC proteins ……. 124
xi. UPF1 knockout mice are embryonic lethal …… 124
xii. UPF2 conditional knock out mice have tissue-specific phenotypes ……. 125
xiii. UPF1 as a phosphoprotein ……. 126
xiv. Rationale of study …….. 126
C. Hypothesis ……...… 126
D. Results
i. HIV-1 virions incorporate UPF1 and MOV10 in a nucleocapsid-dependent manner ……...…… 126
ii. MOV10 and UPF1 have opposite effects ……... 130
iii. Point mutations in UPF1 catalytic domain motifs cause dominant negative effects on HIV-1 single cycle infectivity ……..…… 133
iv. HIV-1 single infectivity involves endogenous UPF1 but not UPF2 137
v. $UPF1_{R865A}$ mutant does not affect viral protein expression and packaging …… 140
vi. $UPF1_{R865A}$ mutant does not affect viral genomic RNA integrity and packaging into virions …….. 143
vii. $UPF1_{R865A}$ mutant does not affect viral entry into target cells …… 146
viii. $UPF1_{R865A}$ mutant decreases viral reverse transcriptase products in target cells ……. 149
E. Discussion
i. Helicases in HIV-1 …….. 152
ii. Opposite effects of MOV10 and UPF1 ……... 154
iii. UPF1 depletion ……... 155

iv. Depletion of UPF1 binding partners ……... 157
v. UPF1 mutant studies ……..……..… 158
vi. Future directions and working hypothesis …….……. 161
Appendix for Chapter IV …… 167
A4.1 Depletion of UPF1 in cell lines …….. 168
A4.2 Depletion of UPF1 in primary cells ……... 170
A4.3 β-galactosidase assay for TZMbl indicator cells to demonstrate HIV-1 single cycle infectivity ……..…… 172
A4.4 Endogenous MOV10 levels ……... 174
A4.5 Biochemical characterization of HIV-1 virions produced with the overexpression of $UPF1_{DE636AA}$*…….…… 176
A4.6 VSV-G-pseudotyped NL4-3 virions produced with the overexpression of $UPF1_{DE636AA}$*…… 178
A4.7 Overexpression of active Nedd4LC2(-) rescues the decrease in p25/p24 in virus-producing cells when $UPF1_{DE636AA}$* is co-expressed … 180-181
Chapter V. References …… 183

List of Figures

Figure 1.1 HIV-1 life cycle 11
Figure 1.2 HIV-1 viral proteins 13
Figure 1.3 Steps in reverse transcription 18
Figure 1.4 Host factors affecting HIV-1 33
Figure 3.1 APOBEC3G deaminates cytosine 51
Figure 3.2 Antiviral effect of exogenous APOBEC3G-YFP on ΔVif virions 58
Figure 3.3 APOBEC3G is a dynamic component of mRNA processing bodies 61
Figure 3.4 Analysis of APOBEC3G point mutants 64
Figure 3.5 Mutations in CD1 and some LR1 residues decreases APOBEC3G protein stability 70
Figure 3.6 Confocal study of P body localization for APOBEC3G mutants 73
Figure 3.7 Depletion of LSM1 by siRNA nucleofection in H9 ΔVif virus-producing cells does not affect endogenous APOBEC3G encapsidation into virions 76
Figure 3.8 Depletion of LSM1 by shRNA transduction in H9 ΔVif virus-producing cells does not affect endogenous APOBEC3G encapsidation into virions 79
Figure 3.9 Dispersion of P bodies in virus-producing cells does not affect viral encapsidation of exogenous APOBEC3G 82
Figure 3.10 RN-18 enhances APOBEC3G protein expression 85
Figure 3.11 Working model for APOBEC3G compartments in the cell 91
Appendix 3.1 Endogenous APOBEC3G expression and localization in resting and activated primary CD4+ T cells 95

Appendix 3.2	APOBEC3G expression and subcellular localization in transiently transfected 293T cells	97-99
Appendix 3.3	P body protein DCP2 interacts with APOBEC3G wild-type and mutant proteins	101
Appendix 3.4	H9 cell viability after Amaxa nucleofection	103
Appendix 3.5	Effect of depletion of P body components on HIV-1 production and single cycle infectivity	105
Appendix 3.6	Effect of miR29a on HIV-1	107
Appendix 3.7	Effect of miR138 on APOBEC3G protein levels	109
Figure 4.1	UPF1 is a multifunctional protein	117
Figure 4.2	HIV-1 virions encapsidate MOV10 and UPF1 in a nucleocapsid-dependent manner	127
Figure 4.3	Opposite effects of overexpression of UPF1 and MOV10 wild-type protein and ATPase mutants on HIV-1 single cycle infectivity	131
Figure 4.4	Overexpression of UPF1 catalytic domain mutants decreases HIV-1 single cycle infectivity	134
Figure 4.5	HIV-1 single cycle infectivity involves endogenous UPF1 but not UPF2 in virus-producing cells	138
Figure 4.6	Effect of UPF1 on virus production, viral protein expression and viral incorporation	141
Figure 4.7	$UPF1_{R865A}$ does not affect viral genomic RNA incorporation or integrity	144
Figure 4.8	$UPF1_{R865A}$ mutant does not affect viral entry	147
Figure 4.9	UPF1 from virus-producing cells is required at an early, post-entry step of the HIV-1 life cycle	150
Figure 4.10	Proposed hypothesis for future experiments	165
Appendix 4.1	Depletion of UPF1 in cell lines	168
Appendix 4.2	Depletion of UPF1 in primary cells	170
Appendix 4.3	β-galactosidase assay for TZMbl indicator cells to demonstrate single cycle infectivity of HIV-1	172
Appendix 4.4	Endogenous MOV10 levels.	174
Appendix 4.5	Biochemical characterization of HIV-1 virions produced with the overexpression of $UPF1_{DE636AA}$*	176
Appendix 4.6	VSVG-pseudotyped NL4-3 virions produced with the overexpression of $UPF1_{DE636AA}$*	178
Appendix 4.7	Overexpression of active Nedd4LC2(-) rescues the decrease in p25/p24 in virus-producing cells when $UPF1_{DE636AA}$* is co-expressed	180-181

List of Tables

Table 3.1	Summary of APOBEC3G mutants	66-67
Table 4.1	Summary of UPF1 mutants	136

List of Abbreviations

ACF	APOBEC1 Complementation Factor
AGO1, AGO2	Argonaute protein 1 and 2
AID	Activation-induced cytidine deaminase
AIDS	Acquired Immune Deficiency Syndrome
APOBEC	Apolipoprotein B mRNA editing enzyme catalytic polypeptide
APOBEC3G	Apolipoprotein B mRNA editing enzyme catalytic, polypeptide-like 3G
Arf1	ADP-ribosylation factor 1
ATP	Adenosine triphosphate
ATR	Ataxia telangiectasia and Rad3 related protein
BLaM-Vpr	β-Lactamase-Vpr recombinant protein
CCR5	Chemokine (C-C motif) receptor 5
CD1, CD2	Cytidine deaminase motif 1 and 2
CDC	Center for Disease Control and Prevention
CDK9	Cyclin-dependent kinase 9
CXCR4	Chemokine (C-X-C motif) receptor 4
CypA	Cyclophilin A
DCP2	mRNA decapping enzyme 2
DMSO	Dimethyl sulfoxide
DNA	Deoxyribonucleic acid cDNA: complementary DNA vDNA: viral DNA
EJC	Exon-junction complex
ELISA	Enzyme-linked immunosorbent assay
EM	Electron microscopy
eRF1, eRF3	Eukaryotic release factor 1 and 3
ESCRT	Endosomal sorting complex required for transport
FDA	Food and Drug Administration
Gag	Group antigen
GAPDH	Glyceraldehyde 3-phosphate dehydrogenase
gp41	Glycoprotein 41
gp120	Glycoprotein 120
gp160	Glycoprotein 160
HAART	Highly active antiretroviral therapy
HBV	Hepatitis B Virus
HIV-1	Human Immunodeficiency Virus Type 1
HMM	High-molecular mass complex
Hsp70	Heat shock protein 70
HTLV-1	Human T cell Lymphotropic Virus Type I
IAP	Intracisternal A-particle
IFNα	Interferon α
Ig	Immunoglobulin (i.e. IgM, IgG, IgA, or IgE)
IN	Integrase

LAV	Lymphadenopathy-associated virus
LC-MS/MS	Liquid chromatography and tandem mass spectrometry
L domain	Late assembly domain
LEDGF	Lens epithelium-derived growth factor
LINE-1	Long-interspersed elements 1
LMM	Low-molecular mass complex
LR1, LR2	APOBEC3G linker region 1 and 2
LTNP	Long-term nonprogressors
LTR	Long-terminal repeats
MA	Matrix protein
MDA5	Melanoma differentiation-associated gene-5
MLV	Murine leukemia virus
MOI	Multiplicity of infection
NC	Nucleocapsid
NC on HAART	Non-controllers on HAART
Nef	Negative factor protein
NIH	National Institutes of Health
NIAID	National Institute of Allergy and Infectious Diseases
NMD	Nonsense-mediated decay
NNRTI	Non-nucleoside reverse transcriptase inhibitor
NRTI	Nucleoside reverse transcriptase inhibitor
nt	Nucleotide
PABP	Poly(A) binding protein
P bodies	mRNA processing bodies
PBS	Primer binding site
PCR	Polymerase chain reaction
p.i.	Post-infection (i.e. after infection)
PIC	Pre-integration complex
Pol	Polymerase
PP2A	Protein phosphatase 2A
PPT	Polypurine tract
	cPPT: central polypurine tract
	3’PPT: 3’ polypurine tract
PR	Viral protease
PRR	Pattern recognition receptor
p.t.	Post-transfection (i.e. after transfection)
PTC	Premature stop codon
R	Repeat sequence
RENT1	Regulator of nonsense transcripts 1
Rev	Regulator of virion
RHA	RNA helicase A
RISC	RNA-induced silencing complex
RNA	Ribonucleic acid
	mRNA: messenger RNA

	miRNA: microRNA
	siRNA: small interfering RNA
	tRNA: transfer RNA
RNP	Ribonucleoprotein complex
RRE	Rev response element
RT	Reverse transcriptase
RTC	Reverse transcription complex
SBLP	Stem loop binding protein
SF1	Super family 1
SIV	Simian Immunodeficiency Virus
SMD	Staufen-mediated decay
SP1, SP2	Spacer peptide 1 and 2
Stau1	Staufen1
Tat	Trans-activator of transcription
TAR	Trans-activation responsive region
TEM	Tetraspanin-enriched microdomain
TERRA	Telomere-repeat containing RNA
TNPO3	Transportin 3
TRIM5	Tripartite motif protein 5
TSG101	Tumor suppressor gene 101
U3	Unique sequence in 3’ end of HIV-1 genome
U5	Unique sequence in 5’ end of HIV-1 genome
UPF1	Up-frameshift 1
UPF2	Up-frameshift 2
UPF3	Up-frameshift 3
UTR	Untranslated region
Vif	Virion infectivity factor
VLP	Virus-like particle
Vpr	Viral protein r
Vpu	Viral protein u
VSV-G	Vesicular stomatitis virus glycoprotein

Chapter I

Introduction to HIV-1 and Host Cellular Factors

This revised chapter was written by Anna Serquiña, incorporating suggestions and comments from the Dissertation Examination Committee, and edited by Heinrich Göttlinger.

CHAPTER I: Introduction

Studies on cellular host factors involved in the HIV-1 life cycle

A. HIV-1/AIDS: Looking back

"…finding the cause of a disease is the alpha but not the omega of its eradication." -R. Gallo and L. Montagnier, NEJM 2003 (Gallo 2003)

1. An epidemic at the turn of the century

Between 1979 and 1981, more than a hundred young men from New York and California sought medical attention for violet-colored skin lesions, enlarged lymph nodes, and pneumonia (CDC 1981b). They were diagnosed with multiple opportunistic infections (bacterial, viral, and fungal) and 40% of reported cases were fatal (CDC 1981a). Epidemiologists from the Center for Disease Control and Prevention (CDC) chronicled the patients' characteristics (CDC 1981a) as Caucasian, aged 25-49, and homosexual or bisexual. Following these was another CDC report describing a cohort of Haitians living in the United States who also manifested opportunistic infections and Kaposi's sarcoma (CDC 1981a). A third group that emerged were male, heterosexual patients diagnosed with hemophilias requiring frequent transfusions of blood products and who died of *Pneumocystis carinii* pneumonias (CDC 1982b). The clustering of all groups' diagnoses (Kaposi's sarcoma skin lesions and *P. carinii* pneumonia) pointed towards an immunocompromised patient, such as those seen in patients on immunosuppressive therapy after a liver transplant. The CDC tested patient blood

specimens and found marked decreases in their levels of CD4+ T helper cells. This disease manifesting as multi-systemic opportunistic infections was eventually called Acquired Immune Deficiency Syndrome (AIDS) (CDC 1982a).

2. The Human Immunodeficiency Virus Type 1 (HIV-1) is the causative agent of AIDS

A few years prior to the emergence of AIDS, Robert Gallo and his group at the National Institutes of Health had identified the first human retrovirus, the Human T cell Lymphotropic Virus Type I (HTLV-1) (Poiesz et al. 1980), which is associated with adult T cell leukemia-lymphoma. Since one of the biomarkers of HTLV-1 infection is depressed CD4+ T cell levels, R. Gallo proposed that HTLV-1 or -2 causes AIDS (Gallo and Montagnier 1987) during the 1983 Cold Spring Harbor Workshop on AIDS. A few months later, R. Gallo's collaborator, Luc Montagnier, and his colleagues published in Science their findings isolating and identifying a non-transforming retrovirus which they dubbed "lymphadenopathy associated virus" (LAV), since the etiologic agent was isolated from lymph nodes of AIDS patients (Barré-Sinoussi et al. 1983). This was later renamed "HIV-1". Although the discovery of the AIDS causative agent was initially contentious, the US and French governments have agreed to acknowledge Gallo's and Montagnier's groups as co-discoverers and to share the intellectual properties associated with the discoveries (Vahlne 2009). In 2008, Montagnier and Barre-Sinoussi received the Nobel Prize for Medicine for their seminal work in the discovery of HIV-1 (Cohen and Enserink 2008).

B. HIV-1/AIDS: Looking forward

"…is there really hope of achieving the vision of an AIDS-free generation?" – Salim S. Abdool Karim (CAPRISA 004 trial co-author), Science 2012 (Abdool Karim 2012)

1. **HIV/AIDS still the world's top infectious killer**

Today, AIDS remains the world's leading infectious killer, with 30 million to date succumbing to its multi-systemic effects. WHO 2010 statistics show that 34 million are currently living with HIV-1, with 2.7 million newly infected cases in 2010. These numbers, though, are starting to plateau in most countries due to prevention programs and availability of treatment, with some exceptions in eastern Europe and Central Asia (Cohen 2010).

2. **More accessible testing for HIV-1**

Widespread public health efforts have fought the initial stigma for HIV-1 testing. Now, it is routinely offered in the outpatient clinics. Also, quantitative PCR protocols have been developed for faster and more sensitive diagnosis, compared to the ELISA-based test. Last July 2012, the Food and Drug Administration (FDA) approved the OraQuick In-Home HIV Test, the first over-the-counter diagnostic kit that can detect antibodies against the virus from a saliva sample, providing results in less than an hour (Chappelle 2012).

3. Improved prognosis for HIV-1/AIDS patients

Today, the diagnosis of "HIV-1 positive" is no longer a death sentence. With several drug regimens now available, the life expectancy of AIDS patients has increased. The highly active antiretroviral therapy (HAART) is a drug regimen initiated when HIV-1 positive patients' CD4+ T cell counts fall below 500/μL (Writing Committee for the CASCADE Collaboration 2011). Starting and maintaining the regimen improves the prognosis for HIV-1 infected patients by delaying disease progression.

The process of HIV-1 replication is error-prone, with several quasispecies existing at the same time in the same patient. Since HIV-1 develops drug resistance quickly due to low-fidelity reverse transcription and recombination, the aim of HAART is to suppress viral replication to very low levels by using 3 or more drugs targeting different steps of the viral life cycle, thereby preventing the emergence of drug-resistant viruses. This still remains challenging due to the development of drug-resistant viruses in patients who have higher viral loads.

4. Vaccine trials and prophylaxis regimens

The search for an HIV-1 vaccine has been a tortuous road, primarily because traditional vaccine approaches have not worked. A live attenuated virus may mutate to a pathogenic strain, since HIV-1 has the propensity to mutate quickly. Also, an inactivated virus or protein-based vaccines do not generate any effective antibodies. Broadly neutralizing antibodies, which would react to a wide range of HIV-1 strains, have shown promising results in primate models. However, clinical trials such as the Microgenesis

and Vaxgen studies failed to elicit the broad response needed to tackle a genetically variable virus (Sekaly 2008).

The focus then shifted to eliciting a robust T cell response by using replication defective adenoviral vectors (Sekaly 2008). Promising results were seen in a limited numbers of macaques (Burton et al. 2004). Novel vaccine regimens that were studied included DNA vectors expressing viral proteins to prime the immune response and a replication-defective recombinant adenovirus serotype 5 (rAd5) vector to boost responses (Robinson and Weinhold 2006). Phase I clinical trials have been published from related NIH Vaccine Research study groups (Graham et al. 2006; Catanzaro et al. 2006).

The "prime-boost" strategy was also utilized by Merck and Company when they began the international STEP trial. However, the study was suspended after an interim review in 2007 showed no efficacy (http://www.hvtn.org/science/1107.html). After further analysis, the Merck STEP trial revealed a disturbing trend towards enhancement of HIV-1 infection among vaccine recipients, especially those with elevated adenoviral immunity at the start of the study (Cohen 2007). The statistical analyses were confusing because, while the P values showed were statistically significant, these analyses may not be appropriate for the study since the "study was not designed to assess potential harm," cautioned S. Self, chief statistician of the HIV Vaccine Trial Network (Cohen 2007).

The first promising study in the field was the RV144 vaccine trial in Thailand, which only showed a modest protection: 31.2% decrease in new infections among vaccine recipients (Pitisuttithum et al. 2011). The vaccine consisted of canarypox vectors (prime) and recombinant gp160 or gp120 (boost) which aimed to induce cell-mediated immune

responses while significantly enhancing antibody responses in HIV-uninfected volunteers (Pitisuttithum et al. 2011). However, the resulting immune responses were not as robust as the researchers expected. Still, the modest protection has been praised as a step in the right direction, and several independent groups continue to study the RV144 samples to glean new correlates of protection (Cohen 2009).

An alternative to the HIV-1 vaccine conundrum is the administration of pre-exposure prophylaxis to high-risk populations. Pre-exposure prophylaxis for HIV-1 with Truvada (combined tenofovir and emtricitabine) has recently been approved by the FDA (Jefferson 2012). The iPREx trial showed that the Truvada treatment group had 44% fewer infections after 1.2 years of daily oral intake of the prophylactic drug among men and transgender women who have sex with men (Grant et al. 2010). However, the FEM-PrEP trial, a related study for Truvada prophylaxis among women, was suspended in April 2011 due to lack of efficacy (van Damme et al. 2012). Blood tests to confirm compliance with daily drug intake showed that only 26% of the participants who became HIV-1 positive (i.e. seroconverted) and 35% of the uninfected participants had optimal target levels of the drug, suggesting that FEM-PrEP study participants did not adhere to dosing schedules (van Damme et al. 2012). In a third related study on HIV-1 serodiscordant couples (one partner was HIV-1 positive and the other was not), called the Partners PrEP trial, Truvada prophylaxis showed a 75% relative reduction of infection compared to the placebo group (Baeten et al. 2012). In this study, only 31% of participants who seroconverted had target-levels of the drug while 82 % of uninfected participants had the desired drug levels (Baeten et al. 2012). L. Van Damme and

colleagues of the FEM-PrEP trial postulate that differences in the biology of men and women with regards to drug responses or HIV-1 susceptibility can be overcome by increased adherence to prophylaxis intake (van Damme et al. 2012). The Truvada projects, which reportedly cost $43.6 M, were supported by the National Institutes of Health and the Bill and Melinda Gates Foundation.

5. A patient is cured

Timothy Ray Brown (a.k.a. “The Berlin Patient”) was an AIDS patient diagnosed with acute myelogenous leukemia. He received an experimental therapy envisioned by hematologist-oncologist Gero Hütter (Cohen 2011), consisting of a bone marrow transplant from a donor with Δ32 CCR5, a polymorphism of the co-receptor which is protective against HIV-1 entry (Liu et al. 1996; Samson et al. 1996). Currently, Mr. Brown has no detectable virus in his system (Cohen 2011). J. Lalezari of Quest Research and R. Mitsuyasu from UCLA embarked on a gene therapy-based clinical trial to determine whether this cure is reproducible. The collaborative study is ongoing and the researchers presented their preliminary data at the 2011 Conference of Retroviruses and Opportunistic Infections (Cohen 2011).

C. HIV-1 Life Cycle

1. Overview

HIV-1 belongs to the Retroviridae family and exhibits the characteristic retroviral life cycle, which involves reverse transcription of the viral RNA genome to DNA and its

insertion into the host genome (see Figure 1.1A). The HIV-1 genome is ~9kb, encoding for three polyproteins and several regulatory and accessory proteins (Frankel and Young 1998). The expression of Gag is sufficient to drive the formation and release of virus-like particles from the host cell (Freed 1998), making it the primary viral polyprotein for viral assembly. Gag is translated as polyprotein Pr55 and is processed by the viral protease (PR) during viral particle maturation into the matrix (MA), capsid (CA), nucleocapsid (NC), p6 and spacer peptides (SP1, SP2) (see Figure 1.2). MA is associated with the inner membrane of the viral particle, while CA forms a shell around the NC in complex with the viral RNA genome. The other major viral polyproteins are Gag-Pol, which autocatalyses into PR, reverse transcriptase (RT), and integrase (IN), and Env (gp160), which is processed by cellular proteases (furin or furin-like proteases) into gp120 (surface protein, SU) and gp41(transmembrane protein, TM). Viral proteins Tat and Rev function in viral transcription and viral RNA export, respectively. Viral accessory proteins such as Vif, Vpr, Vpu and Nef are usually required to overcome cellular restriction factors.

2. Binding to host receptors and viral entry

As the virus docks on its target cell, the viral envelope binds the host receptor CD4, which is necessary for infection (Dalgleish et al. 1984). This binding induces a conformational change in the viral envelope (Sattentau and Moore 1991), promoting an association with co-receptors (Ugolini et al. 1997). After this conformational change in the viral envelope, it is now able to bind the chemokine receptors CCR5 (Deng et al. 1996; Dragic et al. 1996) or CXCR4/fusin (Feng et al. 1996), which are required for viral

Figure 1.1

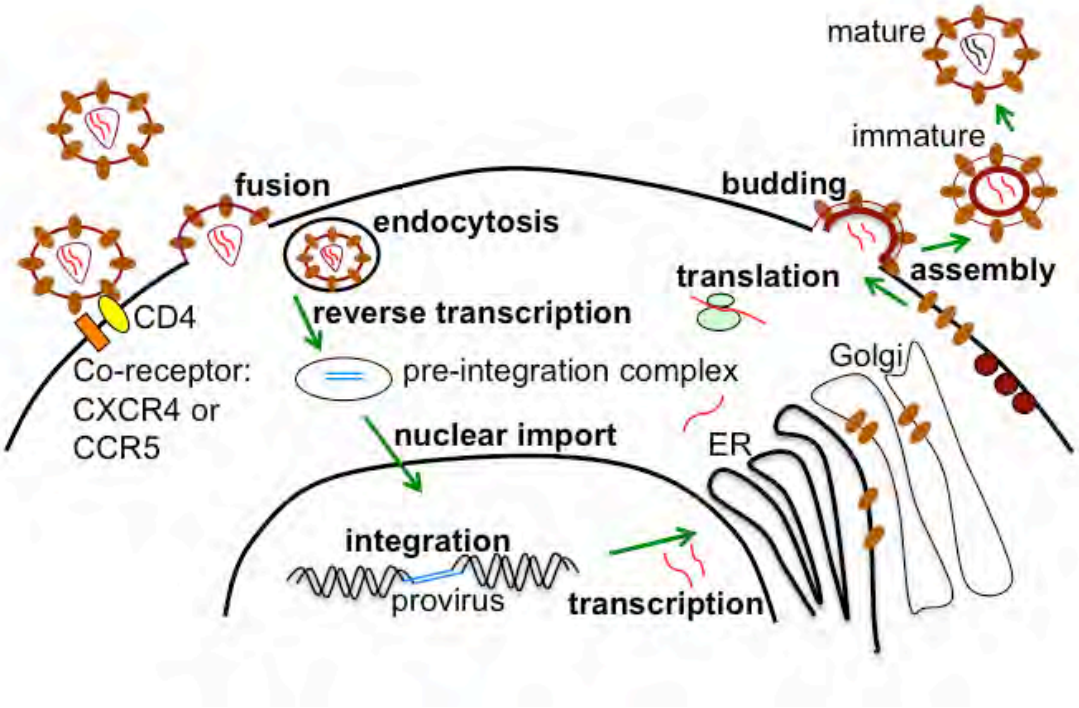
mature
immature
fusion
endocytosis
budding
translation
assembly
CD4
reverse transcription
Co-receptor:
CXCR4 or
CCR5
pre-integration complex
Golgi
ER
nuclear import
integration
provirus
transcription

Figure 1.1 **The HIV-1 Life Cycle.** HIV-1 is a lentivirus that uses CD4 as a primary receptor and either CXCR4 or CCR5 as co-receptor. The virus enters the host cell via fusion or endocytosis. The viral core, containing two copies of the RNA genome, is released into the cytoplasm. Upon completion of reverse transcription, the pre-integration complex is imported to the nucleus, where it is integrated into the host genome. Transcription of the provirus proceeds with Pol II and tat transactivation. The viral proteins are subsequently translated and the nascent virions assemble on the membrane. These bud, and subsequent processing of viral proteins by viral protease transforms the immature virion to a mature, infectious virion.

Figure 1.2

HIV-1 polyproteins

Gag (Pr55):
- Matrix (MA)
- Capsid/p24 (CA)
- Nucleocapsid (NC)
- Spacer peptides (SP1, SP2)
- p6

Env (gp160):
- gp120
- gp41

Gag-Pol:
- Reverse transcriptase (RT)
- Integrase (IN)
- Protease (PR)

Translation from spliced mRNAs

Regulatory:
- Tat
- Rev

Accessory:
- Vif
- Vpu
- Vpr
- Nef

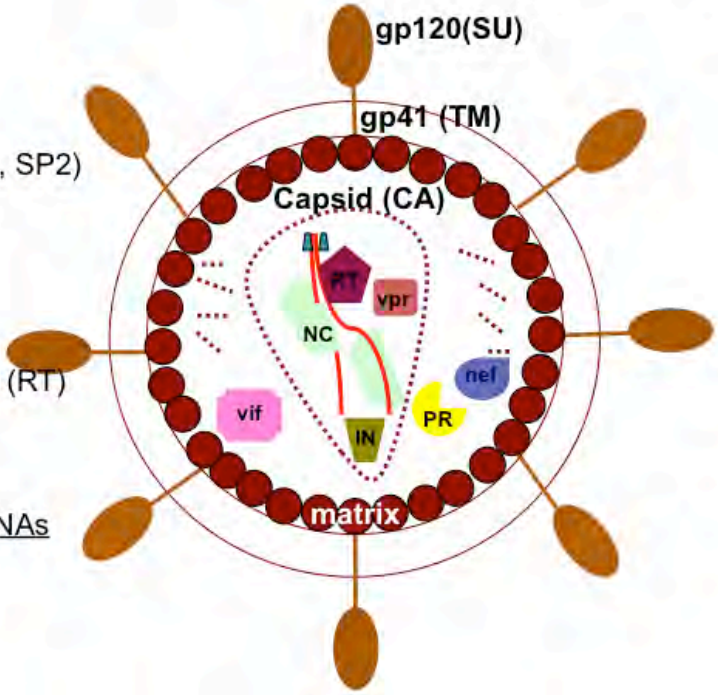

Figure 1.2 **HIV-1 Viral Proteins**. HIV-1 translates three polyproteins: 1) Gag/Pr55 (processed by viral protease into MA, CA, NC, p6, and two spacer peptides), 2) Gag-Pol (autocatalyses to protease, reverse transcriptase, and integrase), 3) Env/gp160 (processed by cellular proteases into gp120 and gp41). HIV-1 also encodes regulatory proteins Tat and Rev and accessory proteins Vif, Vpu, Vpr, and Nef.

entry (Clapham and Weiss 1997). The binding of gp120 to CD4 and the co-receptor causes a conformational change in gp41, exposing a fusion peptide that facilitates entry into the target cell. Viral entry occurs via membrane fusion at the plasma membrane or after endocytosis (Daecke et al. 2005; Miyauchi et al. 2009). As mentioned above, individuals homozygous for the Δ32 CCR5 polymorphism are highly resistant to HIV-1 infection (Liu et al. 1996; Samson et al. 1996).

In 2003, the FDA approved enfurvitide/T-20 (Fuzeon), the first entry inhibitor drug (Robertson 2003). The mechanism of action of enfurvitide is two-fold: it blocks the gp120-CD4 complex from interacting with the CXCR4 co-receptor, and it also targets the gp41 pre-hairpin conformation (Ashkenazi et al. 2011; Kilby et al. 1998). Newer drugs in this class have been categorized as follows: 1) attachment inhibitors, 2) co-receptor binding inhibitors, and 3) fusion inhibitors (Ashkenazi et al. 2011).

3. Uncoating and reverse transcription

Once the virion enters the cell, it undergoes uncoating and reverse transcription. The viral uncoating step involves dissociation of CA units to release the NC-RNA complex. Uncoating can occur in vitro upon synthesis of full-length viral DNA (vDNA) by the virion core-associated RT, suggesting that any cellular factors required for uncoating are present within HIV-1 virions (Arhel et al. 2007). Reverse transcription may initiate inside the core prior to entry, but uncoating has to occur for reverse transcription to proceed. The completion of reverse transcription and the formation of the central DNA flap trigger or facilitate uncoating (Arhel et al. 2007). Conversely, unsuccessful reverse transcription

(e.g. by using RT inhibitor Nevirapine or a DNA flap mutant) prevents uncoating (Arhel et al. 2007). The following models for uncoating have been put forth (Arhel 2010):

- Quick uncoating: due to a change in CA amounts, from high concentration inside the virion to low concentration in the cytoplasm, the viral core disassembly occurs immediately after delivery of the viral core to the cytoplasm
- Slow uncoating: the viral core remains intact after entry, but slowly disassembles as reverse transcription proceeds, with the resulting viral cDNA and associated proteins being transported to the nuclear periphery
- Uncoating at the nuclear pore: viral core disassembly occurs at the nuclear pore prior to nuclear import to keep the reverse transcriptase enzyme associated with the viral genome

The reverse transcription complex (RTC) is the viral nucleoprotein complex undergoing reverse transcription to yield double-stranded viral DNA from the viral RNA genome. The efficiency of reverse transcription is reported to be ~30% (Thomas et al. 2007). The steps of reverse transcription are as follows (see Figure 1.3):

i. Synthesis of minus strand: reverse transcriptase catalyzes the minus-strand using a cellular tRNA primer annealed to the primer binding site (PBS) near the 5’ end of the viral genome. Reverse transcriptase extends the minus strand towards the 5’ end of the genome, including the unique 5’ (U5) genomic sequence and the 5’ repeat (R) sequence (identical sequences found near the 5’ and 3’ end of the viral genome). While the reverse transcriptase extends the primer, the RNase H activity of the reverse transcriptase also degrades the genomic RNA in the RNA-DNA

hybrid, with the exception of the polypurine tract (PPT) at the central and 3' positions

ii. Minus-strand strong stop: occurs once the reverse transcriptase reaches the 5'-most end of the genome

iii. First strand transfer: the minus-strand moves to the 3' end of the second copy of the viral genome, annealing at the 3' R sequence; reverse transcription proceeds towards the 5' end with the reconstitution of the unique 3' (U3) sequence next to the R sequence, the coding region, and the PBS; recombination for vDNA occurs during this intermolecular strand transfer step

iv. The PPT (cPPT and 3'PPT) primes the plus strand synthesis, using the minus strand as the template

v. Second strand transfer: the plus strand moves towards the 5'end of the minus strand and extends the plus strand. The 3'PPT primed-plus strand extension occurs through the cPPT and ends downstream at the central termination sequence, forming an overlap called the central DNA flap

As reverse transcription is completed, the RTC is transported from the entry point to the nucleus. These complexes move rapidly toward the nuclear compartment, using microtubules and actin filaments to reach the nuclear pore, as seen in fluorescently-labeled HIV-1 cores which traffic along microtubules (Arhel et al. 2006; McDonald et al.). However, a kinetics study showed that inhibitors of the cytoskeleton do not totally block transport of the RTC to the nucleus, suggesting that actin is not required for

Figure 1.3

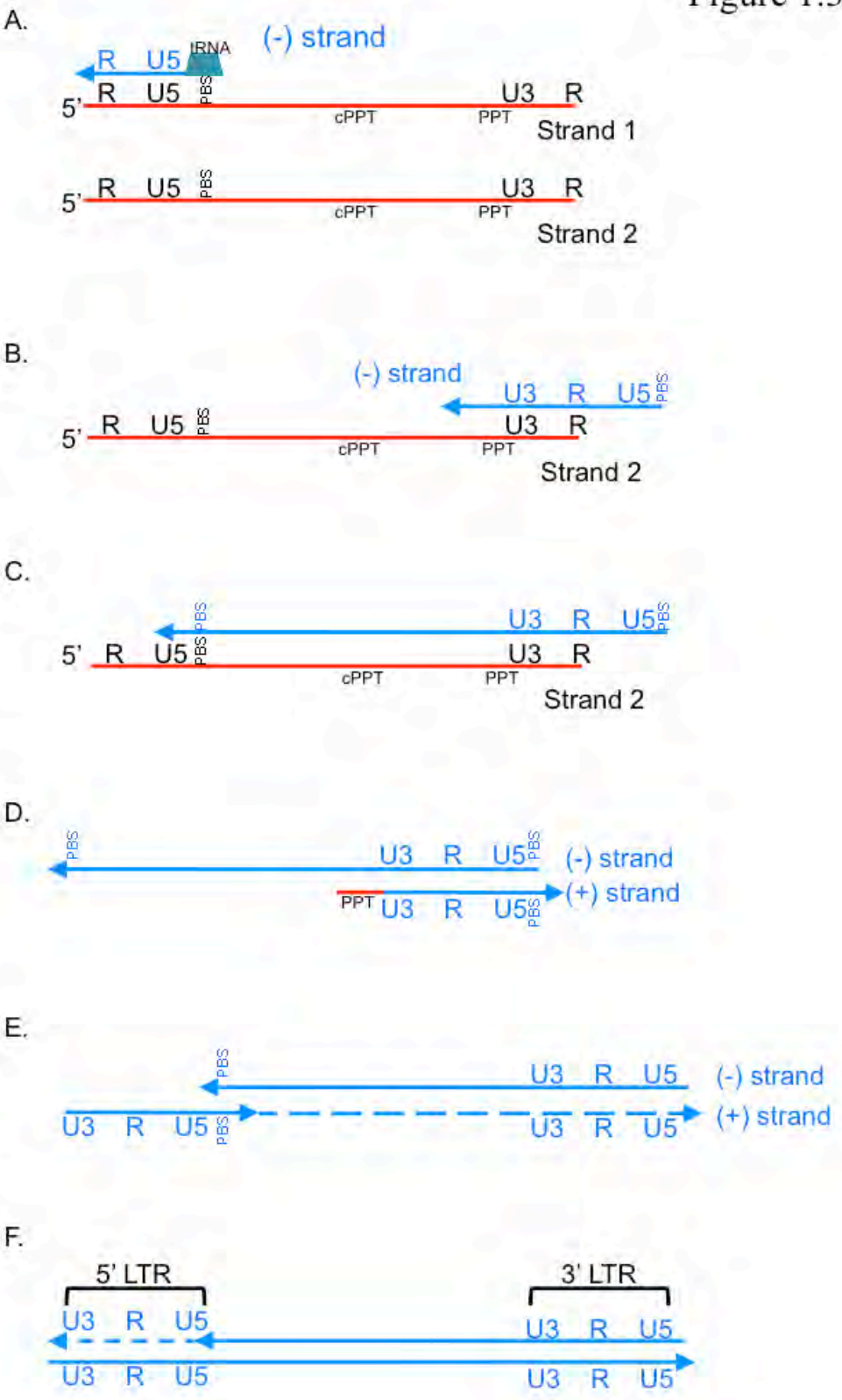
A.
(-) strand
tRNA
R U5
PBS
5' R U5
cPPT
U3 R
PPT
Strand 1
5' R U5
cPPT
U3 R
PPT
Strand 2
B.
(-) strand
U3 R U5
PBS
5' R U5
cPPT
U3 R
PPT
Strand 2
C.
PBS
U3 R U5
PBS
5' R U5
PBS
cPPT
U3 R
PPT
Strand 2
D.
PBS
U3 R U5
PBS
(-) strand
PPT
U3 R U5
PBS
(+) strand
E.
PBS
U3 R U5
(-) strand
U3 R U5
PBS
U3 R U5
(+) strand
F.
5' LTR
3' LTR
U3 R U5
U3 R U5
U3 R U5
U3 R U5

Figure 1.3 **Steps in HIV-1 reverse transcription.** (A) Reverse transcription is initiated by $tRNA^{Lys}$ annealed to the primer binding site (PBS) and extended towards the 5’ end of the genome. (B) The minus strand jumps from the 5’ end to the 3’ end of the genome, with base pairing occurring in the repeat (R) region. This jump may also occur from one RNA copy to the other. (C) Minus strand extension moves toward the 5’ end of the genome, reconstituting the PBS. (D) Initiation of plus strand polymerization occurs either at the cPPT or the 3’PPT, both of which remain intact after RNase H digestion (see below). The minus strand is used as the template. (E) The plus strand jumps to the 5’ end of the minus strand and extends the plus strand towards the 3’ end. (F) The 5’ and 3’ long-terminal repeats (LTRs) are completed.

RNase H digestion: as reverse transcription proceeds, the RNase H activity of the reverse transcriptase degrades the RNA strand in the RNA-DNA pairing that is formed.

RTC movement (Arfi et al. 2009). Also, some functional RTCs are lost during transport towards the nucleus (McDonald et al.).

A comparison of the vDNA quantities produced within cells relative to the amount of viral RNA genomes in the inoculum shows that only 5% of virus particles present actually initiated reverse transcription, with 0.41% of the genomes proceeding all the way to a provirus (Thomas et al. 2007).

The drug class of HIV-1 RT inhibitors is divided into non-nucleoside RT inhibitors (NNRTIs) and nucleoside RT inhibitors (NRTIs). NNRTIs (ex. Nevirapine) inhibit DNA polymerization by binding to an allosteric site, resulting in a conformational change in the active site of the reverse transcriptase and causing a decrease in its binding to nucleosides (Adams et al. 2010). NRTIs (ex. Zidovudine/AZT) are nucleotide mimics that lack the 3'OH. They compete with endogenous nucleotides and block further elongation by HIV-1 reverse transcriptase (Cihlar and Ray 2010).

4. Nuclear import and integration

The pre-integration complex (PIC) is composed of the vDNA, with associated viral and cellular proteins, after reverse transcription is completed. The PIC is transported into the nucleus through the nuclear pore and is integration-competent. The PIC sheds most of its CA (Fassati and Goff 2001; Miller et al. 1997), in contrast to the RTC discussed above.

The viral integrase (IN) is the third enzyme from the Gag-Pol polyprotein and it facilitates the insertion of the vDNA into the host genome by removing 2-3 nucleotides

on the 3’ end to produce a recessed end. IN also nicks the cellular target DNA and joins the viral 3’ recessed end to the 5’ overhang of cellular DNA. The cellular machinery performs gap repair to complete the integration process. At this point, the integrated vDNA is now called a provirus.

Occasionally, vDNA forms episomes called 1-LTR circles (containing one copy of the long-terminal repeat, LTR, due to homologous recombination) or 2-LTR circles (has 2 copies of LTR joined end-to-end). These unintegrated forms may persist but are diluted out during cell division (Pierson et al. 2002; Butler et al. 2002).

The lens epithelium-derived growth factor (LEDGF, also called p75) is a nuclear transcription co-activator that tightly binds to IN (Cherepanov et al. 2004) and stabilizes IN (Llano et al. 2004). LEDGF activates IN and is required for provirus formation and infection (Emiliani et al. 2005; Llano et al. 2006) and also for the nuclear entry of PICs (Llano et al. 2004). LEDGF protects IN from degradation by the proteasome, but depletion of LEDGF does not affect HIV-1 infection efficiency (Ciuffi et al. 2005; Emiliani et al. 2005; Llano et al. 2004; 2006).

The DNA damage response proteins have also been implicated in integration. Mutant cells undergo apoptotic cell death after viral infection (Daniel et al. 1999; Smith and Daniel 2006). These proteins do not seem to be directly involved in integration but probably fill single-stranded gaps and nicks after integration (Ariumi et al. 2005; Dehart et al. 2005). Other viral factors required for integration include NC, which enhances the efficiency of integration (Buckman et al. 2003; Gao et al. 2003), and the central DNA flap (Zennou et al. 2000).

In 2007, the FDA approved the first IN inhibitor, Raltegravir. This drug binds to the active site of IN, blocking its activity (Cocohoba and Dong 2008). The PIC is therefore unable to integrate into the host DNA, and is rendered noninfectious. Merck & Co. spearheaded the research on lead compounds, which led to the development of Raltegravir (Quashie et al. 2012).

5. Transcription of provirus and export of viral RNA

As mentioned above, the long-terminal repeat (LTR) is generated during reverse transcription and exists as repeats in the 5' and 3' ends of the viral DNA. In the context of integrated viral DNA, the major function of the LTR is the regulation of viral RNA synthesis. Expression from the HIV-1 LTR is trans-activated by Tat. Together with cyclin T1 and CDK9, Tat binds the RNA TAR element in nascent HIV-1 transcripts, directs the phosphorylation of RNA Pol II, and thereby improves its processivity (Yankulov and Bentley 1998).

After transcription, both spliced and unspliced viral transcripts are transported to the cytoplasm. Rev (regulator of virion) facilitates the transport of unspliced and singly spliced viral RNA out of nucleus. Rev binds the structured RRE (Rev response element) and functions as an adaptor to link the viral RNA to the host protein export pathway.

Viral RNA can be found in 3 forms. The 9kb RNA (unspliced) is translated into Gag and Gag-Pol, with the latter produced due to a frame shift in a slippery sequence. Two copies of the full-length Gag RNA are also incorporated as the genome of nascent virions (Butsch and Boris-Lawrie 2002). The 4kb RNA (partially spliced or singly spliced) codes

for Env, Vif, Vpu, and Vpr, while the 2kb RNA (multiply spliced) is translated into Rev, Tat, and Nef (Emerman and Malim 1998). The route of mRNA export from the nucleus predetermines the subsequent route of trafficking of Gag protein that is translated from that mRNA and host factors that interact with it (Swanson et al. 2004).

6. Translation of viral proteins and assembly of viral particles

As mentioned above, Gag is translated as a polyprotein and is subsequently processed by the viral protease (PR) during viral particle maturation into MA, CA, NC, p6 and spacer peptides (Frankel and Young 1998). In immature virions, these are arranged radially, with MA found under viral envelope and NC found in the innermost portion of particle. As the virions mature, CA forms a shell around the NC, which is in complex with the viral RNA genome. This is visualized by electron microscopy as an electrodense, conical structure called the viral core. NC functions as a chaperone protein for the viral RNA genome. NC interacts with viral or cellular RNA nonspecifically, but has the propensity to package full-length viral RNA with the psi signal found in the 5' region of the viral RNA. This psi signal is lost in spliced viral RNA. Not all viral particles contain RNA (Coffin et al. 1997). NC is substantially enriched relative to CA in preparations of purified viral cores (Welker et al. 2000; Forshey and Aiken 2003).

Several attempts have been made to estimate the Gag content in viral particles. Empirical determination of the ratio of viral genomic RNA to CA, which corresponds to ~104 virions pg–1 CA antigen (Piatak et al. 1993). In a study by S. Layne and colleagues linking CA concentration with the number of particles counted by thin-section EM

compared to a known standard, they estimate 1,200 ± 700 CA proteins per virion (Layne et al. 1992). In an independent study by P. Zhu and colleagues, they compared the concentrations of CA and Env proteins in purified virus preparations coupled with counting Env trimers per viral particle by negative stain EM, estimating 1,400 CA proteins per virion (Zhu et al. 2003).

A newer report by J. Briggs et al. estimates ~5,000 copies of Gag for an average immature HIV particle, while only 1,000-1,500 CA molecules comprise the mature viral core (Briggs et al. 2004). This implies that less than one-third of immature Gag contributes to the mature viral core and that a considerable amount of free CA may be found inside the viral particle (Briggs et al. 2004). Also, about one-third of viral particles have 2 cores but very few have 3 cores (Briggs et al. 2004). As for efficiency of infection, only one in eight virus particles that initiate an infection results in an integrated copy of the viral DNA in the host genome (Thomas et al. 2007). The ratio of infectious to noninfectious particles has been estimated to be between 1 in 1,000 and 1 in 60,000 (Andreadis et al. 2000; Dimitrov et al. 1993; Kimpton and Emerman 1992; Marozsan et al. 2004). However, infectivity may be underestimated because of cell-free viral particles not encountering a target cell. A recent study attempting to address this issue concluded that there is approximately 1 infectious particle in 8 to 20 viral particles (Thomas et al. 2007).

Aside from measuring Gag in viral particles, efforts have been made to characterize other components of the viral particle. An older report by J. Coffin estimates that 2,000 Gag (Pr55) molecules, along with 50 to 100 Gag-Pol precursor proteins, form

homodimers and then capture and encapsidate two copies of the viral RNA genome with about 20 copies of host $tRNA^{Lys}$ isoacceptors ($tRNA^{Lys}$) (Coffin et al. 1997). An estimated 40–100 IN molecules are encapsidated within each HIV particle (Pommier et al. 2005). Also, ~400 transmembrane glycoproteins (gp120 and gp41) trimers surround the nucleoprotein core (Vogt 1997). An average 145-nm immature HIV-1 virion would contain ~700 molecules of Vpr, which would be 1:7 ratio compared with Gag (Müller et al. 2000).

Since the maturation of virions is essential for viral infectivity, the viral PR has been a feasible drug target. First-generation protease inhibitors (P.I., e.g. Indinavir, Saquinavir, Nelfinavir) had significant side-effects and complicated dosing systems (Tejerina and Bernaldo de Quirós 2011). With newer P.I. (Darunavir/Ritonavir), monotherapy is a viable option for maintenance therapy once virological suppression is achieved (Estébanez and Arribas 2012).

D. Cellular host factors

Since viruses are, by their nature, obligate parasites, they hijack the cellular machinery to complete their life cycle. On the other hand, the cell has evolved factors which target and restrict the spread of infection. Therefore, increasing our knowledge of host factors that may be essential or may modulate steps in the viral life cycle leads to a better understanding of the host-pathogen relationship and of potential therapeutic targets (Goff 2007).

The last couple of years have seen the advent of genome-wide screens to identify candidate factors that may be “pro”-viral or antiviral. siRNA-based platforms facilitate genome-wide hunts for these “HIV-dependency factors”, first published by A. Brass and colleagues (Brass et al. 2008) and subsequently published by independent groups (König et al. 2008; Zhou et al. 2008). R. Konig, et al. have also used additional criteria, which they have dubbed “evidence score” and have cross-referenced different databases (ex. Hynet: yeast two-hybrid human protein-protein interaction database) to provide a stringent analysis of new hits (König et al. 2008). Zhou, et al. on the other hand, applied criteria for druggable targets (Hopkins and Groom 2002), narrowing 311 hits to 56 candidates (Zhou et al. 2008). The overlap between the two genome-scale siRNA screens (Brass, et al. vs. Zhou, et al.) for HIV cofactors is greater than the amount of overlap that would be expected by chance (Zhou et al. 2008). This is an attractive direction for drug development, since antiviral medicines targeting host factors required for HIV infection or replication may provide a higher barrier to the development of resistance (Flexner 2007). Currently, the NIH curates a database for these host factors in the NIH NIAID HIV-1 Human Protein Interaction Database found in this website: (http://www.ncbi.nlm.nih.gov/RefSeq/HIVInteractions/).

One host factor discovered in siRNA screens from A. Brass, et al. is Transportin 3 (TNPO3), a nuclear import protein that is required for HIV-1 infection (Brass et al. 2008). Several independent groups have since explored the role for TNPO3 in nuclear import and maturation of the HIV-1 PIC (Diaz-Griffero 2012; Krishnan et al. 2010; Lee et al. 2010; Christ et al. 2008).

Another approach for identifying HIV-related host factors is to identify host proteins incorporated into HIV-1 virions (Ott 2008). This methodology, however, has some technical issues that need to be addressed. First, the protocol for purifying virions is of paramount importance, since contaminating proteins may cause spurious results (Bess et al. 1997; Gluschankof et al. 1997). Traditionally, virus may be purified from cell culture supernatants by ultracentrifugation through a sucrose cushion (Bess et al. 1992). An alternative or additional ultracentrifugation method is to use gradients of 60% w/v iodixanol (commercial name: OptiPrep), which allow the separation of cellular vesicles from virions. Another alternative method is CD45 immunodepletion of the supernatant, since HIV-1 virions do not have CD45 in their membranes while cellular vesicles do (Ott 2008).

After obtaining purified viral samples, the next step is the analysis of samples by mass spectrometry. However, failure to identify a protein by LC-MS/MS does not conclusively demonstrate that the protein is not present, since the absence of identifiable peptides can be due to several technical factors (Ott 2008). To confirm a candidate protein, detection by mass spectrometry must be complemented by functional data.

E. Chertova and colleagues reported on host proteins isolated and identified by μRPLC-MS/MS from CCR5-tropic HIV-1 virions produced in monocyte-derived macrophages (Chertova et al. 2006). These virions were purified by density centrifugation and CD45 immunoaffinity depletion prior to μRPLC-MS/MS. Electron microscopy after CD45 depletion was performed to confirm purification of HIV-1 virions.

A. Saphire and colleagues also reported a study on CXCR4-tropic HIV-1 virions produced from 293T cells and from Jurkat cells and purified through a sucrose cushion (Saphire et al. 2006). No significant difference was seen between identified proteins from the 293T set and from the Jurkat set. A. Saphire et al. identified previously known host factors incorporated into virions, such as cyclophilin A and Hsp70 (Saphire et al. 2006). They also identified proteins not previously known to be incorporated into HIV-1: histones and CD48 antigen (Saphire et al. 2006).

D. Ott has proposed a classification of incorporated host proteins based on their functional significance to the virions (Ott 2002; 2008):

1. **Partners: ex. Staufen 1**

The overexpression of Staufen1 in virus-producing cells increases viral RNA and Staufen1 packaged in virions (Mouland et al. 2000). Interestingly, depletion of Staufen1 in virus-producing cells also increases the amount of packaged viral RNA (Abrahamyan et al. 2010), possibly causing deregulation of assembly of newly synthesized virions. The current hypothesis is that Staufen1 assists in viral genome packing to produce fewer empty viral particles. The RNA may serve as a scaffold on which Gag organizes and assembles (Muriaux et al. 2001).

2. **Assassins: ex. APOBEC3G**

Since incorporation of this host factor potently inhibits HIV infectivity (reviewed in (Strebel et al. 2009)), this type of protein is actively excluded from virions. In this case,

the HIV-1 accessory protein Vif promotes the proteasomal degradation of cellular APOBEC3G, decreasing the amount available for encapsidation in nascent virions. APOBEC3G will be discussed further in Chapter III.

3. Hostages/Captives: ex. Hsp70

Heat shock protein 70 (Hsp70), a protein-folding chaperone, has transiently increased expression after HIV-1 infection (Wainberg et al. 1997). Incorporated Hsp70 associates with the mature viral core and is included at a 1:20 molar ratio relative to Gag (Gurer et al. 2002). It is postulated to play a role in maintaining the mature virion structure (Ott 2008).

4. Bystanders: ex. Tetraspanins

A bystander protein is a host protein incorporated into nascent virions due to its proximity to the sites of viral budding on the plasma membrane. Its inclusion into virions, therefore, has no known function (Ott 2008). Tetraspanins, which are integral membrane proteins, are examples of this group. HIV-1 has been proposed to bud from tetraspanin-enriched microdomains (TEMs), based on microscopy, cell fractionation data (Khurana et al. 2007; Nydegger et al. 2006) and the presence of tetraspanins in HIV-1 membranes (Ott 2002; Chertova et al. 2006).

Cyclophilin A (CypA) was formerly classified as a captive. It has been shown to be required for optimal infectivity but not virus production (Thali et al. 1994; Franke et al.

1994). It is incorporated at 1:10 molar ratio with Gag (Ott 2002) and binds directly to CA (Luban et al. 1993). However it has since been shown that it is the CypA in target/infected cell, not the virion-associated CypA, which provides this function (Hatziioannou et al. 2005; Sokolskaja et al. 2004). It promotes DNA synthesis early after infection, perhaps by facilitating uncoating (Braaten et al. 1996; Sokolskaja et al. 2004). Since target cell-associated CypA functions in HIV-1 infectivity, virion-associated CypA has been proposed for re-classification as a bystander (Ott 2008).

E. Host factors affecting HIV-1

1. APOBEC3G: from the Old Guard of antivirals

The HIV-1 virion infectivity factor (Vif) is required for viral replication in primary cells (CD4+ T cells) and some nonpermissive cell lines. This Vif requirement was presumably to overcome the presence of a restriction factor, since complementation assays using heterokaryon cell lines, which result from fusing a permissive cell line producing HIV-1 ΔVif virions to a nonpermissive cell line, produced noninfectious virions (Madani and Kabat 1998; Simon et al. 1998). To identify this restriction factor, A. Sheehy and colleagues adopted a subtractive hybridization approach, gleaning a gene product present in a nonpermissive cell line but not expressed in permissive cell lines (Sheehy et al. 2002). Initially called CEM15 after the nomenclature of the nonpermissive cell line, it was later identified as APOBEC3G (apolipoprotein B mRNA-editing, enzyme-catalytic, polypeptide-like 3G), one of seven genes in a cluster on chromosome 22 which code for cytidine deaminases (Jarmuz et al. 2002). These seven genes most

likely arose through gene duplication, as rodent APOBEC3 only has a single gene. All APOBEC3 proteins have either one or two copies of a cytidine deaminase zinc-coordinating motif, which has histidine and cysteine residues, and a glutamic acid that serves as a proton shuttle (Jarmuz et al. 2002).

APOBEC3G most potently inhibits HIV-1, but APOBEC3F, APOBEC3B, and APOBEC3DE also have anti-HIV-1 activities (Bishop et al. 2006; 2004; Doehle et al. 2005a; Holmes et al. 2007). APOBEC3G also suppresses Simian Immunodeficiency Virus (SIV) (Gaddis et al. 2004; Mangeat et al. 2003) and Murine Leukemia Virus (MLV) (Harris et al. 2003; Bishop et al. 2004; Doehle et al. 2005b). APOBEC3F and APOBEC3DE inhibit SIV (Yu et al. 2004a; Dang et al. 2006). APOBEC3B inhibits MLV (Doehle et al. 2005b) and HIV-1, and is also Vif-resistant (Doehle et al. 2005a).

Anti-Hepatitis B Virus (HBV) activity is also exhibited by APOBEC3G (Köck and Blum 2008; Noguchi et al. 2007), APOBEC3F (Bonvin et al. 2006; Rösler et al. 2005), APOBEC3B (Bonvin et al. 2006), and APOBEC3C (Baumert et al. 2007; Köck and Blum 2008). APOBEC3A, a nuclear protein, inhibits adeno-associated Virus (AAV) (Chen et al. 2006) and HIV-1 in target macrophages and dendritic cells (Berger et al. 2011).

APOBEC3 proteins can also restrict mobile genetic elements (reviewed in (Chiu and Greene 2008)). This restriction is important for genome stability because retrotransposons can generate new copies of themselves through reverse transcription and re-insertion into the genome can potentially result in disease-causing mutations. APOBEC3C, APOBEC3F, and APOBEC3G can inhibit yeast Ty1 retrotransposons by

decreasing the number of transposed cDNAs and by extensive editing (Dutko et al. 2005; Schumacher et al. 2005). APOBEC3A, APOBEC3B, and APOBEC3G all inhibit mouse IAP and MusD elements (Esnault et al. 2005). It has been hypothesized that the expansion of the APOBEC3 locus evolved with the need to restrict and inactivate endogenous retroviruses and other mobile elements in the genome (Chiu and Greene 2008).

2. Tetherin: thwarting the viral escape

HIV-1 accessory protein Viral protein u (Vpu) is required in certain nonpermissive cell lines to successfully release nascent virions; otherwise viral particles are retained on the cell surface, apparently tethered, and subsequently endocytosed (Neil et al. 2006; Varthakavi et al. 2003). This nonpermissive phenotype is interferon α (IFNα)-inducible (Neil et al. 2007). To identify the restriction factor responsible, a microarray was performed and a candidate gene called BST-2/CD317, also dubbed “tetherin”, was identified. It is IFNα-inducible, recapitulated the Vpu-requiring phenotype and colocalized with Vpu (Neil et al. 2008) and Gag (Van Damme et al. 2008) on the cell surface.

Tetherin is a type II single pass transmembrane protein with a transmembrane anchor on the N-terminus, an extracellular a helix, and a C-terminal glycophosphatidyl inositol (GPI) anchor (Kupzig et al. 2003). Disulfide bonds are formed between the three cysteines in the extracellular domain and the corresponding cysteines in the other tetherin monomer of the coiled-coil dimer (reviewed in (Malim and Bieniasz 2012)). The activity

Figure 1.4

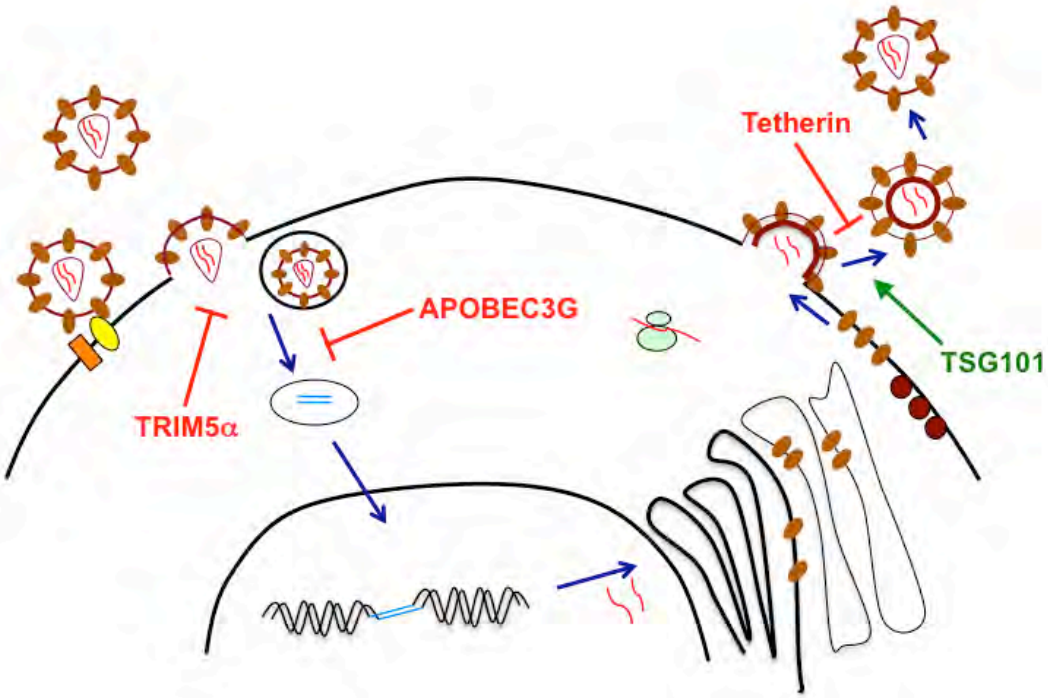

Figure 1.4 **Host factors affecting HIV-1 and other viruses.** The host cell has evolved restrictions factors to limit the infection and propagation of unwanted invaders such as HIV-1. TRIM5α is postulated to be a pattern-recognition receptor that interacts and recognizes the incoming viral capsid. APOBEC3G is from the APOBEC3 family of cytidine deaminases that can restrict a wide-range of unwanted cellular parasites such as viruses and endogenous retrotransposons by mutating viral genomic material to render them noninfectious. Tetherin, a transmembrane protein, presents a final effort to restrict viral spread by preventing viruses from budding off the cell membrane. On the other hand, viruses have likewise developed mechanisms to co-opt host cellular functions, such as utilizing TSG101 and the ESCRT machinery to complete viral budding from the plasma membrane.

of tetherin seems to be fairly nonspecific, since a wide variety of viruses are restricted (Jouvenet et al. 2009). The mode of action of tetherin is thought to be simply cross-linking the plasma membrane to the viral particles that have budded off. Tetherin tolerates mutations, including swapping whole domains with no detrimental effect (Perez-Caballero et al. 2009). Retroviruses which do not possess Vpu have evolved other tetherin antagonists (e.g. Nef protein for SIV) (Malim and Bieniasz 2012).

3. TRIM5α: intruder sensor alert

TRIM5α was initially identified in a screen for rhesus macaques cellular factors that could restrict HIV-1 but were susceptible to SIV or MLV (Stremlau et al. 2004). Conversely, human TRIM5α can inhibit MLV but cannot restrict HIV-1 (Hatziioannou et al. 2004). Therefore, TRIM5α proteins are roadblocks to cross-species transmission since they cannot restrict retroviruses occurring in the same species but can effectively block other retroviruses.

An independent report from Sayah et al. showed that owl monkeys are not susceptible to HIV-1 due to the presence of TRIMCyp, a fusion protein of TRIM5α with cyclophilin A replacing the SPRY domain, arising from a retrotransposon insertion (Sayah et al. 2004). This restriction to HIV-1 is removed when the interaction of cyclophilin with the HIV-1 capsid is interrupted.

The current model for the mechanism of action of TRIM5α is that it accelerates uncoating after viral entry, resulting in abortive reverse transcription (Malim and Bieniasz 2012). New data from T. Pertel et al. (Pertel et al. 2011) additionally show that

TRIM5α may be acting as a pattern recognition receptor (PRR) by its ability to identify the retroviral lattice of the capsid and to activate pathways of innate immunity.

4. TSG101: a partner for cell break out

Located on the C-terminal end of the Gag polyprotein is p6, which contains the late assembly domains (L domains), designated as such because they mediate the completion of viral budding from the plasma membrane (reviewed in (Weiss and Göttlinger 2011; Martin-Serrano and Neil 2011)). The importance of p6 was discovered when mutations on p6 resulted in the accumulation of budded viral particles still tethered to the plasma membrane of adherent cells, as visualized by transmission and scanning electron microscopy (Göttlinger et al. 1991). These p6 mutations also impaired proteolytic processing, with the accumulation of a Gag p25 intermediate (Göttlinger et al. 1991). The p6 domain contains a P(T/S)AP motif, which is highly conserved among primate lentiviruses (Strack et al. 2000) and constitutes the primary HIV-1 L domain required for budding (VerPlank et al. 2001). Other retroviruses have equivalent motifs that are required for virus release, and these different motifs are functionally interchangeable (Parent et al. 1995). These studies led to the hypothesis that L domains are docking sites for cellular factors necessary for virus release (Strack et al. 2000; Parent et al. 1995). Subsequently, several independent groups identified TSG101 (tumor suppressor gene 101, also called Vps23) in yeast two-hybrid screens as specifically interacting with the PTAP motif of HIV-1 p6 (Martin-Serrano et al. 2001; Garrus et al. 2001; VerPlank et al. 2001). PTAP-containing sequences in HIV-1 and the unrelated Ebola virus are required

for the recruitment of TSG101 (Martin-Serrano et al. 2001). Also, TSG101 recruitment is necessary for the formation of viral particles. TSG101 is a component of a 350-kDa complex, ESCRT-I (endosomal sorting complex required for transport–I), one of several ESCRT complexes tasked of packaging ubiquitinated cargo into multivesicular bodies for eventual degradation by lysosomes (Wollert and Hurley 2010). By utilizing TSG101, HIV-1 has the ability to co-opt the cellular machinery for forming vesicles, in this case facilitating the process of pinching off viral particles from the plasma membrane to release nascent virions.

Chapter II

Materials and Methods

A. APOBEC3G Study

i. **Cell culture and cell lines.** Human embryonic kidney (HEK) 293 and H9 T cell lines were generous gifts from Dr. Eicke Latz and Dr. Mario Stevenson, respectively. HEK293, HEK 293T, and HeLa cell lines were maintained in DMEM (Invitrogen) supplemented with 10% FBS. H9 cells were maintained in RPMI (Invitrogen)-10% FBS media. All cell lines were grown at 37^{o}C in a humidified incubator (5% CO_2). Stable cell lines expressing A3G-YFP and point mutants were established by transfecting HEK293 and selecting for 12-14 days with 800 μg/mL G418 (Invitrogen) in DMEM-10% FBS following standard procedures.

ii. **Plasmids and transfections.** Plasmids for expression of A3G-YFP and A3G-HA were previously described (Wichroski et al. 2006). Vectors for expressing APOBEC3G point mutants, except C100S and C291S, were constructed by site-directed mutagenesis using PCR. Amplicons were inserted into the *HindIII* and *Sac II* sites of pEYFP-N1 (BD Biosciences). C100S and C291S were derived from plasmids pGST-APO3G C100S and C291S plasmids, which were generously provided by Dr. Judith Levine (Iwatani et al. 2006). The coding regions were amplified and modified to introduce restriction sites *HindIII* and *SacII* by PCR. Amplicons were inserted into pEYFP-N1 as above. All constructs were confirmed by sequencing. Single-cycle HIV-1 luciferase reporter proviral vectors pNL4-3.Luc.E^{-}R^{-} and pNL4-3.Luc.E^{-}R^{-} ΔVif were generous gifts of Dr. Nathaniel Landau (Mariani et al. 2003). pLTR-VSV-G and full-length provirus

pLAI ΔVif were kindly provided by Dr. Mario Stevenson. The HIV-1 subgenomic vectors pNL-A1 and pNL-A1 ΔVif were generous gifts of Dr. Klaus Strebel (Kao et al. 2003). Transfections were carried out using Lipofectamine 2000 (Invitrogen) for HEK 293 and 293T following manufacturer's instructions. HeLa was transfected using Lipofectamine (Invitrogen). Unless otherwise specified, transfections for virus production of pGIPZ (Open Biosystems, see below) lentiviral particle production were carried out using standard calcium phosphate procedure.

iii. **Virion production.** Vectors coding for A3G-HA were co-transfected with pNL4-3.Luc.E$^-$R$^-$ ΔVif and pLTR-VSV-G using Lipofectamine 2000. After 48 hours, supernatants containing virus were collected, clarified by low-speed centrifugation, and filtered (0.4 μm, Millipore). For packaging experiments, amounts of virions were quantified by p24 ELISA (Zeptometrix, Buffalo, NY) followed by ultracentrifugation of equal amounts of virions at 27000xg for 2 hours at 4^{o}C through a sucrose cushion. Antibodies α-p24 (Gag monoclonal #24-4 from Dr. Michael Malim, NIAID, NIH), α-GFP (JL-8, Clontech) or α-HA (Santa Cruz Biotech) and α-APOBEC3G (affinity purified polyclonal rabbit antibody, Antibody Solutions, Palo Alto, CA; published in (Wichroski et al. 2006)). For luciferase infectivity assays, target 293T cells were infected in triplicate with 10 ng of virus as determined by p24 ELISA. After 48 hours, total cell extracts were prepared from target cells and luciferase activity was measure after addition of Luciferase Substrate (Promega).

iv. **Immunostaining and confocal microscopy.** Preparation of samples for confocal microscopy was previously described (Wichroski et al. 2006; Chu and Rana 2006). Primary antibodies α-DDX6/RCK (Bethyl) and α-myc (Santa Cruz Biotech) were used at 1:500 and 1:400, respectively.

v. **siRNA and shRNA knockdown.** siRNAs (Dharmacon) targeting RCK, LSM1 and GW182 were previously described (Chu and Rana 2006). 293T producer cells were transfected with 50 nM siRNA using Lipofectamine 2000. After 24 hours, cells were reseeded and transfected with a second dose of 50 nM siRNA plus proviral DNA pNL4-3.Luc.E$^-$R$^-$ ΔVif or subgenomic pNL-A1 ΔVif (mock) and pLTR-VSV-G. Virions were prepared as above. siLSM1 nucleofection of H9 cells by Amaxa were performed following manufacturer's recommendations. Knock down of LSM1 in H9 cells was accomplished using pGIPZ shRNA against LSM1 (shLSM1, source ID V2LHS_213130, Open Biosystems). These lentiviral particles were produced by transfecting subconfluent 293T in a 100 mm dish with 21 μg pGIPZ, 21 μg PAX2 (Gag-Pol, from AddGene), and 10.5 μg pMD2.G (VSV-G, from Addgene) using a standard calcium phosphate procedure. Virus supernatant was harvested after 48 hours, clarified by low speed centrifugation, filtered, and stored in aliquots at -80^{o}C. Virus titers were determined according to manufacturer's protocol. H9 cells were transduced at MOI=10 using spinoculation at 1200xg for 2 hours at room temperature with 8 μg/mL polybrene (Millipore). Fresh RPMI media was added the next day. Four days after transduction, H9 cells were treated with 0.5 μg/mL puromycin to select for transduced cells. After 2

days of selection, H9 was infected by spinoculation with 450 ng p24 equivalent of full-length LAI ΔVif per $1x10^6$ target cells. Three days after infection, virus supernatant was collected, clarified, and filtered. Virions were prepared and analyzed as above.

vi. **H9 infection and RNA extraction for miRNA microarray study.** 293T cells in DMEM-10% FBS were transfected with pNL4-3 using Lipofectamine 2000. Supernatant was collected after 48 hours, cleared for cellular debris by a low-speed spin, and passed through a 0.45 μM pore size filter (Millipore). Viral content was quantitated using p24 ELISA (Zeptometrix). Supernatant aliquots were stored in at -20^{o}C. The H9 infection protocol was adapted from published methods by D. Baltimore and colleagues and R. Gallo's group (Kim et al. 1989; Popovic et al. 1984). Briefly, $1x10^7$ H9 cells were washed and pre-treated with 10 μg/mL polybrene (Chemicon) in RPMI-10% FBS at 37^{o}C for 1 hour. Afterwards, the cells were again washed and split two-ways: one set ($0.5x10^7$ cells for infection) was resuspended in virus supernatant equivalent to 125 ng p24 and another set ($0.5x10^7$ cells for mock treatment) was resuspended in DMEM-10% FBS. Cells were incubated at 37^{o}C, 5% CO_2 for four hours, washed, and resuspended in RPMI-10% FBS. Infection was allowed to proceed for 5 passages and was monitored by p24 ELISA. H9 mock-treated and infected cells were collected after two weeks and washed with cold PBS. RNA was extracted using Trizol (Invitrogen), resuspended in nuclease-free water, and submitted to LC Sciences (Houston, TX) for miRNA profiling.

B. UPF1 Study

i. **Transfection of proviral constructs and over-expression vectors.** All proviral constructs in this study are pNL4-3 env fs complemented with SR α NL4-3 env in trans. UPF1 was amplified from a pSPORT vector (accession number BC039817) and inserted into pcDNA3.1+, with an engineered HA tag in the N-terminus of the protein (HA-UPF1). Vectors containing point mutations were constructed from this HA-UPF1. Transfections were carried out using standard calcium phosphate methods in T25 flasks using 2 μg proviral construct, 1 μg envelope, and 0.2 μg HA-UPF1.

ii. **siRNA experiments.** Transfections for siRNA experiments were carried out in 293T cells in 6-well format using standard Lipofectamine 2000 protocol. 10 nM siRNA against UPF1 were co-transfected with 0.76 μg proviral construct and 0.38 μg envelope. Cells were washed 1 day after transfection and supernatant was collected 2 days after transfection for infectivity assays.

iii. **Assaying viral infectivity.** Infectivity assays were performed in T25 flasks seeded previously with 50,000 GHOST CD4 CXCR4, which were infected with 40 ng p24 equivalent supernatant as measured by ELISA. Infected cells were assayed for GFP expression 2 days p.i. by FACS.

iv. **Immunoblotting.** Total cell lysates were resolved on SDS-PAGE and immunoblots were performed using the following antibodies: anti-HA from Covance, anti-HIV CA serum from NIH AIDS, anti-UPF1 (a generous gift from

Dr. Jens Lykke-Andersen; also from Bethyl), anti-gp120 (Fitzgerald Industries), anti-IN (IN-2) and anti-UPF2 (C-18) from Santa Cruz Biotech.

v. **Analysis of viral particles.** Virions released in the medium from 293T cells transfected with pNL4-3 env fs were isolated as previously described (Popova et al. 2010). For UPF1 incorporation into virions, HA-UPF1 was co-transfected with proviral DNA. For determining nucleocapsid dependence, SVC vpu+ (with nucleocapsid) or SVC vpu+ GCN4p6 (without nucleocapsid) constructs were used. An additional spin using an OptiPrep gradient, as previously described (Dettenhofer and Yu 1999), was utilized to purify the virions away from microvesicles.

vi. **Analysis of virion-associated genomic RNA.** After saving an aliquot for p24 ELISA, virions produced from 293T were pelleted as above and viral RNA was recovered using the QiAMP Viral RNA kit (Qiagen). The viral RNA was then reverse transcribed using EcoDry strips (Clontech). The resulting cDNA was diluted 1:20 using TE/carrier DNA before use in Sybr Green-based assay using primers specific for full-length viral RNA(Buckman et al. 2003) . The raw signal was then normalized to the amount of p24 in the supernatant volume that was used for RNA extraction.

vii. **Analysis of viral fusion.** The BLaM-Vpr protocol used for this study was modified from W. Greene and colleagues (Cavrois et al. 2002)and L. Brandano and M. Stevenson (Brandano and Stevenson 2012). Briefly, virus supernatant were produced from 293T transfected with 2 μg pNL4-3 env fs, 1 μg SRαNL4-3

env, 2 μg pMM310 (BLaM-Vpr construct), and 0.2 μg HA-UPF1 or mutant HA-$UPF1_{R865A}$. Virus supernatants were harvested, spun down, and filtered prior to addition to TZMbl cells plated previously at 30,000 cells per well in a 96-well plate. Infection was allowed to proceed for 2 hours at 37^{o}C in a humidified incubator. Afterwards, the supernatant was removed and dye solution (LiveBLAzer FRET-B/G CCF4-AM kit from Invitrogen) was added and the plate was incubated overnight at room temperature, protected from light. The next day, the dye solution was washed off and replaced by supplemented Hanks' balanced salt solution (20 mM HEPES, 2 mM L-Glutamine). Blue cells were counted under a fluorescence microscope with Chroma filter set 41031 (Beta-Lactamase, Blue/Aqua, EX HQ405/20X, BS 425DCXR, EM HQ430LP) for 5 random fields, under 20x magnification and normalized to p24 content.

viii. **Analysis of post-entry events.** Virus stocks were produced from 293T transfected with pNL4-3 env fs complemented with SRαNL4-3 env used and were treated with DNase prior to infection for early RT and late RT assays. GHOST CD4 CXCR4 target cells were infected in triplicate. The DNA from target cells was extracted 2 days p.i. using DNA Blood Mini Kit (Qiagen). Methods and primers previously described in Mbisa et al. (Mbisa et al. 2009) were used to prepare infected target cells for this assay. The primer sets/probes used were: 1) Early RT: hRU5-F2, hRU5-R; 2) Late RT: MH531, MH532, LRT-P; 3) 2-LTR circles: SS-4, LTR-R5, P-HUS-SS1. For the standard curves for early RT and late RT assays, 10-fold dilutions of linearized pNL4-3 plasmid

were used. For the 2-LTR circle assay, the plasmid standard was kindly provided by Dr. Mark Sharkey (Sharkey et al. 2000). DNA was normalized prior to quantitative PCR performed on a 7500 Fast Real-time PCR machine by Applied Biosystems using the standard format. Final values were obtained by subtracting corresponding “no env ctrl” (i.e. DNase-treated supernatants from samples not transfected with env expression vector) values.

Chapter III

Disassembly of APOBEC3G ribonucleoprotein complexes in mRNA processing bodies does not affect APOBEC3G incorporation into HIV-1

Mentor: Tariq Rana, Ph.D.

Michael Wichroski and Anna Serquiña cloned the expression vectors for the APOBEC3G point mutants. Michael Wichroski carried out the experiment in Appendix 3.1. Chih-chung Lu performed the experiments in Figure 3.9, with Figure 3.9 B in collaboration with Anna Serquiña. Chia-ying Chu provided the microscopy data in Appendix 3.2A. Hong Cao analyzed the microarray data for Appendices 3.6 and 3.7. RNA samples for Appendix 3.6 were prepared by Anna Serquiña. All other experiments were performed by Anna Serquiña. Appendix 3.5A, 3.5B and 3.6 were published in R. Nathans, et al. Mol Cell 2009.

A. Abstract

APOBEC3G is a cytidine deaminase that inhibits HIV-1 lacking the virion infectivity factor (Vif). Newly-translated APOBEC3G are found in low-molecular mass (LMM) complexes and are subsequently recruited into high-molecular mass (HMM) ribonucleoprotein (RNP) complexes. Our group has previously shown that this APOBEC3G RNP is in processing bodies (P bodies), which are cytoplasmic foci of mRNA suppression and decay, but the role of this localization is unclear. To explore the functional relevance of APOBEC3G in P bodies, we constructed tagged APOBEC3G point mutations of amino acids in known motifs of the protein, including regions recognized to be essential for enzymatic activity, virion packaging, Vif sensitivity, and RNA binding. We then characterized their effect on expression level, subcellular localization, and packaging into virions. We found that none of the mutations abrogate P body localization. The importance of P body localization of APOBEC3G on virion packaging was also studied by disrupting P bodies through knockdown of P body components such as LSM1, RCK, and GW182. However, we did not see any significant changes in APOBEC3G viral packaging after the dispersal of P bodies. These findings suggest that APOBEC3G localized in P bodies do not constitute the pool of APOBEC3G that is recruited into HIV-1 virions; rather, APOBEC3G in P bodies may serve another purpose, such as to sequester and inactivate the enzyme in a subcellular component.

B. Background and rationale for study

1. Discovery of APOBECs

As discussed in Chapter I, APOBEC3G is a restriction factor against HIV-1 ΔVif discovered in nonpermissive cell lines (Sheehy et al. 2002) but is downregulated by Vif (Marin et al. 2003; Sheehy et al. 2003). APOBEC3G belongs to a family of cytidine deaminases called APOBECs (apolipoprotein B mRNA editing enzyme catalytic polypeptide). They catalyze the hydrolytic deamination of the C4 position of the cytosine base (see Figure 3.1), converting cytidine to uridine. The cytidine deaminase motif is His-X_{aa}-Glu-$X_{aa23-28}$-Pro-Cys-X_{aa2-4}-Cys, with a histidine and two cysteines coordinating a Zn^{++} ion and a glutamate residue for proton shuttling (Jarmuz et al. 2002).

The first cytidine deaminase described in this family is APOBEC1, which was cloned in 1993 (Teng et al. 1993) and is expressed in small intestines to regulate cholesterol metabolism (Breslow 1988). Together with the APOBEC1 Complementation Factor (ACF), APOBEC1 edits ApoB100 mRNA (Navaratnam et al. 1995) by cytidine deamination (CAA→UAA corresponding to amino acid position 2153) (Johnson et al. 1993; Navaratnam et al. 1993), introducing an in-frame stop codon to produce ApoB48, in contrast to full-length ApoB100 protein. Tight control of protein expression appears to be an important characteristic of this enzyme since editing becomes nonspecific when APOBEC1 is overexpressed in rat hepatomas cell lines (Sowden et al. 1996). Transgenic rabbits and mice ectopically overexpressing APOBEC1 in liver tissue developed hepatic dysplasia and hepatocellular carcinoma (Qian et al. 1998). Another way of regulating APOBEC1 activity is by shifting its subcellular localization (Wedekind et al. 2003).

Figure 3.1

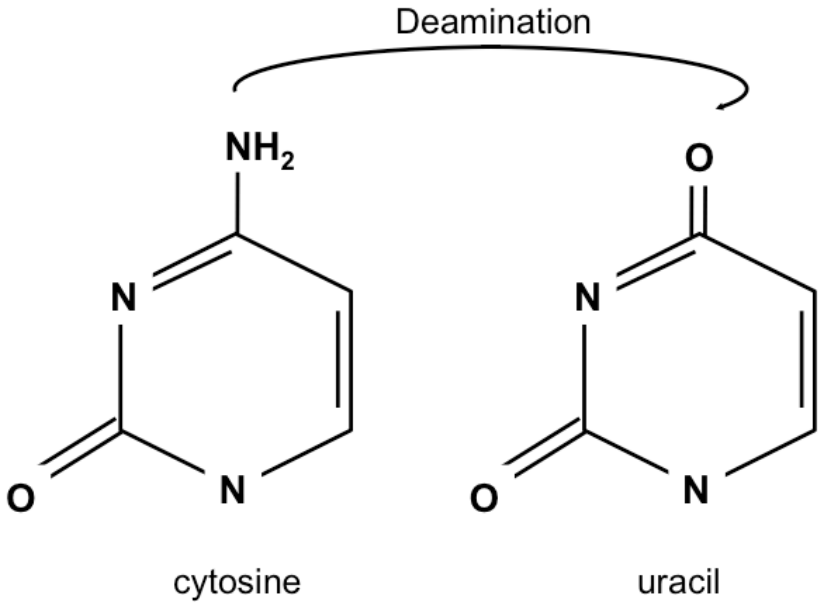

Figure 3.1 **APOBEC3G deaminates cytosine at position C4, converting the base into uracil.**

ApoB mRNA editing occurs in the cell nucleus. However, most of APOBEC-1 and ACF reside as inactive 60S complexes in the cytoplasm (Sowden et al. 2002; Yang et al. 1997). This may be a mechanism for regulating the entry of editing complexes into the nucleus and preventing unwanted, nonspecific editing due to high levels of APOBEC1 activity (Wedekind et al. 2003).

Activation-induced cytidine deaminase (AID), another member of this family, mediates somatic hypermutation and class-switch recombination (Okazaki et al. 2002). Somatic hypermutation creates a population of B cells with increased affinity for a particular antigen by mutating the immunoglobulin variable region. On the other hand, class-switch recombination diversifies the immunoglobulin heavy-chain class: IgM, IgG, IgA, or IgE. These genetic modifications are essential for a normal immune response. However, overexpression of AID leads to lymphomas, probably due to increased amount of unrepaired DNA damage and translocations after AID-induced mutations (Lenz and Staudt 2010). AID functions as a DNA mutator (Petersen-Mahrt et al. 2002; Yoshikawa et al. 2002), in contrast to the RNA-editing APOBEC1 enzyme.

2. Vif-mediated degradation of APOBEC3G

The HIV accessory protein Vif mediates downregulation of APOBEC3G to prevent its incorporation into nascent virions. This Vif-mediated downregulation is accomplished via proteasome degradation of APOBEC3G. Vif recruits E3 ubiquitin ligase (cullinB-ElonginB-ElonginC-Rbx complex) and induces poly-ubiquitination of APOBEC3G,

which targets APOBEC3G for proteasomal degradation (Marin et al. 2003; Sheehy et al. 2003).

A non-proteasome-mediated mechanism has also been postulated because Vif causes a 4.6-fold decrease in the synthesis of APOBEC3G protein, pointing towards transcriptional or translational modulation by Vif (Mariani et al. 2003). Additionally, Vif mutant S144A still induces APOBEC3G degradation (Mehle et al. 2004a) but does not fully rescue infectivity of virions (Yang and Gabuzda 1998). Vif depletes intracellular APOBEC3G by impairing translation of its mRNA (Kao et al. 2003; Mariani et al. 2003; Stopak et al. 2003) by binding to the 3'UTR and the 5' UTR of APOBEC3G mRNA (Mercenne et al. 2010).

3. Vif sensitivity of APOBEC3G

A single amino acid at position 128 in APOBEC3G governs its sensitivity to HIV-1 Vif (Bogerd et al. 2004; Mangeat et al. 2004; Mariani et al. 2003; Schröfelbauer et al. 2004). When negatively charged D128 is mutated to positively charged K128, APOBEC3G gains resistance against HIV-1 Vif while becoming sensitive to Vif SIV_{agm}.

4. APOBEC3G structure

APOBEC3G forms homo-multimers and is packaged as oligomers bound to RNA in virions. Multimerization is not required for its catalytic and antiviral activities (Opi et al. 2006). The APOBEC3G C-terminal CD has five β strands flanked by an α helix on each side plus connecting loops (Chen et al. 2008; Holden et al. 2008; Zhang et al. 2007).

5. Dissecting APOBEC3G antiviral activity

Initially, APOBEC3G's mode of action in the HIV-1 life cycle was ascribed to its ability to incorporate into nascent virions and subsequently hypermutate the viral cDNA during reverse transcription in newly-infected target cells (Mangeat et al. 2004; Zhang et al. 2003). The hypermutation results from deamination of cytidines into uridines during reverse transcription in the ssDNA minus strand, resulting in G → A conversions in the plus strand. APOBEC3G deaminates cytidine in the context of the CC dinucleotide at multiple spots on the HIV-1 proviral DNA (Yu et al. 2004b; Suspène et al. 2006). Twin gradients of APOBEC3G editing with the maxima occur at the 5' to the cPPT and the 3'PPT (Suspène et al. 2006), which are the locations during reverse transcription where priming of the positive strand occurs (described in Chapter I). It is hypothesized that prior to this priming event, the single stranded minus strand at the cPPT and 3' PPT are hotspots for the deaminase activity of APOBEC3G (Suspène et al. 2006). Only the C-terminal cytidine deaminase (CD) domain is catalytically active, with the second domain functioning in nucleic acid binding and virus encapsidation (see Figure 3.4A). However, several studies show that APOBEC3G mutants lacking deaminase activity (i.e. alterations in the C-terminal CD motif) still demonstrate considerable residual antiviral effects (Bishop et al. 2006; Newman et al. 2005). Conversely, APOBEC3G-APOBEC3F chimeras retain deaminase activity but demonstrate diminished antiviral activity (Bishop et al. 2006). These findings suggest that deaminase-dependent hypermutation may not be a requirement for antiviral activity. One proposed mechanism for this deaminase-independent antiviral activity is that APOBEC3G remains bound to viral genomic RNA,

preventing the viral reverse transcriptase from accessing its template (Soros et al. 2007). Since this deaminase-independent activity is an incomplete block, reverse transcription will occasionally occur, generating the minus-strand and providing the substrate for the deamination reaction.

6. APOBEC3G complexes in the cell

Several independent groups have demonstrated that APOBEC3G can be found in distinct complexes in the cell. Initially, APOBEC3G was reported to be in low-molecular mass (LMM) complexes and shift into high-molecular mass complexes (HMM) upon activation of CD4+ T cells (Chiu et al. 2005). Later, this paper was retracted (Chiu et al. 2010) since the claim that APOBEC3G presents a post-entry restriction in inactivated cells was not repeatable (Kamata et al. 2009; Santoni de Sio and Trono 2009). However, subsequent work from W. Greene's group have shown that APOBEC3G being found in LMM and HMM is reproducible (Chiu et al. 2006; 2010).

At least two independent groups have demonstrated that newly translated APOBEC3G ("new A3G") resides in these LMM complexes while "old A3G" assembles into HMM complexes (Goila-Gaur et al. 2009; Soros et al. 2007). This assembly has been shown to occur within 30-60 minutes after translation by pulse-chase assays. However, these reports have conflicting data as to which APOBEC3G is packaged into virions: V. Soros et al. reported that APOBEC3G in LMM are recruited into virions and become part of an intra-virion associated complex (Soros et al. 2007). However, R. Goila-Gaur et al.

demonstrated that APOBEC3G packaged into virions come from both the LMM and HMM populations (Goila-Gaur et al. 2009).

These HMM A3G complexes are ribonucleoprotein assemblies, the identity of which have been variably described by several groups as either Staufen granules (Chiu et al. 2006), stress granules (Gallois-Montbrun et al. 2007; Kozak et al. 2006), polysome-associated complexes (Kozak et al. 2006), or mRNA processing (P) bodies (our group (Wichroski et al. 2006) and (Gallois-Montbrun et al. 2007)). P bodies are punctate structures in the cytoplasm where mRNA degradation and mRNA translation repression occur (reviewed in (Eulalio et al. 2007)). In a related study, we have also shown evidence that implicates P body components in the suppression of HIV-1 (Nathans et al. 2009).

We therefore want to explore the possibility that APOBEC3G located in P bodies may have a functional relevance to its antiviral effect against HIV-1.

C. Hypothesis:

APOBEC3G localization in processing bodies contributes to its antiviral function.

D. Results

1. APOBEC3G is a dynamic component of P bodies

We first tested whether our current conditions for transfecting YFP-tagged APOBEC3G would yield an antiviral effect. We co-transfected luciferase-expressing proviral DNAs (+Vif or –Vif) with 15 fmol of APOBEC3G-YFP. We then assayed for infectivity of the resultant virus stocks by measuring for luciferase in infected 293T

Figure 3.2

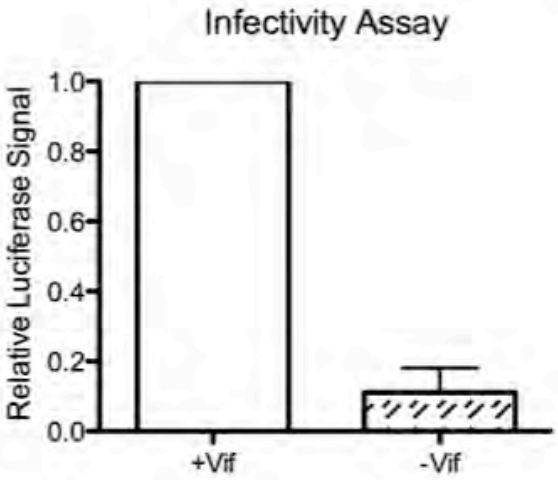
Infectivity Assay
Relative Luciferase Signal
1.0
0.8
0.6
0.4
0.2
0.0
+Vif
-Vif

Figure 3.2 **APOBEC3G-YFP is antiviral.** 293T cells were co-transfected with wild-type HIV-1 (+Vif) or ΔVif (-Vif) luciferase-expressing proviral plasmid and APOBEC3-YFP. VSV-G-pseudotyped viral supernatants were normalized to particle number (p24) prior to infecting target cells and single cycle luciferase infectivity assay was measured 2 days after infection.

target cells after normalizing for p24 content. As expected, -Vif virus (ΔVif Luc) produced in the presence of 15 fmol APOBEC3G-YFP has ~10-fold decreased infectivity compared to +Vif (i.e. wild-type) virus supernatant (Figure 3.2). These results demonstrate that exogenous, YFP-tagged APOBEC3G has potent antiviral activity against HIV-1 ΔVif virus.

APOBEC3G, together with Vif, localizes to mRNA processing bodies (P bodies). To test whether this subcellular localization is due to aggregates of APOBEC3G protein as opposed to functional APOBEC3G complexes, we utilized a diagnostic drug previously reported by N. Kedersha and P. Anderson that can differentiate dynamic P bodies versus transfection-induced protein aggregates in the cell (Kedersha and Anderson 2007). They have shown that treatment of mammalian cells with emetine, a translation inhibitor, disperses P bodies, but not protein aggregates. To observe the effect of emetine in our system, we treated empty vector-transfected HEK293 cells with either 40 μg/mL emetine or DMSO (vehicle control) for 2 hours and immunostained for RCK (a P body marker, (Cougot et al. 2004)). Empty vector-transfected cells lost their P bodies when treated with emetine, as seen by dispersal of RCK into the cytoplasm, while DMSO-treated cells retained the RCK signal in punctate structures (Figure 3.3A).

Next, we transiently transfected HEK293 cells with APOBEC3G-YFP (A3G-YFP) and treated the cells with emetine. Similarly, A3G-YFP is also dispersed in emetine-treated HEK293, but not in DMSO-treated cells (Figure 3.3C). In addition, there is co-localization of A3G-YFP with RCK in DMSO-treated cells, indicating that in our current system, APOBEC3G is located in *bona fide* P bodies and is not forming protein

Figure 3.3

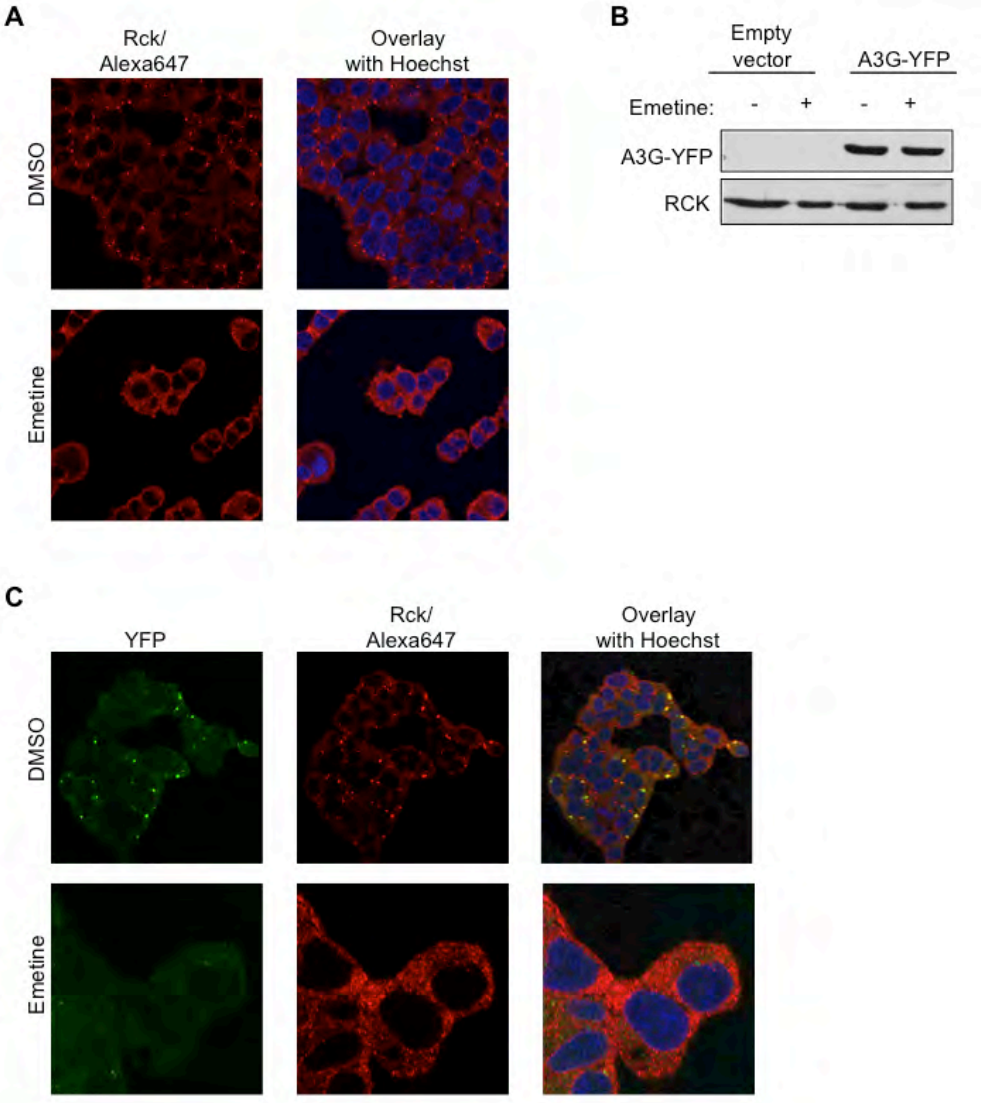
A
Rck/
Alexa647
Overlay
with Hoechst
DMSO
Emetine
B
Empty
vector
A3G-YFP
Emetine:
- + - +
A3G-YFP
RCK
C
YFP
Rck/
Alexa647
Overlay
with Hoechst
DMSO
Emetine

Figure 3.3 **APOBEC3G is a dynamic component of processing bodies.** (A) Emetine treatment (40 μg/mL, 2 hr incubation) disperses processing bodies in HEK293 cells, as seen by cytoplasmic redistribution of endogenous RCK (indirect immunostaining with RCK antibody), compared to DMSO vehicle control. Nuclei were stained with Hoechst 33258 and images were merged digitally. (B) Emetine treatment does not affect protein levels of endogenous RCK or A3G-YFP. Total cell extracts from HEK293 cells transiently transfected with 0.5 μg empty vector or A3G-YFP were analyzed by immunoblot with antibodies against RCK or GFP. (C) Emetine treatment disperses processing body-localized A3G-YFP, resulting in diffuse cytoplasmic staining. A3G-YFP was detected by direct YFP fluorescence while RCK was detected as above.

aggregates. These results suggest that with our current overexpression conditions, APOBEC3G is a dynamic component of processing bodies that disperses into the cytoplasm when protein synthesis is halted. These results are also in agreement with previously published observations from our group using cycloheximide as a translation inhibitor (Wichroski et al. 2006). Our data suggests that APOBEC3G localization in P bodies is RNA-dependent, since emetine and cycloheximide inhibit translation elongation by stabilizing polysomes and blocking mRNA recruitment into P bodies (Kedersha et al. 2005). Figure 3.3B shows that emetine treatment does not change total levels of RCK or A3G-YFP.

2. Point mutations in APOBEC3G cytidine deaminase motif 1 and some residues on linker region 1 results in lower protein expression but still exhibit P body localization

APOBEC3G contains two cytidine deaminase motifs (CD1, CD2, see Figure 3.4A) and 2 linker regions (LR1, LR2). Both cytidine deaminase motifs contain the characteristic catalytic domain but only CD2 is enzymatically active. Mutations in the CD1 residues has been reported to decrease virion packaging and modestly affect protein stability (see Table 1) (Newman et al. 2005; Navarro et al. 2005) but antiviral and deaminase activities remain intact (Shindo et al. 2003; Navarro et al. 2005; Newman et al. 2005). As for CD2 mutant E259Q, the deaminase activity is removed (Newman et al. 2005; Navarro et al. 2005) but reports on antiviral activity are conflicting. Studies with tagged recombinant proteins showed that E259Q partially lost its antiviral activity

Figure 3.4

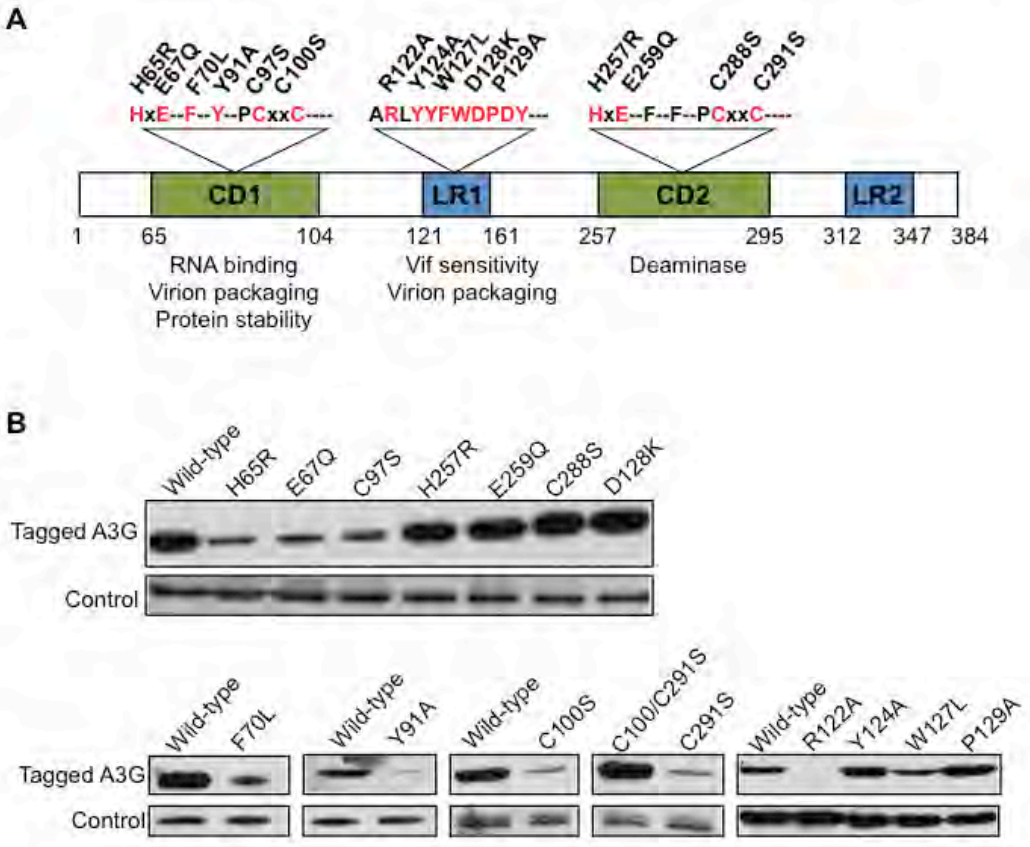
A
H65R
E67Q
F70L
Y91A
C97S
C100S
HxE--F--Y--PCxxC----
R122A
Y124A
W127L
D128K
P129A
ARLYYFWDPDY---
H257R
E259Q
C288S
C291S
HxE--F--F--PCxxC----
CD1
LR1
CD2
LR2
1
65
104
121
161
257
295
312
347
384
RNA binding
Virion packaging
Protein stability
Vif sensitivity
Virion packaging
Deaminase
B
Wild-type
H65R
E67Q
C97S
H257R
E259Q
C288S
D128K
Tagged A3G
Control
Wild-type
F70L
Wild-type
Y91A
Wild-type
C100S
C100/C291S
C291S
Wild-type
R122A
Y124A
W127L
P129A
Tagged A3G
Control

Figure 3.4 **Analysis of APOBEC3G point mutants.** (A) Schematic diagram of APOBEC3G cytidine deaminase (CD) motifs and linker regions (LR), with corresponding functions and relevant residues. (B) YFP and HA-tagged point mutants of APOBEC3G were constructed for this study. Shown here are relative protein expression levels of tagged APOBEC3G mutants (HA-tagged: F70L, Y91A; YFP-tagged for the rest) compared to wild-type from total cell extracts of transiently transfected 293T cells.

Table 3.1

	Protein level	Antiviral activity	Virion packaging	Vif sensitive	Deaminase activity	Comments
H65R	+*,e, ++b	+a, ++b	+b,e	**Yes***	++b	
E67Q	+*; ++b, ++e (E67A)	+a; +++b, +++e (E67A)	+++b ++e(E67A)	**Yes***	++b, +++e (E67A)	
F70L	+*, ++a	0a	0e	**?**	**?**	
Y91A	+*, ++a	0a	0e	**?**	**?**	
C97S	+*,a	+a, ++b	0e, +++b	**Yes***	++b	
C100S	+a	+a, ++b	++d,e, +++b	**?**	++	
R122A	+*,d, ++a	0d	0d	**No**d	+++d	
Y124A	+++*a,d	+	+	**Yes**d	+++d	
W127L	++*,d	0d	+d	**No**d	+++d (W127A)	**W127A Vif sensitive**
D128K	+++*,d	+++d	+++d	**No**d	**?**	**Also antiviral against wild-type HIV-1 (Vif+)**
P129A	+++*,d	++d	**?**	**No**d	**?**	**Also antiviral against wild-type HIV-1 (Vif+)**
H257R	+++*b, +c	++b	+++b	**Yes***	0b	
E259Q	+++*,b,e, ++c	+++b, 0c, ++e	+++b,e	**Yes***	0b,e	**Tag on protein may interfere**
C288S	+++*,b	+++b	+++b	**Yes***	+b	
C291S	+++*,b	+++b; 0c	+++b,d	**?**	+b	

Like wild-type APOBEC3G: +++
Slightly decreased: ++
Significantly decreased: +
No activity (<10%): 0
No data available: ?

[a]Zhang KL, Mangeat B, Ortiz M, Zoete V, Trono D, Telenti A, Michielin O. PLoS One. 2007 Apr 18;(4):e378.
[b]Newman EN, Holmes RK, Craig HM, Klein KC, Lingappa JR, Malim MH, Sheehy AM. Curr Biol. 2005 Jan 26;15(2):166-70.
[c]Shindo K, Takaori-Kondo A, Kobayashi M, Abudu A, Fukunaga K, Uchiyama T. J Biol Chem. 2003 Nov 7;278(45):44412-6. Epub 2003 Sep 11.
[d]Huthoff H, Malim MH. J Virol. 2007 Apr;81(8):3807-15. Epub 2007 Jan 31.
[e]Navarro F, Bollman B, Chen H, König R, Yu Q, Chiles K, Landau NR. Virology. 2005 Mar 15;333(2):374-86.
*Our unpublished data

(Shindo et al. 2003; Navarro et al. 2005); however, E. Newman et al., while working with untagged proteins, showed that E259Q still retains its antiviral activity, demonstrating that the deaminase activity is separate from its anti-HIV-1 properties (Newman et al. 2005). The presence of the tag in recombinant proteins may therefore be interfering with the activity being measured (Newman et al. 2005).

There are also conserved aromatic residues (F70, Y91 in CD1; F262, F282 in CD2) in both motifs, which were shown to be required for RNA binding in APOBEC1 (Navaratnam et al. 1995).

LR1 contains residues which determine Vif sensitivity and virion packaging (Huthoff and Malim 2007). D128 has been identified as the residue responsible for determining species-specific susceptibility to Vif (Janini et al. 2001; Mariani et al. 2003; Pace et al. 2006; Mangeat et al. 2004; Bogerd et al. 2004; Schröfelbauer et al. 2004). When D128 is mutated to lysine, it is incorporated into HIV-1 virions despite the presence of Vif. Other important residues in LR1 (see Table 1) include R122 (mutant defective in virion packaging while deaminase activity is intact; low-expressing), Y124 (phenotype similar to R122, except expression level is like wild-type), W127 (leucine mutant is Vif-resistant), and P129 (mutant phenotype same as D128K).

To determine whether P body localization is linked to any of the functional motifs, we mutated relevant residues to inactivate specific functions of the APOBEC3G protein (Figure 3.4A, in red). Figure 3.4B shows a comparison of the protein expression among these tagged mutants relative to wild-type protein. We observed that all mutations in CD1 and some in LR1 (specifically: H65R, E67Q, C97S, C100S, F70L, Y91A,

R122A, and W127L) resulted in lower protein expression, suggesting that these residues contribute to protein stability (Figure 3.4B).

To confirm this, we determined the mRNA abundance of representative low-expressing mutants (E67Q, W127L) and compared them to the mRNA levels of wild-type APOBEC3G and high-expressing mutants Y124A and E259Q by quantitative PCR. As expected, the mRNA levels of the low-expressing mutants were similar to wild-type and high-expressing mutants (Figure 3.5A).

To take a snapshot of newly-synthesized low-expressing mutant proteins, we performed metabolic labeling on tagged E67Q. Synchronized 293T cells previously transfected with either wild-type APOBEC3G (A3G-HA) or mutant E67Q (E67Q-HA) were pulsed with S^{35}-labeled methionine. Cell lysates were then collected at several time-points up to 30 minutes (APOBEC3G $t_{1/2}$ ~29 min, (Mehle et al. 2004b)) during the pulse process, followed by immunoprecipitation with an HA antibody. In Figure 3.5B, we show that the amount of newly-synthesized, radiolabeled mutant E67Q lags behind wild-type APOBEC3G, suggesting that the mutation in the glutamate of CD1 might be altering the stability of the newly-synthesized mutant protein in our current system.

We then asked if the low-expressing mutants are being turned over quickly by the proteasome. We addressed this, utilizing ALLN, a proteasome inhibitor, to determine whether we can rescue the low-expressing mutant proteins. Cells transiently transfected with representative low-expressing and high-expressing mutants were treated with 100 μM ALLN overnight prior to harvesting. As a positive control for protein recovery, wild-type A3G-YFP was co-transfected with or without Vif expression vector and similarly

Figure 3.5

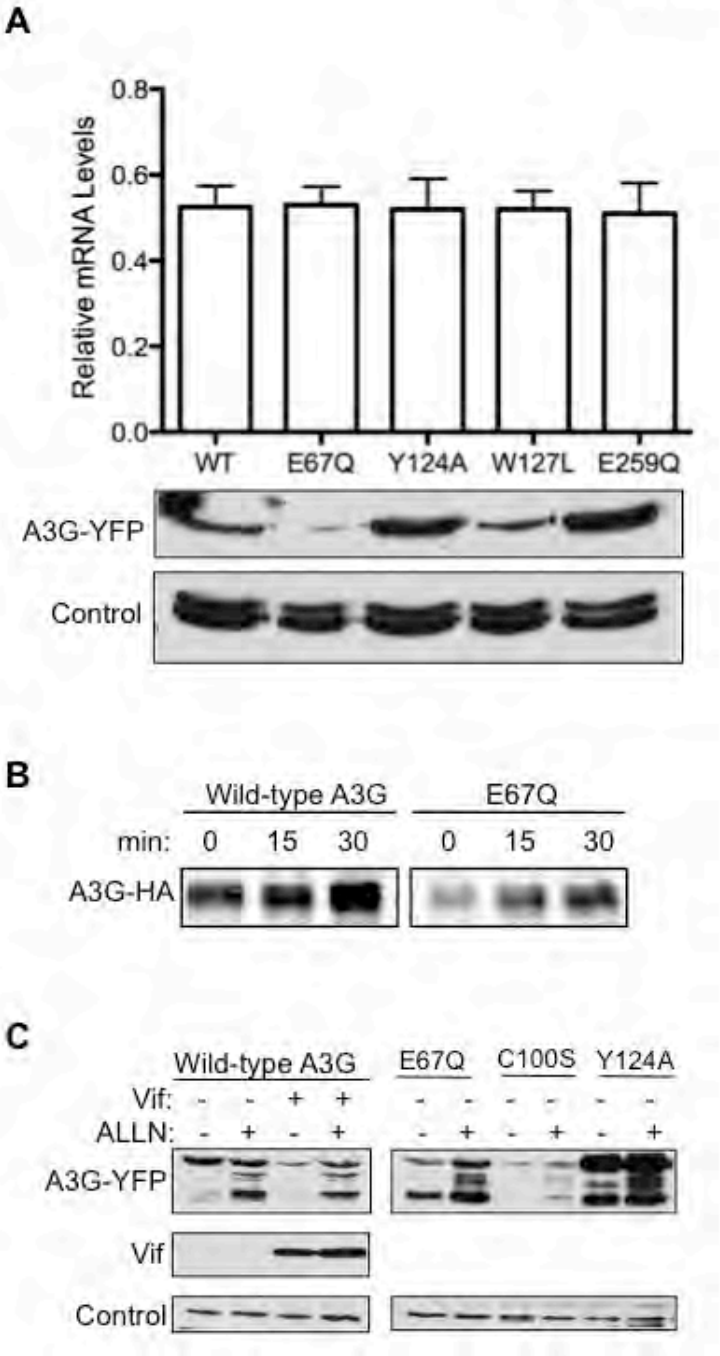
A
Relative mRNA Levels
0.8
0.6
0.4
0.2
0.0
WT
E67Q
Y124A
W127L
E259Q
A3G-YFP
Control
B
Wild-type A3G
E67Q
min:
0
15
30
0
15
30
A3G-HA
C
Wild-type A3G
E67Q
C100S
Y124A
Vif:
ALLN:
A3G-YFP
Vif
Control

Figure 3.5 **Mutations in CD1 and some LR1 residues decreases APOBEC3G protein stability.** (A) Relative mRNA and protein levels of representative APOBEC3G mutants compared to wild-type APOBEC3G, normalized to GAPDH and neomycin (vector internal control) mRNA levels (B) Synchronized 293T cells transiently transfected with either wild-type A3G-HA or E67Q-HA were pulsed with S^{35}-methionine and collected at indicated time points followed by IP with α-HA (C) Proteasome inhibition with ALLN partially recovers protein levels of low-expressing APOBEC3G mutants E67Q and C100S. Wild-type A3G-YFP recovery in the presence of Vif was used as positive control for ALLN.

treated with 100 μM ALLN. Total cell lysates analyzed by immunoblotting (Figure 3.5C, left panel) showed diminished wild-type A3G-YFP when co-expressed with Vif, but with recovery to near normal levels (i.e. without Vif) upon treatment with ALLN. There is also the appearance of bands migrating faster than full-length protein, which are presumably polyubiquitinated products. APOBEC3G low expressing mutants also show some recovery of protein levels with proteasome inhibition (Figure 3.5C, right panel) but are still not on par with the high-expressing mutant Y124A. These results indicate that the low protein expression of CD1 mutants and some LR1 mutants is partially due to faster turnover of the mutant proteins.

To characterize P body localization even under conditions of low protein expression, we propagated HEK293 cells stably expressing representative YFP-tagged mutant proteins with G418 as a selection marker. Confocal microscopy was performed using indirect immunofluorescence against endogenous RCK and direct immunofluorescence for APOBEC3G protein localization. As seen in Figure 3.6, most of the signal of wild-type A3G-YFP co-localizes with RCK in P bodies, while the rest of the signal was diffused in the cytoplasm. Representative CD2 mutants C291S-YFP and E259Q-YFP displayed a pattern of localization similar to wild-type protein. Mutants C100S and E67Q, which have mutations in CD1 on the corresponding residues, showed lower signal intensity on confocal microscopy, reflecting lower protein expression. However, some signal can still be clearly seen to colocalize with RCK in P bodies. D128K also showed wild-type subcellular localization. Y124A, which is not encapsidated

Figure 3.6

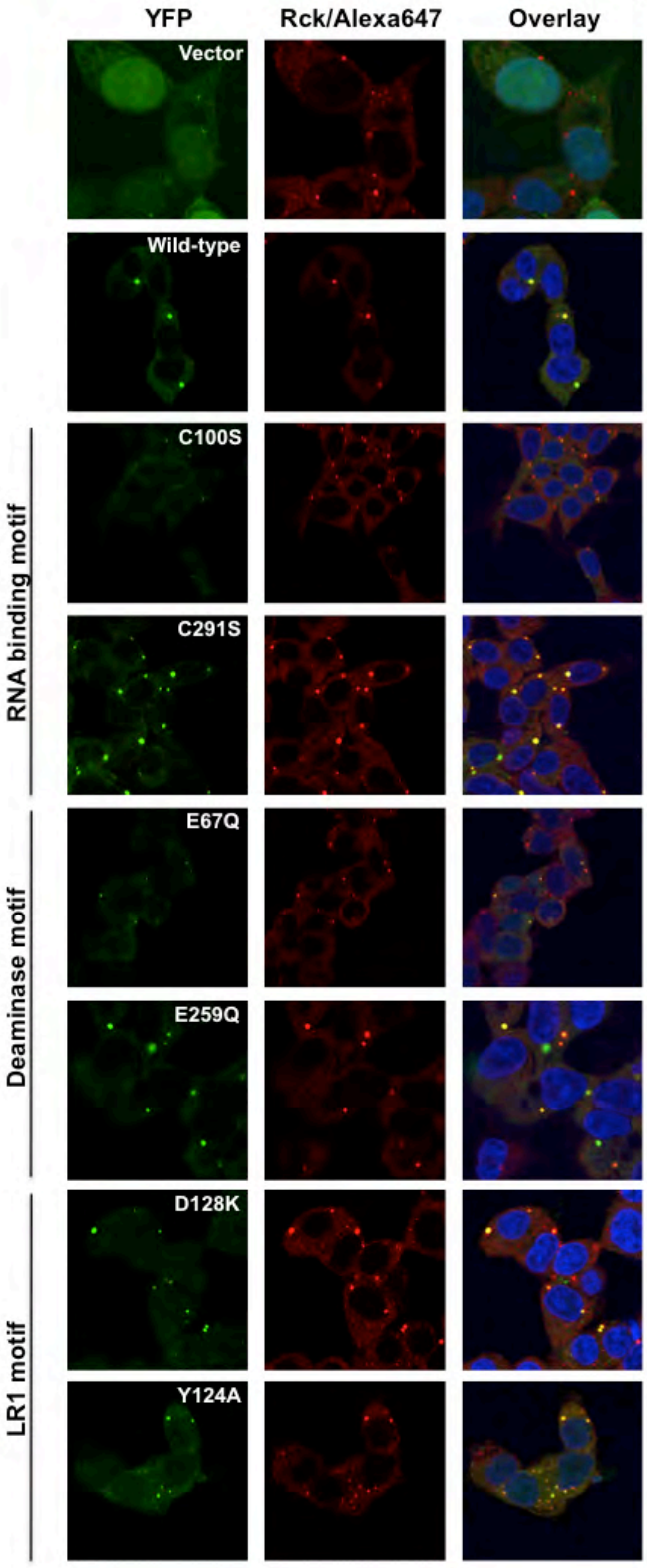
YFP
Rck/Alexa647
Overlay
Vector
Wild-type
C100S
C291S
E67Q
E259Q
D128K
Y124A
RNA binding motif
Deaminase motif
LR1 motif

Figure 3.6 **Confocal study of P body localization for APOBEC3G mutants.** HEK293 stable cell lines expressing representative YFP-tagged APOBEC3G mutants demonstrate decreased over-all signal for low-expressing mutants E67Q and C100S but localization to processing bodies is still observed.

in virions, also displayed wild-type localization. Our results suggest that localization to P bodies does not correlate to packaging of APOBEC3G in virions.

3. P body depletion does not affect virion packaging of endogenous or exogenous APOBEC3G

APOBEC3G requires encapsidation in newly-assembled ΔVif virions to restrict the next round of infection. We therefore wanted to test whether we can perturb APOBEC3G viral packaging by disruption of processing bodies in virus-producing cells. To examine this, we depleted LSM1, another P body protein (Cougot et al. 2004), in H9 cells by Amaxa nucleofection, as H9 cells are not amenable to siRNA transfection with Lipofectamine 2000. We then infected these H9 cells with fully-replicating ΔVif virus. To check whether LSM1 was depleted in H9 cells, we assayed LSM1 mRNA levels by quantitative PCR and LSM1 protein levels by immunoblotting. Transfection of H9 cells with either 300 nM or 1 μM siRNA depleted LSM1, as seen in Figure 3.7A. We decided to use 300 nM for subsequent experiments since using the lowest needed concentration of siRNA would minimize any off target effects.

H9 cells depleted of LSM1 were infected with ΔVif and the virus supernatants were collected four days post-infection (p.i.). Virions were purified from the supernatants and normalized for particle production. Viral lysates were then analyzed by immunoblotting for APOBEC3G and p24. We saw no significant difference in APOBEC3G content of virions produced after LSM1 depletion compared to si_Ctrl-treated samples (Figure 3.7B). LSM1 knockdown in H9 cells was confirmed by qPCR

Figure 3.7

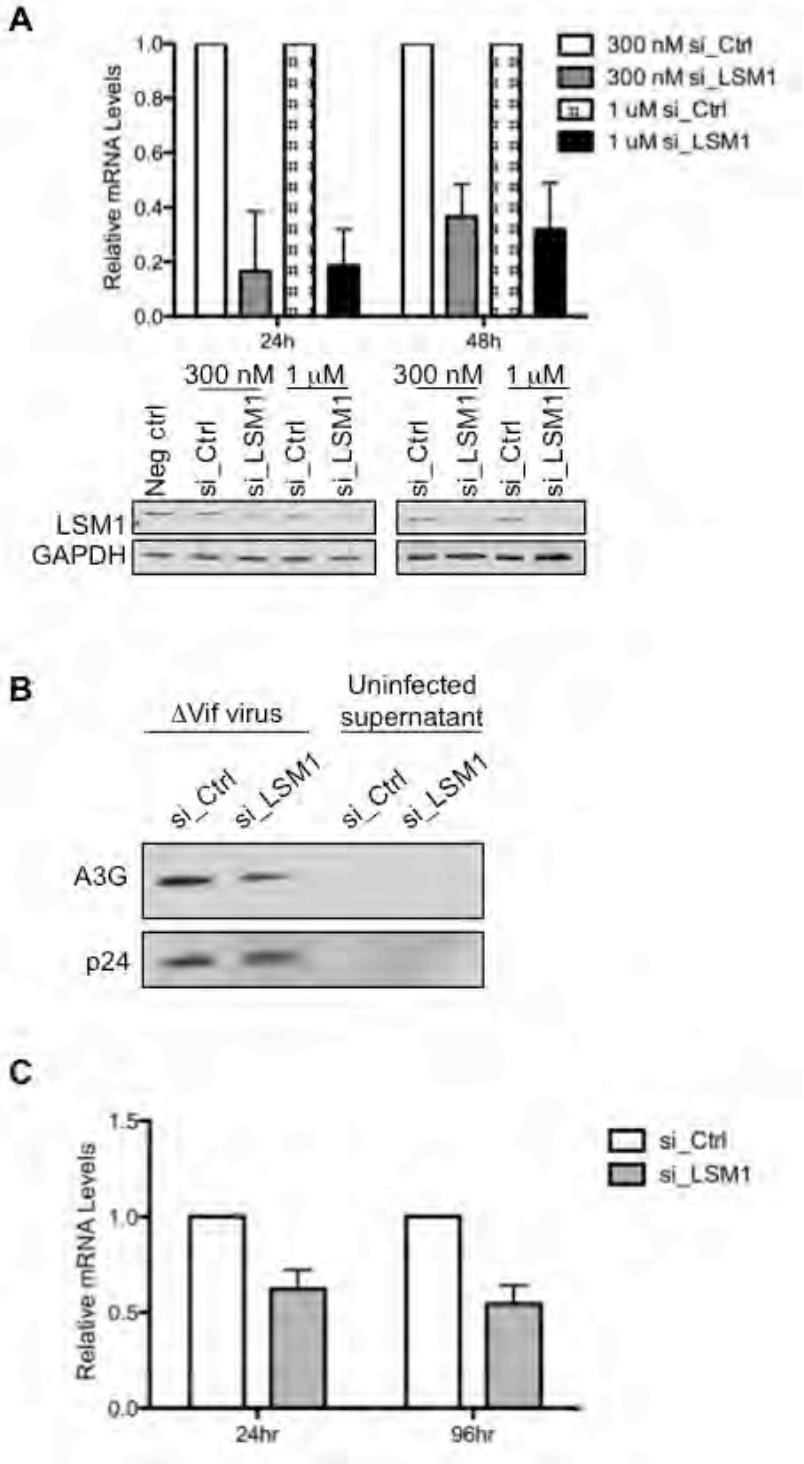
A
Relative mRNA Levels
1.0
0.8
0.6
0.4
0.2
0.0
300 nM si_Ctrl
300 nM si_LSM1
1 uM si_Ctrl
1 uM si_LSM1
24h
48h
300 nM
1 μM
300 nM
1 μM
Neg ctrl
si_Ctrl
si_LSM1
si_Ctrl
si_LSM1
si_Ctrl
si_LSM1
si_Ctrl
si_LSM1
LSM1
GAPDH
B
ΔVif virus
Uninfected supernatant
si_Ctrl
si_LSM1
si_Ctrl
si_LSM1
A3G
p24
C
Relative mRNA Levels
1.5
1.0
0.5
0.0
si_Ctrl
si_LSM1
24hr
96hr

Figure 3.7 **Depletion of LSM1 by siRNA nucleofection in H9 ΔVif virus-producing cells does not affect endogenous APOBEC3G encapsidation into virions.** (A) Optimization of siRNA conditions in nucleofected H9 cells shows depletion of LSM1, as assayed by qPCR and immunoblotting. (B) Purified virions produced from LSM1-depleted H9 cells are assayed by immunoblotting for virion-associated endogenous APOBEC3G. (C) Depletion of LSM1 in virus-producing H9 cells was assayed by qPCR.

(Figure 3.7C). These results suggest that disruption of processing bodies by LSM1 depletion does not affect packaging of endogenous APOBEC3G in ΔVif virions. However, it is possible that we do not see an effect since LSM1 depletion is not efficient using this method. Additionally, we observed that Amaxa nucleofection resulted in increased cytotoxicity for H9 cells, as seen by Trypan blue exclusion (Appendix 3.4). Therefore, we sought another method to deplete LSM1.

We tested several clones from the pGIPZ library targeting LSM1 (shLSM1) and found that shLSM1_343 resulted in the most efficient knockdown of our target protein (Figure 3.8A). We also compared spinoculation, wherein high speed centrifugation is performed during incubation with the shRNA supernatant (O'Doherty et al. 2000), as a method of transducing H9 cells, in contrast to incubation only. With our current conditions, we found no difference between the two methods (Figure 3.8C). While optimizing for MOI (multiplicity of infection) and puromycin selection conditions, we observed that increasing MOI resulted in increased GFP signal (i.e. transduction efficiency) but also increased cytotoxicity, as seen with Trypan Blue exclusion. This is probably due to the increased amount of VSV-G in the virus supernatant, which was used to pseudotype the shRNA viral-like particles (VLPs). We therefore used the lowest MOI (MOI=10) that results in successful transduction for subsequent experiments.

In brief, we produced shRNA virus-like particles (VLPs) in 293T cells and transduced H9 cells by spinoculation. After two days of selection with puromycin, we then infected the H9 cells with ΔVif virions and collected virus supernatant four days p.i. Virions were purified and analyzed as above. In Figure 3.8C, left panel, we show that

Figure 3.8

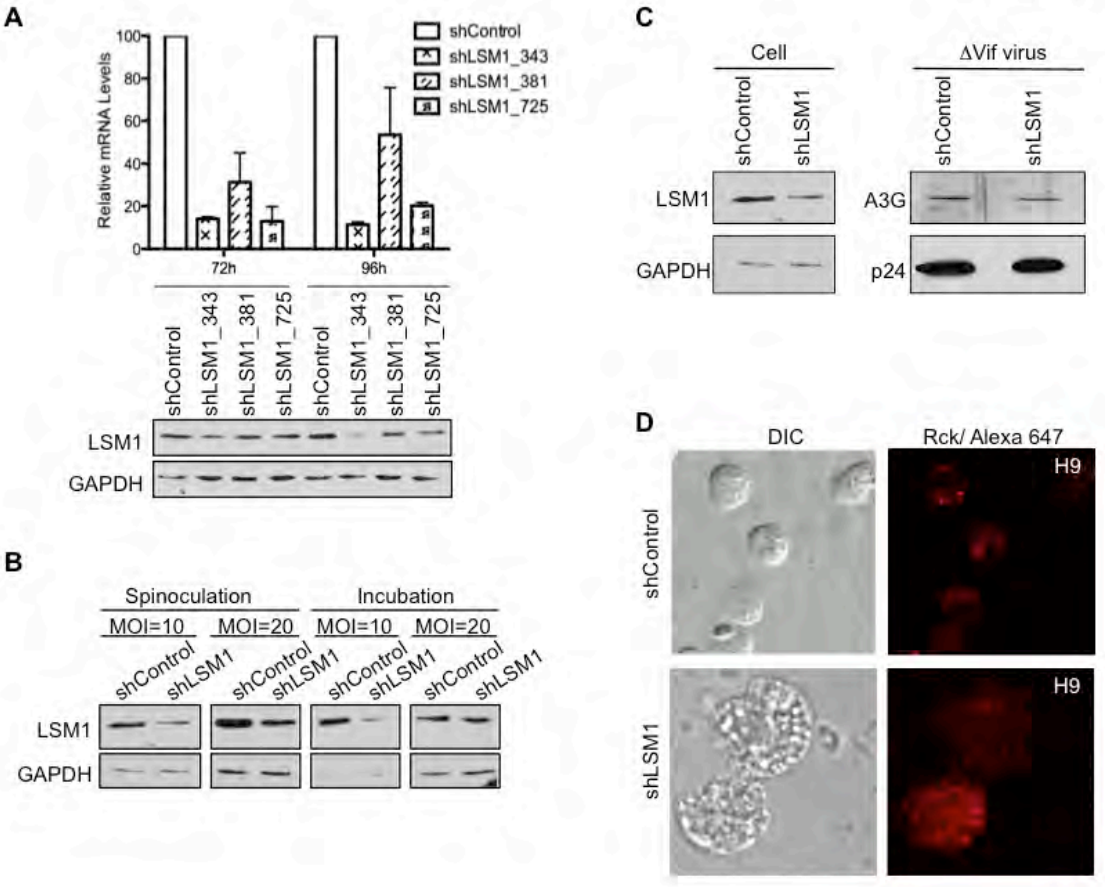
A
Relative mRNA Levels
100
80
60
40
20
0
shControl
shLSM1_343
shLSM1_381
shLSM1_725
72h
96h
shControl
shLSM1_343
shLSM1_381
shLSM1_725
shControl
shLSM1_343
shLSM1_381
shLSM1_725
LSM1
GAPDH
B
Spinoculation
Incubation
MOI=10
MOI=20
MOI=10
MOI=20
shControl
shLSM1
shControl
shLSM1
shControl
shLSM1
shControl
shLSM1
LSM1
GAPDH
C
Cell
ΔVif virus
shControl
shLSM1
shControl
shLSM1
LSM1
A3G
GAPDH
p24
D
DIC
Rck/ Alexa 647
shControl
shLSM1
H9
H9

Figure 3.8 **Depletion of LSM1 by shRNA transduction in H9 ΔVif virus-producing cells does not affect endogenous APOBEC3G encapsidation into virions.** (A) Optimization of shRNA conditions in transduced H9 cells shows depletion of LSM1, as assayed by qPCR and immunoblotting. (B) Transduction methods (spinoculation vs. incubation) and MOI conditions were compared for efficiency of transduction, as measured by immunoblotting for LSM1 and GAPDH (loading control). (C) LSM1 depletion in H9 cells were assayed by immunoblotting (total cell lysates, left panel). Purified virions produced from LSM1-depleted H9 cells were assayed for virion-associated endogenous APOBEC3G by immunoblotting. (D) Depletion of LSM1 in H9 cells results in disruption of P bodies, as seen in confocal microscopy.

LSM1 is depleted in H9 total cell lysates. Also, endogenous APOBEC3G encapsidation in ΔVif virions is unaffected despite LSM1 depletion (Figure 3.8C, right panel). In parallel, we confirmed P body disruption upon shLSM1 transduction in H9 using indirect immunostaining for RCK (Figure 3.8D, lower right panel).

Concurrently, we also investigated the effect of depleting other P body proteins on the packaging of exogenous A3G-HA into ΔVif virions. Figure 3.9A (lanes 1-3) shows the efficient knockdown of GW182, another P body marker (Cougot et al. 2004), using siRNA in 293T total cell lysates. The ΔVif virion lysates showed no difference in the packaging of A3G-HA upon depletion of GW182 (lane 7) compared to si_Ctrl (lane 10) for 293T cells transfected with 1 μg A3G-HA expression vector. Unexpectedly, when 2 μg A3G-HA expression vector is transfected, there is no A3G-HA packaged in both si_GW132 and si_Ctrl ΔVif virions. Figure 3.9B shows the disruption of P bodies upon GW182 depletion using indirect immunofluorescence in 293T cells.

We also repeated these experiments using siRNA against RCK and saw similar results (Figures 3.9C, lane 7 vs. lane 10). As a negative control for virion encapsidation, we utilized APOBEC3G Y124A, which is excluded from virions. As expected, Y124A mutant was not detected in the virion lysates (Figure 3.9C, lane 8 and lane 11).

Taken together, our results demonstrate that P bodies can be disrupted by depleting a P body resident protein (LSM1, GW182, or RCK) but dispersing P bodies does not affect encapsidation of exogenous or endogenous APOBEC3G. This suggests that the APOBEC3G fraction in P bodies is not the source of APOBEC3G included in nascent virions, since manipulating this P body fraction does not affect virion packaging

Figure 3.9

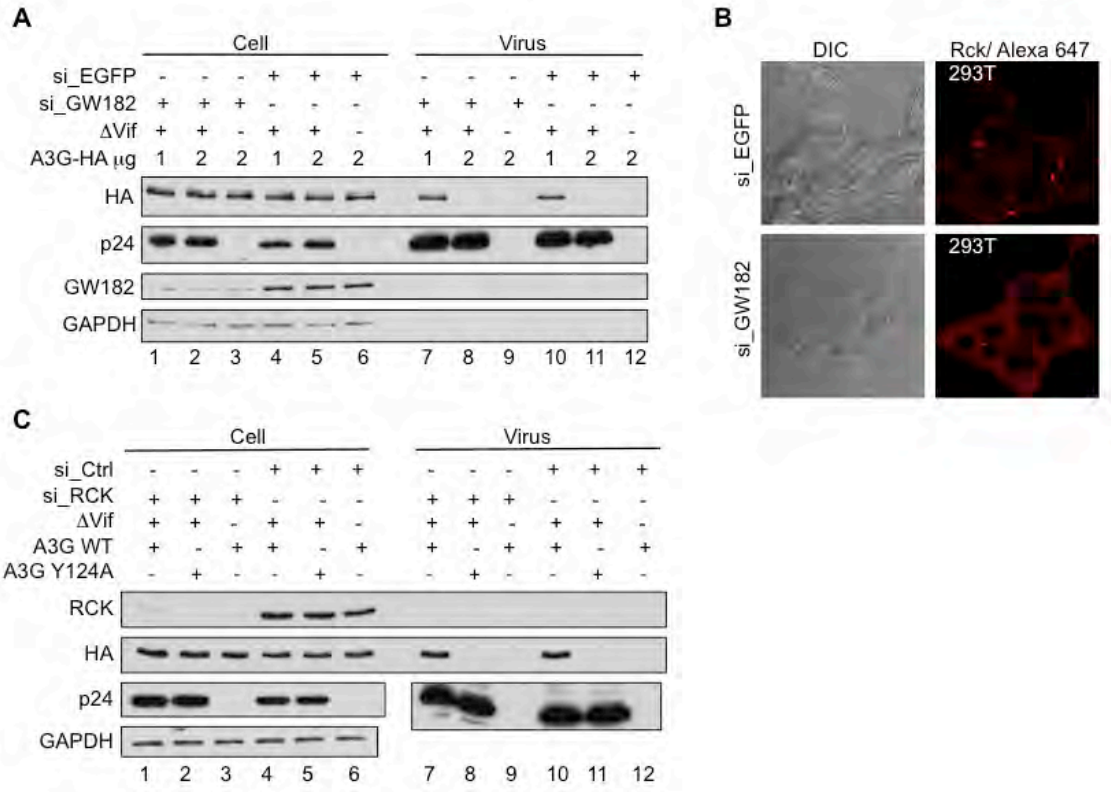
A
Cell
Virus
si_EGFP
si_GW182
ΔVif
A3G-HA μg
HA
p24
GW182
GAPDH
1 2 3 4 5 6 7 8 9 10 11 12
B
DIC
Rck/ Alexa 647
si_EGFP
si_GW182
293T
293T
C
Cell
Virus
si_Ctrl
si_RCK
ΔVif
A3G WT
A3G Y124A
RCK
HA
p24
GAPDH
1 2 3 4 5 6 7 8 9 10 11 12

Figure 3.9 **Dispersion of P bodies in virus-producing cells does not affect viral encapsidation of exogenous APOBEC3G.** (A) 293T cells were co-transfected with indicated siRNAs, proviral DNA, and APOBEC3G-HA plasmid. Total cell lysates were immunoblotted for GW182 depletion and expression of A3G-HA and p24. Purified virions were assayed for virion-associated A3G-HA. (B) Depletion of GW182 disperses P bodies in 293T cells, as seen using indirect immunofluorescence for RCK staining. (C) 293T cells were co-transfected with indicated siRNAs, proviral DNA, and APOBEC3G-HA wild-type or Y124A mutant. Total cell lysates were immunoblotted for RCK depletion and expression of A3G-HA and p24. Purified virions were assayed for virion-associated A3G-HA.

of APOBEC3G. Our results agree with V. Soros et al. (Soros et al. 2007) because they demonstrated that APOBEC3G which associates with virions is from the newly-synthesized APOBEC3G found in the LMM A3G fraction and not the HMM A3G complexes. In contrast, R. Goila-Gaur et al. (Goila-Gaur et al. 2009) have reported that new A3G in LMM and old A3G in HMM are packaged in virions at similar efficiencies.

4. Vif inhibitor RN-18 increases total APOBEC3G protein levels that localize to P bodies.

The Vif inhibitor RN-18 was identified by our group in a small molecule library screen as an enhancer of APOBEC3G expression in the presence of Vif through a pathway independent of general proteasome inhibition (Nathans et al. 2008). We were curious, therefore, whether RN-18 would affect APOBEC3G localization in processing bodies. In Figure 3.10A (left panels), A3G-YFP is expressed with or without Vif expression vector, demonstrating baseline APOBEC3G localization and expression level in P bodies in the presence and absence of Vif. As expected, co-expression of Vif obliterates APOBEC3G signal both in P bodies and in the cytoplasm (Figure 3.10A, left lowermost panel). K. Stopak and colleagues have previously shown that co-expression of Vif with APOBEC3G shortens its half-life (Stopak et al. 2003). However, cells treated with increasing amounts of RN-18 display increased APOBEC3G signal in the P body compartment above the baseline signal (Figure 3.10A, right panels) and accompanied by increased number of P bodies, suggesting that total APOBEC3G expression in the cells may be increased by the drug. To confirm this, we analyzed total cell lysates by

Figure 3.10

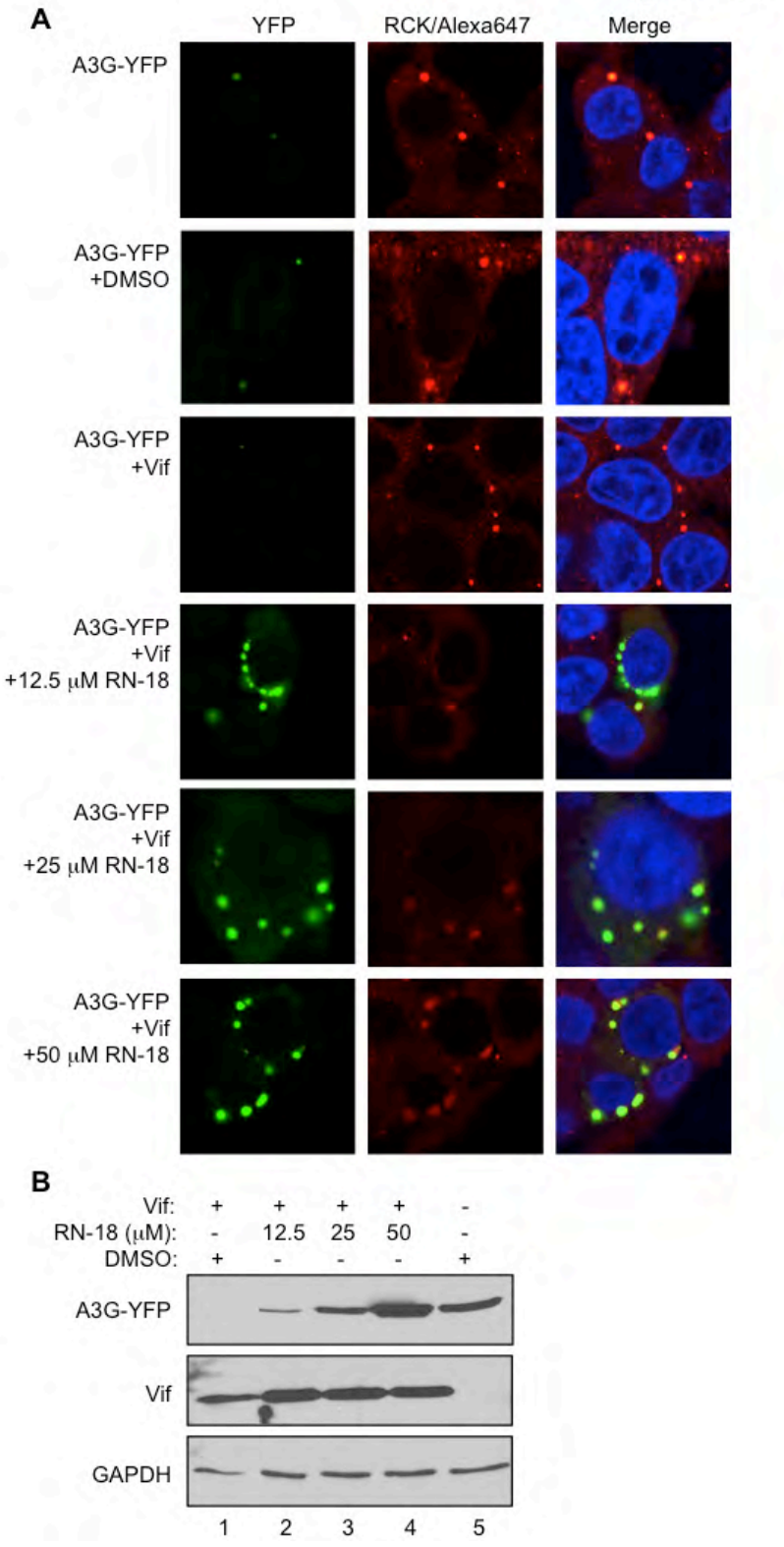
A
YFP
RCK/Alexa647
Merge
A3G-YFP
A3G-YFP +DMSO
A3G-YFP +Vif
A3G-YFP +Vif +12.5 μM RN-18
A3G-YFP +Vif +25 μM RN-18
A3G-YFP +Vif +50 μM RN-18
B
Vif: + + + + -
RN-18 (μM): - 12.5 25 50 -
DMSO: + - - - +
A3G-YFP
Vif
GAPDH
1 2 3 4 5

Figure 3.10 **RN-18 enhances APOBEC3G protein expression.** (A) HeLa cells were co-transfected with APOBEC3G-YFP, with or without a Vif-expressing construct, and were treated with either DMSO or increasing concentrations of inhibitor RN-18. Cells were then fixed and analyzed using confocal microscopy. (B) Total cell lysates were analyzed for A3G-YFP and Vif protein levels with immunoblotting.

immunoblotting. Figure 3.10B demonstrates increasing amounts of A3G-YFP protein levels upon RN-18 treatment in a dose-dependent manner, despite the presence of Vif. With the highest RN-18 dose (50 μM), A3G-YFP protein levels are even higher (Figure 3.10B, lane 4) than A3G-YFP expressed without Vif (Figure 3.10B, lane 5). These data are in agreement with previously published observations from our group, which showed APOBEC3G protein stabilization in the presence of Vif upon RN-18 treatment (Nathans et al. 2008). Taken together, these results indicate that RN-18 increases the total APOBEC3G levels in the cells, resulting in increased APOBEC3G content of different subcellular compartments, including the APOBEC3G fraction in P bodies. This increase in total APOBEC3G also explains why there is increased APOBEC3G packaged in virions when treated with RN-18.

E. Discussion

1. APOBEC3G and AIDS progression

Hypermutation in clinical samples of HIV-1 proviruses has previously been reported, showing an over-representation of G→A substitutions (Janini et al. 2001; Pace et al. 2006). However, there are conflicting reports as to whether these G→A hypermutations are APOBEC3-mediated (specifically, APOBEC3G and APOBEC3F) and whether they contribute toward slowing progression to AIDS. K. Gandhi et al. (Gandhi et al. 2008) showed that there is no correlation between A3G expression and hypermutation rate or disease state when long-term nonprogressors (LTNP) were compared to non-controllers (NC) on HAART. On the other hand, Y. Kourteva and

colleagues (Kourteva et al. 2012) have found a strong inverse correlation between HIV-1 plasma RNA and A3G-mediated hypermutation after stratifying subject samples by their "Hypermutation Index", which corrects for length of sequences and RT error rate. Also, they have brought up the issue of using unselected, HAART-naïve patients since some of them might turn out to be spontaneous controllers. Careful dichotomy of patient subjects (LNTP vs. NC on HAART) and larger study populations have been recommended.

While APOBEC3G's contribution to the clinical progression (or non-progression) of HIV-1/AIDS is still unclear, it nevertheless clearly acts as a restriction factor with several modes of action. It is of interest to study APOBEC3G biology to elucidate the pathways involved and to continue efforts in developing therapeutic targets related to it (e.g. Vif inhibitors). Also, measuring hypermutation as a footprint of APOBEC3G's activity may underestimate the antiviral activity since hypermutation and antiviral activities are separable. The amount of reverse transcripts in infected cells appear to be a stronger correlate for antiviral activity (Holmes et al. 2007; Mbisa et al. 2007).

2. An independent study of APOBEC3G and P bodies

During the preparation of this manuscript, R. D'Aquila and colleagues published a report detailing how A3G complexes affect HIV-1 virus production (Martin et al. 2011). Similar to our work, they analyzed several tagged APOBEC3G mutants (C97A, Y124A, W127L, and D128K) with respect to subcellular localization. They report that the C97A mutant has a predominantly nuclear localization at 24 hours but this reverts to wild-type APOBEC3G localization at 48 hours, which they describe as mostly diffuse

cytoplasmic signal and with punctate structures that partially co-localize with RNA granules (RCK, GW182) and late endosomes (CD63). We did not see this phenotype with our C97S mutant, although our time frame for analysis is ~18–24 hr post-transfection. Also, we transfect 0.5 μg plasmid or less while they transfected 2 μg expression vector. In their hands, treatment with a translation inhibitor (cycloheximide) had no effect on the A3G complexes, while our use of emetine disperses the punctate structures (Figure 3.3C). However, they checked the expression level of exogenous APOBEC3G and found that it is similar to endogenous APOBEC3G in CEM cells and activated CD4+ T cells. It is therefore difficult to conclude whether the phenotype they see with the C97A mutant is due to protein aggregates or not. Alternatively, it is possible that the alanine mutant of C97 has a different phenotype compared to the serine mutant.

R. D'Aquila and colleagues also report that ΔVif HIV-1 production is decreased in the presence of A3G complexes while RCK depletion, which disperses the A3G complexes, results in increased HIV-1 production. This is similar to what we previously observed (Appendix 3.5, (Nathans et al. 2009)). However, they do not see any increase in virus production for wild-type (Vif+) HIV-1.

3. Small molecules enhance APOBEC3G protein expression

Our group has previously described the effect of Vif inhibitor RN18 on APOBEC3G levels: RN18 rescues APOBEC3G protein levels in a Vif-dependent manner (Nathans et al. 2008). In this study, RN-18 increases APOBEC3G levels beyond baseline levels (i.e. without Vif, Figure 3.10B), with increased signal in P body-associated

APOBEC3G by confocal microscopy (Figure 3.10A). It is possible that Vif may be recruiting APOBEC3G into HMM/PB complexes (Goila-Gaur et al. 2009). Alternatively, RN-18 may be increasing the total amount of APOBEC3G in all the subpopulations in the cell, either by stabilizing APOBEC3G in complex with Vif or by increasing APOBEC3G translation. As a result, more APOBEC3G is packaged into virions, resulting in less infectious virus despite the presence of Vif (Nathans et al. 2008).

An independent group has reported another anti-HIV drug called SN-2, that also increases APOBEC3G levels above baseline despite the presence of Vif (Ejima et al. 2011). The authors demonstrated an increase in APOBEC3G protein levels assayed by western blot after drug treatment (Ejima et al. 2011). Both SN-2 and RN18 have similar scaffolds. It would be interesting to find out if confocal data using SN-2 would be similar to our results, as these two drugs may have similar mechanisms in counter-acting Vif.

4. Proposed model for APOBEC3G compartments in the cell

Our data support a model (Figure 3.11) wherein APOBEC3G distributes into several compartments in the cell. Newly-translated APOBEC3G is found in LMM A3G complexes and these are recruited into HMM A3G complexes such as P bodies. Activation of cells results in a shift from LMM A3G complexes into HMM A3G complexes. This would explain why APOBEC3G in P bodies is seen more clearly in activated CD4+ T cells compared to unstimulated cells (see Appendix 3.5). Interestingly, Rose et al. (Rose et al. 2004) have reported that activating cells with phorbol myristate acetate results in increased transcription and translation of APOBEC3G in H9 cells. The

Figure 3.11

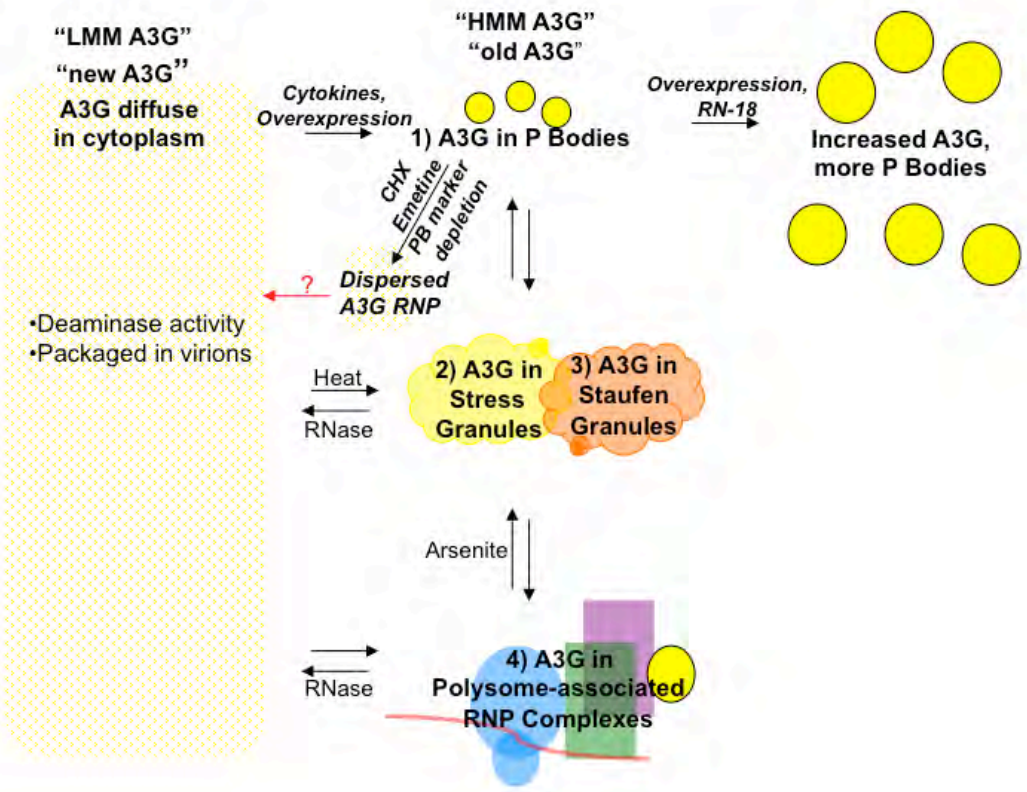
"LMM A3G"
"new A3G"
A3G diffuse
in cytoplasm
Cytokines,
Overexpression
"HMM A3G"
"old A3G"
1) A3G in P Bodies
Overexpression,
RN-18
Increased A3G,
more P Bodies
CHX
Emetine
PB marker
depletion
?
Dispersed
A3G RNP
•Deaminase activity
•Packaged in virions
Heat
RNase
2) A3G in
Stress
Granules
3) A3G in
Staufen
Granules
Arsenite
RNase
4) A3G in
Polysome-associated
RNP Complexes

Figure 3.11 **Proposed model for APOBEC3G compartments in the cell.** Newly-synthesized APOBEC3G proteins are found in low-molecular mass (LMM) complexes, which are localized diffusely throughout the cytoplasm. APOBEC3G that associates with assembling virions presumably come from this population. Within 30 minutes, these APOBEC3G proteins are recruited into high-molecular mass (HMM) ribonucleoprotein (RNP) complexes, which may be processing bodies, stress granules, and/or polysome-associated RNP complexes, possibly to sequester and inactivate the APOBEC3G deaminase. RNase-treatment converts these HMM RNP complexes into LMM complexes, with APOBEC3G recovering its deaminase activity. On the other hand, depletion of P body components apparently disrupts these HMM RNP, as seen by its dispersal in confocal microscopy, but these dispersed HMM RNP complexes may still be distinct from the LMM complexes, since encapsidation of APOBEC3G into virions is unaffected. Overexpression of APOBEC3G or stabilization of APOBEC3G protein (ex. with RN-18) results in increased total APOBEC3G levels, including APOBEC3G found in P bodies.

shift into HMM may therefore be a reflection of increased total amounts of APOBEC3G, either by upregulating transcription and translation or by adding a drug like RN-18, which may slow down the turn-over of the protein. Also, similar to APOBEC1 (Wedekind et al. 2003), moving APOBEC3G to HMM complexes may possibly be a mechanism to sequester and inactivate APOBEC3G. The HMM can be converted to LMM by RNase treatment, which restores deaminase activity (Chiu et al. 2005). The HMM may also be disassembled by utilizing translation inhibitors (emetine, cycloheximide) or by depleting P body proteins, although loss of the structural P bodies does not seem to shift the HMM A3G into the LMM fraction, since APOBEC3G packaging is not affected. It is possible that the HMM A3G complexes are simply dispersed in the cytoplasm but are still in sub-microscopic ribonucleoprotein complexes that are distinct from the LMM fraction. Further experiments need to done to address this possibility.

Appendix for Chapter III

Appendix 3.1

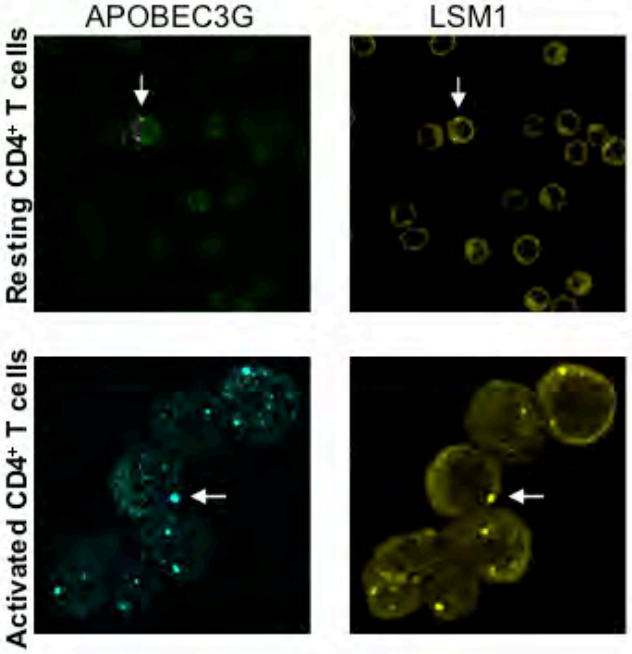

Appendix 3.1 **Endogenous APOBEC3G expression and localization in resting and activated primary CD4+ T cells.** Resting primary CD4+T cells show relative low APOBEC3G expression, with less than 10% of cells showing punctate spots that co-localize with LSM1 (P body marker). Upon activation, the APOBEC3G signal is increased, with almost all cells demonstrating LSM1-co-localizing spots. Primary CD4+ T cells were obtained from peripheral blood mononuclear cells. Cells were treated with Cell-Tak to promote adherence to cover slips and were fixed with 4% paraformaldehyde, followed by permeabilization prior to immunolabeling with LSM1 and APOBEC3G antibodies.

Appendix 3.2

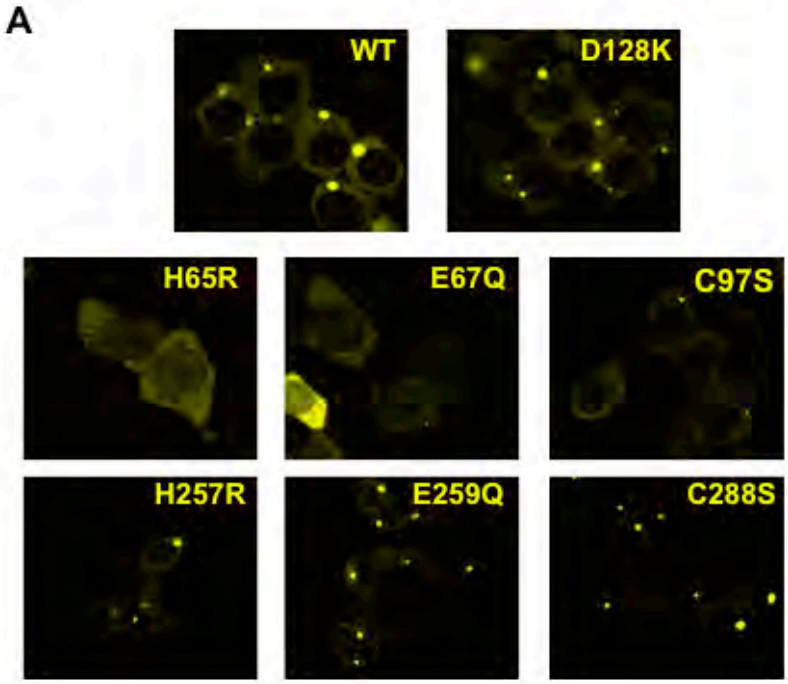

Appendix 3.2

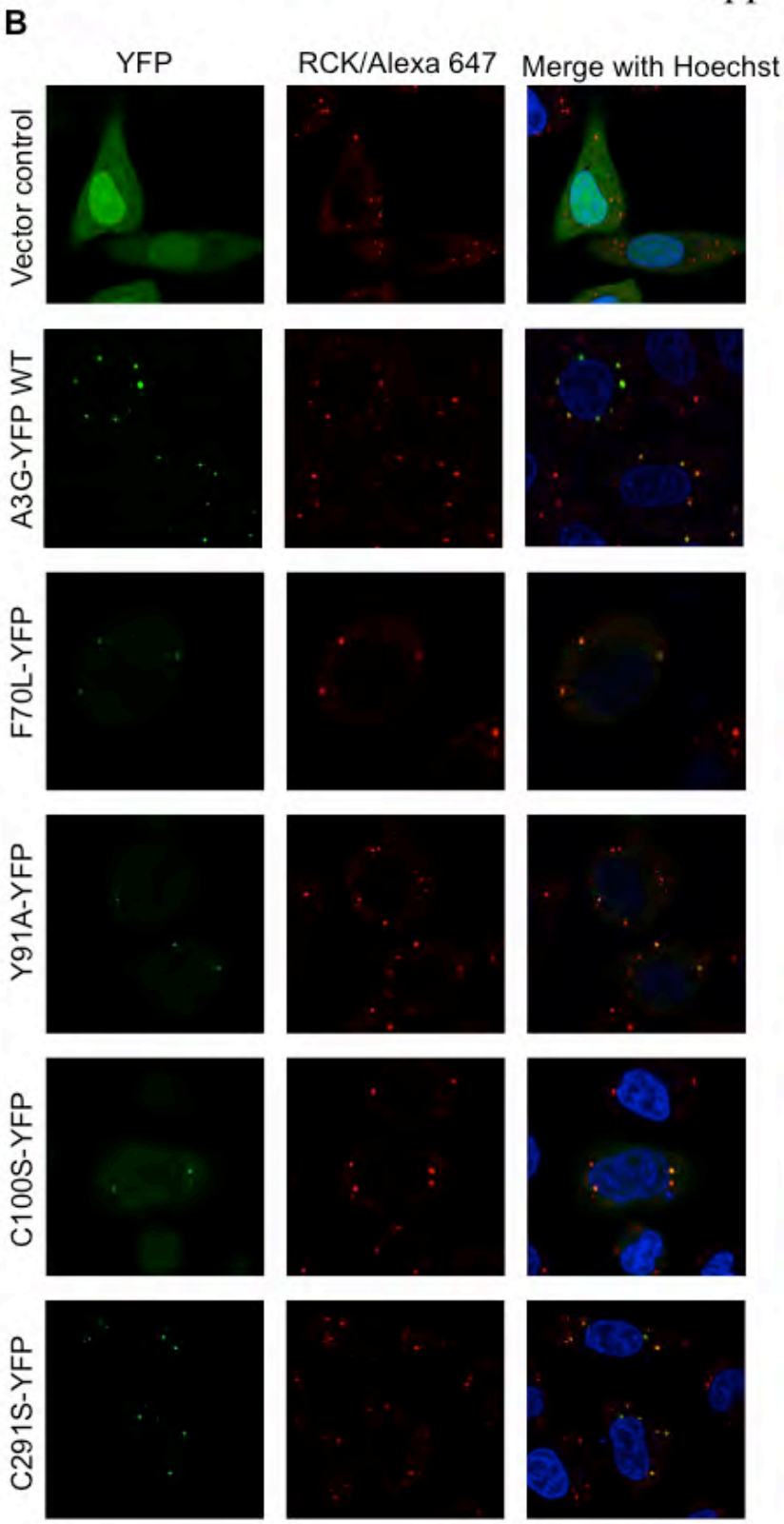
B
YFP
RCK/Alexa 647
Merge with Hoechst
Vector control
A3G-YFP WT
F70L-YFP
Y91A-YFP
C100S-YFP
C291S-YFP

Appendix 3.2

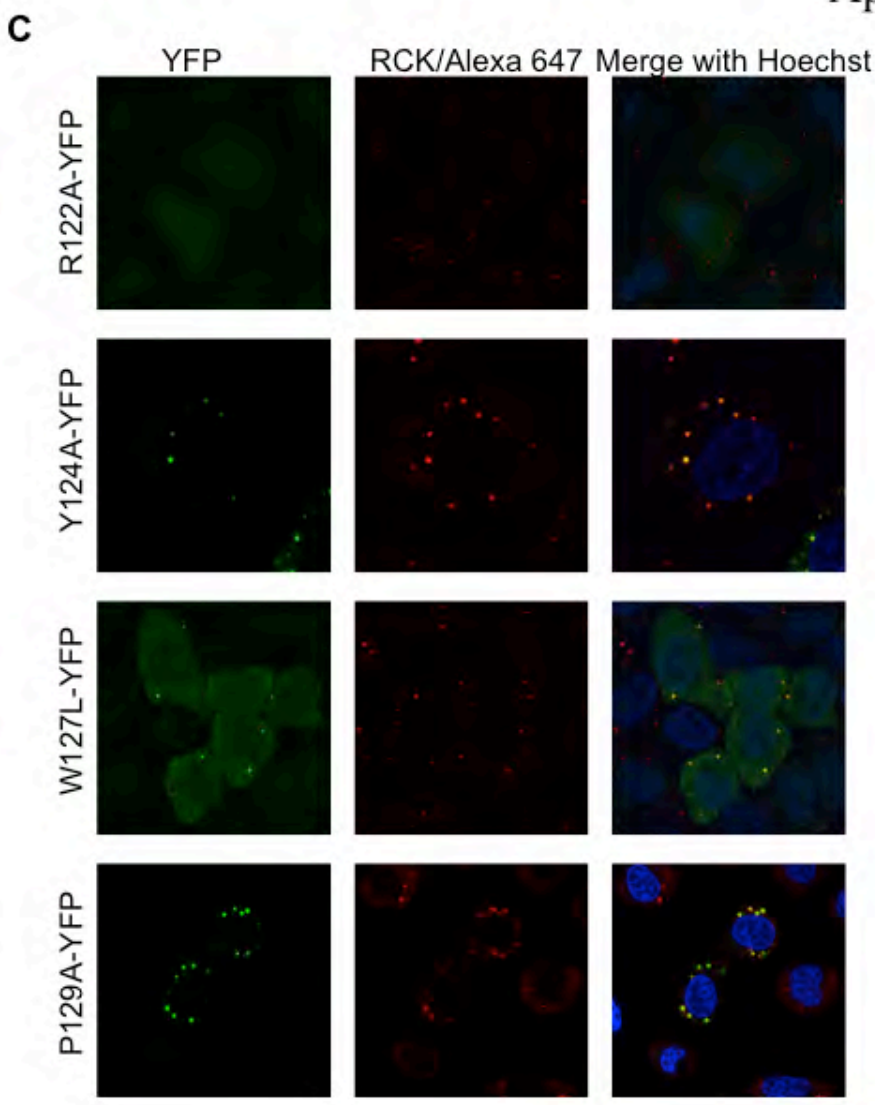
C
YFP
RCK/Alexa 647
Merge with Hoechst
R122A-YFP
Y124A-YFP
W127L-YFP
P129A-YFP

Appendix 3.2 **APOBEC3G expression and subcellular localization in transiently transfected 293T cells.** (A) To determine whether mutations in known APOBEC3G motifs disrupt its localization to P bodies, HeLa cells were transiently transfected with YFP-tagged APOBEC3G constructs. At 1 day post-transfection (p.t.), cells were fixed and analyzed by direct immunofluorescence microscopy. (B) 293T cells were transiently transfected with YFP-tagged APOBEC3G with mutations in residues important for RNA binding and analyzed by confocal microscopy after immunostaining for RCK at 1 day p.t. (C) 293T cells were transiently transfected with YFP-tagged APOBEC3G LR1 mutants (except D128K) and analyzed as in above.

Appendix 3.3

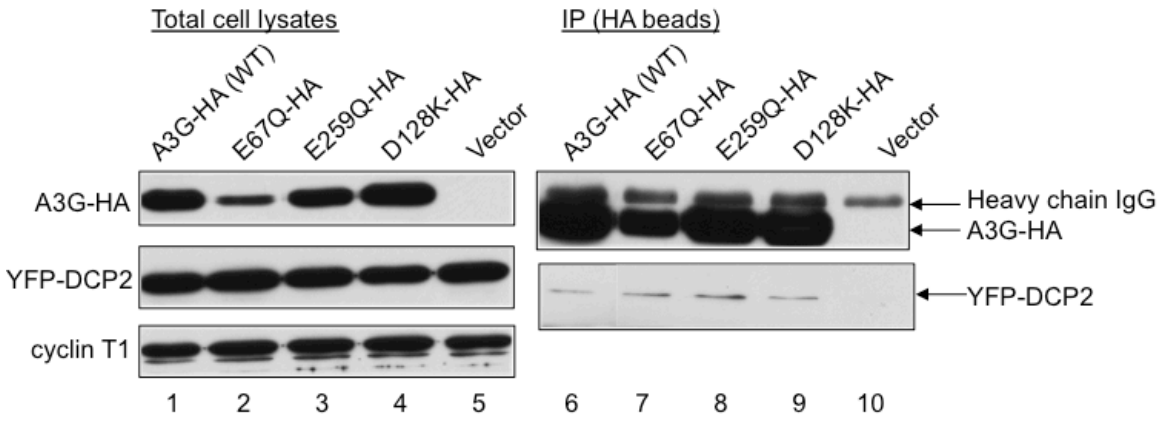
Total cell lysates
IP (HA beads)
A3G-HA (WT)
E67Q-HA
E259Q-HA
D128K-HA
Vector
A3G-HA
YFP-DCP2
cyclin T1
Heavy chain IgG
A3G-HA
YFP-DCP2
1 2 3 4 5 6 7 8 9 10

Appendix 3.3 **P body protein DCP2 interacts with APOBEC3G wild-type and mutant proteins.** To determine whether APOBEC3G mutations abrogate interactions with P body components, 293T cells were co-transfected with YFP-DCP2 (a P body protein) and representative HA-tagged APOBEC3G constructs. Total cell lysates were immunoprecipitated with α-HA and analyzed by immunoblotting.

Appendix 3.4

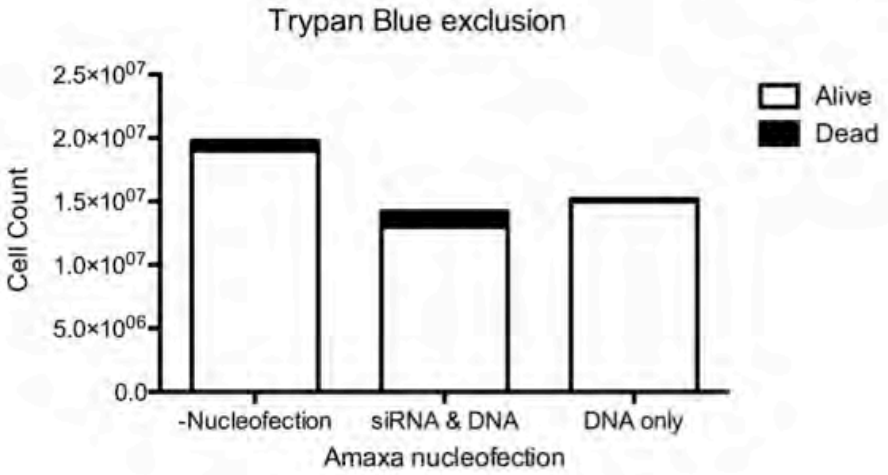
Trypan Blue exclusion
Alive
Dead
Cell Count
2.5×10^07
2.0×10^07
1.5×10^07
1.0×10^07
5.0×10^06
0.0
-Nucleofection
siRNA & DNA
DNA only
Amaxa nucleofection

Appendix 3.4 **H9 cell viability after Amaxa nucleofection.** To determine whether Amaxa nucleofection conditions were cytotoxic, H9 cells were counted using the Trypan Blue exclusion method.

Appendix 3.5

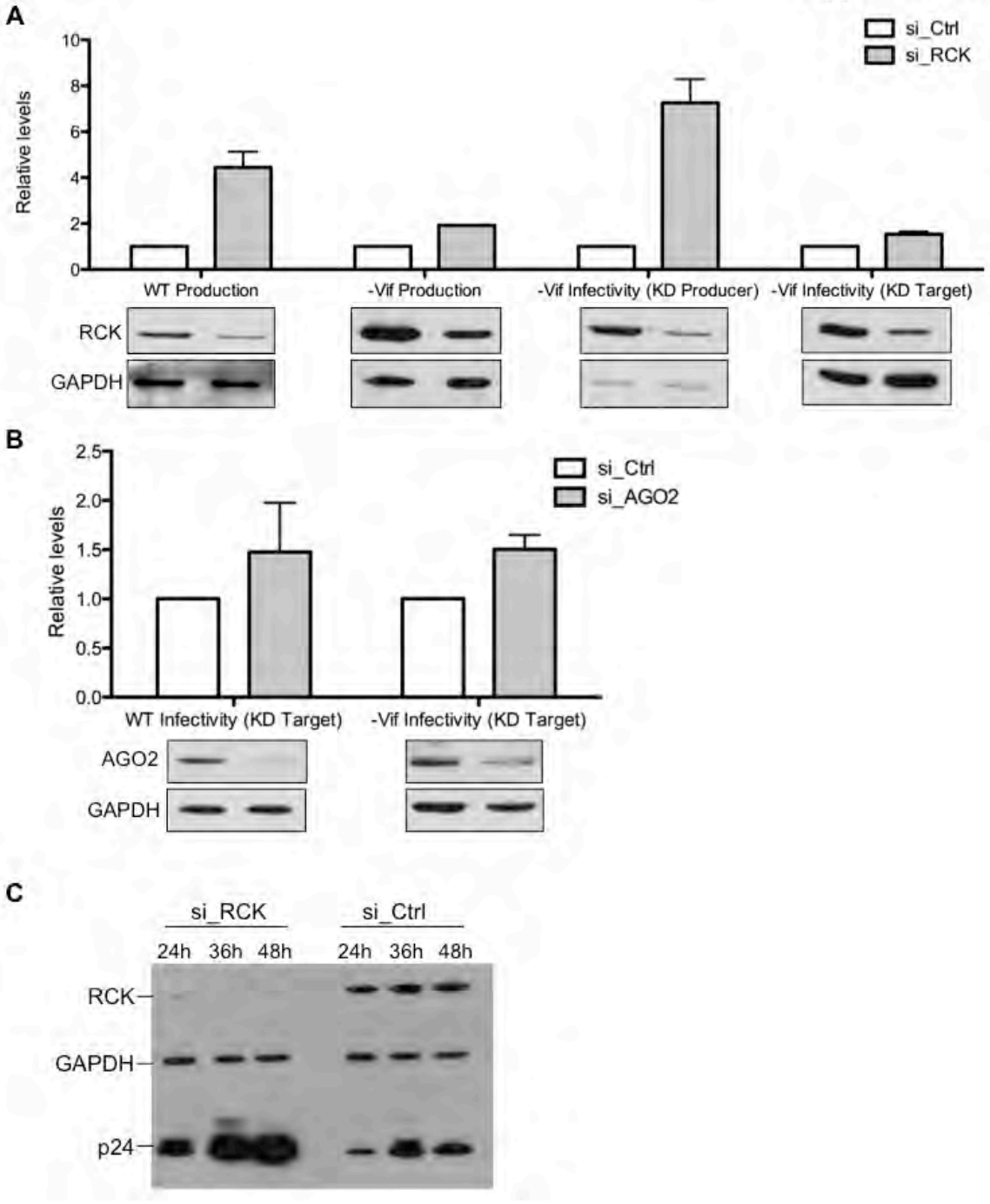
A
si_Ctrl
si_RCK
Relative levels
10
8
6
4
2
0
WT Production
-Vif Production
-Vif Infectivity (KD Producer)
-Vif Infectivity (KD Target)
RCK
GAPDH
B
si_Ctrl
si_AGO2
Relative levels
2.5
2.0
1.5
1.0
0.5
0.0
WT Infectivity (KD Target)
-Vif Infectivity (KD Target)
AGO2
GAPDH
C
si_RCK
si_Ctrl
24h 36h 48h
24h 36h 48h
RCK
GAPDH
p24

Appendix 3.5 **Effect of depletion of P body components on HIV-1 production and single cycle infectivity.** (A) To determine whether P bodies play a role in the HIV-1 life cycle, RCK (a P body marker) was depleted by siRNA transfection in either ΔVif virus-producing (KD Producer) or virus-infected (KD Target) 293T cells and assayed for single cycle infectivity, as seen in the right panels. Target cells were transfected by siRNA one day prior to infection. Virus production of wild-type and ΔVif-producing 293T cells were also measured by 24 ELISA after depletion of RCK in virus-producing cells, as seen in the left panels. RCK depletion was assayed by immunoblotting cell lysates for RCK and GAPDH (loading control). (B) AGO2, another P body protein, was likewise depleted in 293T cells which were subsequently infected with either wild-type or ΔVif virions pseudotyped with VSV-G and single cycle infectivity was measured. (C) Total cell lysates for a time-course experiment in RCK-depleted virus-producing 293T cells were immunoblotted for RCK, p24, and GAPDH (loading control).

Appendix 3.6

A

H9 cell line	miR29a levels
HIV-1 Infected	24,409
Uninfected	19,920

B

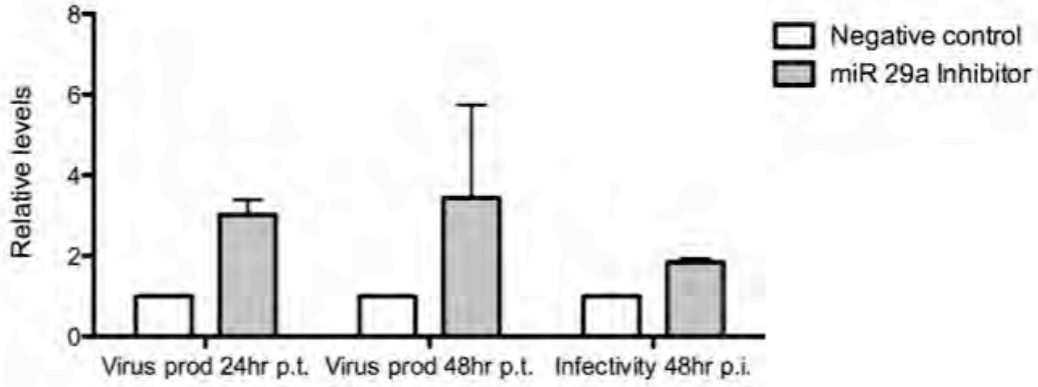

Appendix 3.6 **Effect of miR29a on HIV-1.** (A) RNA samples from mock and HIV-infected H9 cells were prepared and submitted for miRNA profiling. During analysis of the microarray data, miR29a was found to target the HIV-1 3'UTR (3'LTR) and is highly expressed in H9 cells, with increased levels upon HIV-1 infection. (B) To determine whether miR29a modulates HIV-1, we utilized 2'-O-methyl oligonucleotides complementary to miR29a to inhibit miR29a (20 nM miR29a Inhibitor) in virus-producing cells and assayed for virus production (p24 ELISA) and single cycle infectivity.

Appendix 3.7

A

Cell line	miR138 levels	Endogenous APOBEC3G expression
HeLa	38.2	No
293T	167.6	No
H9	undetectable	Yes

B

```
A3G 3'UTR          98 TCTCCAGCTGATCACAGACACCAGCAAAGCAATGCACTCCTGACCAAGTA 147
pGL3_A3G_3UTR_5 651 TCTCCAGCTGATCACAGACACCAGCAAAGCAATGCACTCCTGACCAAGTA 700
```

C

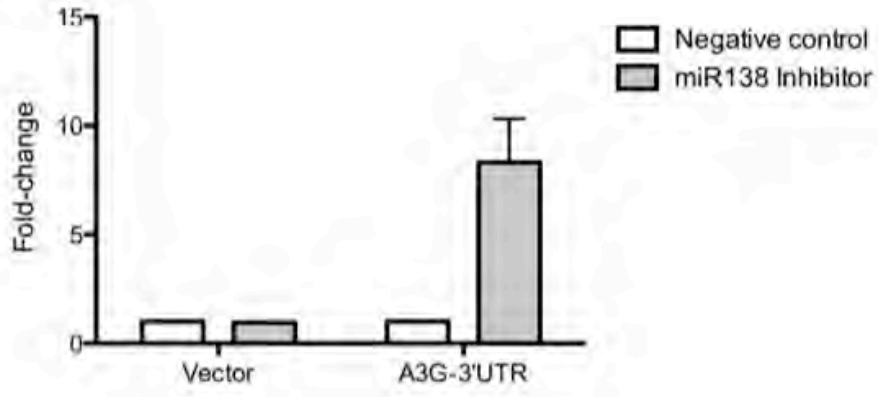

Appendix 3.7 **Effect of miR138 on APOBEC3G protein levels.** (A) H9 cells, which express APOBEC3G, have undetectable levels of miR138. On the other hand, 293T and HeLa cells, which do not express endogenous APOBEC3G, have measurable levels of miR138. (B) Target sequence of miR138 on APOBEC3G 3'UTR (A3G-3'UTR, numbering corresponds to 3'UTR only) and on cloned reporter construct pGL3-A3G-3'UTR. (C) To determine whether miR138 affects APOBEC3G protein levels, a dual luciferase assay was performed with reporter construct pGL3-A3G-3'UTR after transfection of 20 nM miR138 inhibitor.

CHAPTER IV

Cellular host factor UPF1 is required in an early, post-entry step of the HIV-1 life cycle

Mentor: Heinrich Göttlinger, M.D.

Suman Das performed Figure 4.2A and cloned the UPF1 DE636AA mutant in Appendix 4.6. Suman Das and Elena Popova collaborated on experiments shown in Figure 4.3. Anna Serquiña and Elena Popova performed the experiment presented in Figure 4.7C and Appendix 4.5D. Christian Roy and Ogooluwa Ojelabi carried out the experiment in Figure 4.7D. Anna Serquiña cloned the vectors expressing UPF1 wild-type and mutant proteins and the pNL4-3 env fs Vpr fs vector (Appendix 4.3B). All other experiments were performed by Anna Serquiña.

A. Abstract

The putative RNA helicase MOV10 is packaged into HIV-1 virions and inhibits their infectivity at the level of reverse transcription. UPF1 (also known as RENT1) is a ubiquitously expressed helicase related to MOV10 with well-documented roles in regulating nonsense-mediated decay in organisms from yeast to mammals. We have observed that UPF1, like MOV10, is packaged into HIV-1 virions in a nucleocapsid-dependent manner. Unlike MOV10, UPF1 did not inhibit the infectivity of progeny virions when overexpressed. However, the depletion of UPF1 or the overexpression of UPF1 mutants defective for ATP binding, ATP hydrolysis, or RNA binding in virus-producing cells significantly decreased the single-cycle infectivity of HIV-1 virions. In contrast, MOV10 was ineffectual in restricting HIV-1 when mutated to prevent ATP hydrolysis. To determine which step in the HIV-1 life cycle requires UPF1, we utilized a dominant-negative UPF1 mutant and assayed different steps of the life cycle. The dominant-negative UPF1 mutant did not affect HIV-1 Gag processing or the incorporation of Gag-Pol, Env, or of viral genomic RNA into virions. The same nonfunctional mutant did not affect the integrity of encapsidated genomic viral RNA or viral entry into target cells. However, virions produced in the presence of the dominant negative UPF1 mutant yielded decreased amounts of early and late reverse transcriptase products and of 2-LTR circles in infected cells. Taken together, our findings reveal an important role for UPF1 during the early phase of the HIV-1 life cycle.

B. Background and rationale for study

MOV10 was initially identified as a host protein incorporated in HIV-1 virions produced by monocyte-derived macrophages (Chertova et al. 2006). More recently, several independent groups have described MOV10 as an antiviral host protein that, when overexpressed in virus-producing cells, restricts the infectivity of virions in the target cells (Arjan-Odedra et al. 2012; Burdick et al. 2010; Furtak et al. 2010; Wang et al. 2010). However, depletion of endogenous MOV10 does not affect viral production or infectivity (Arjan-Odedra et al. 2012). Although the mechanism of its antiviral action is still unclear, it has been shown to decrease early reverse transcription and nuclear transport of the proviral DNA (Arjan-Odedra et al. 2012; Burdick et al. 2010; Furtak et al. 2010; Wang et al. 2010).

MOV10 is the human homolog of the Mov10 protein from the synonymously named mouse strain infected with the Moloney murine leukemia virus (Jaenisch et al. 1981; Mooslehner et al. 1991). Human MOV10 has been documented to localize in processing bodies (P bodies) (Meister et al. 2005; Gallois-Montbrun et al. 2007). An earlier report by T. Tuschl and colleagues showed that MOV10 is required for miR21-guided mRNA cleavage (Meister et al. 2005). However, recent work by M. Malim and colleagues demonstrated that MOV10 is not necessary for endogenous let7 miRNA-mediated mRNA repression in HeLa cells (Arjan-Odedra et al. 2012).

MOV10, like APOBEC3G, also restricts mobile genetic elements. MOV10 inhibits transposition of human endogenous retrotransposons LINE-1 and Alu, and also of mouse endogenous retrovirus IAP (Arjan-Odedra et al. 2012). Armitage, the MOV10

ortholog in Drosophila, has likewise been shown to curb endogenous mobile elements (Olivieri et al. 2010; Tomari et al. 2004).

MOV10 and UPF1, a MOV10-related protein, were identified concurrently by protein sequencing in our lab as host proteins incorporated in HIV-1 virions produced in 293T cells (H. Göttlinger, unpublished observations). Interestingly, both UPF1 and MOV10 belong to the same subfamily of SF1 helicases: SF1-Bα (B directionality is 5'→3' while type α translocation occurs on a single-stranded substrate; also designated as Upf1-like helicases (Fairman-Williams et al. 2010; Koonin 1992; Singleton et al. 2007)). Both have the characteristic 7 helicase motifs in the C-terminal half of the protein. However, a helicase function for MOV10 has not yet been reported. The stoichiometry of both in purified virions is currently not known.

A. Mouland et al. have also documented UPF1 as a host protein that is packaged into HIV-1 virions (Abrahamyan et al. 2010). Preliminary data from their group suggested that UPF1 stabilizes Gag mRNA in the cytoplasm of virus-producing cells (Ajamian et al. 2008). Increased UPF1 incorporation into virions was seen when Staufen1 (Stau1), a UPF1-interacting protein, is depleted in virus-producing cells. Notably, Stau1 depletion causes decreased viral infectivity and an increased amount of packaged viral genomic RNA (Abrahamyan et al. 2010). Overexpression of Stau1 in virus-producing cells also increases viral RNA and Stau1 packaged into virions (Mouland et al. 2000). A. Mouland and colleagues have proposed that Stau1 plays a role in viral assembly, especially in the packaging of exactly two copies of the genomic RNA (Abrahamyan et al. 2010), since more or less than two copies would result in decreased viral infectivity.

UPF1 (for up-frameshift 1; also known as RENT1, regulator of nonsense transcripts 1) was initially discovered in a genetic screen in yeast (Upf1, also called NAM7 in *S. cerevisiae*) (Leeds et al. 1992). Homologs have been described in *D. melanogaster* (Upf1), *C. elegans* (SMG2), and mammals (reviewed in (Nicholson et al. 2009)). UPF1 is an ATP-requiring 5'→ 3' helicase and unwinds both RNA and DNA in vitro (Bhattacharya et al. 2000; Czaplinski et al. 1995). In these experiments, UPF1 forms complexes with both kinds of nucleic acids in the absence of ATP and requires its ATPase activity to release the bound nucleic acid (Czaplinski et al. 1995; Weng et al. 1998). More recent work demonstrated that UPF1's ATPase activity is dependent on RNA (Chamieh et al. 2008), with ATP binding and hydrolysis inducing a conformational change in the UPF1 helicase domain, probably altering its RNA binding capacity (Cheng et al. 2007). In general, RNA-dependent ATPases can clamp onto the RNA and unwind nucleic acids, hence the term "helicase" (Chakrabarti et al. 2011). Alternatively, helicases can function as translocases, displacing proteins associated to an RNA substrate (Jankowsky et al. 2001).

UPF1 has a well-characterized role in the nonsense-mediated decay (NMD) pathway (see Figure 4.1A, also (Czaplinski et al. 1995), reviewed in (Amrani et al. 2006; Brogna and Wen 2009; Isken and Maquat 2008; Singh and Lykke-Andersen 2003)), which maintains error-free RNA in the cell and regulates genomic noise (Mendell et al. 2004). UPF1, UPF2, and UPF3 (isoforms UPF3a and UPF3b in mammalian cells) are the

Figure 4.1

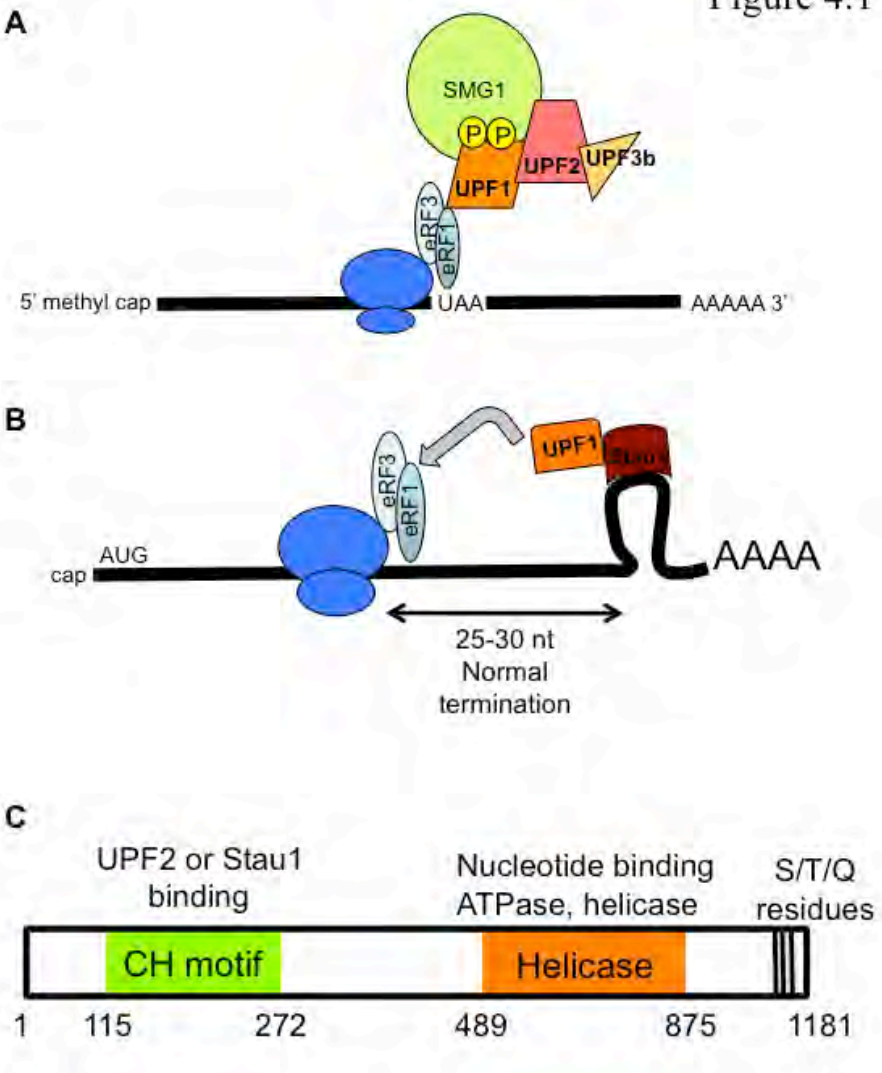
A
SMG1
P
P
UPF1
UPF2
UPF3b
eRF3
eRF1
5' methyl cap
UAA
AAAAA 3'
B
UPF1
eRF3
eRF1
AUG
cap
AAAA
25-30 nt
Normal
termination
C
UPF2 or Stau1
binding
Nucleotide binding
ATPase, helicase
S/T/Q
residues
CH motif
Helicase
1
115
272
489
875
1181

Figure 4.1 **UPF1 is a multifunctional protein.** (A) UPF1 is one of the core proteins, together with UPF2 and UPF3a/b, of the nonsense-mediated decay (NMD) pathway. (B) UPF1 is recruited by Staufen1 (Stau1) and interacts with eukaryotic release factors in the Staufen-mediated decay (SMD) pathway. (C) Schematic diagram of the UPF1 protein showing the CH domain (binding site for UPF2 and Stau1), the helicase domain, and S/T/Q residues for phosphorylation.

highly-conserved, core proteins in a surveillance complex for this NMD pathway (He et al. 1997; Serin et al. 2001). The stoichiometry of yeast Upf1, Upf2, and Upf3 per cell has been estimated as follows: ~1,600 molecules of Upf1, ~160 molecules of Upf2, ~ 80 molecules of Upf3 (Maderazo et al. 2000). As for localization within the cell, the following quantitation of immunofluorescent signal in the nucleus was performed in HeLa cells: UPF1 ~14%, UPF2 ~25%, UPF3 ~46% (Iborra et al. 2004), suggesting that UPF1 and UPF2 are mostly in the cytoplasm.

When translation termination factors eukaryotic release factor 1 (eRF1) and eRF3 encounter a stalled ribosome due to a premature stop codon (PTC), they recruit UPF1, which links the surveillance machinery to translation termination events (Czaplinski et al. 1998; Ivanov et al. 2008; Kashima et al. 2006). UPF1 bound to eRF1 and eRF3 is phosphorylated by SMG1, and this allows UPF2 binding. UPF2 is an activator of UPF1 (Chakrabarti et al. 2011), since UPF2 bound to UPF1 alters UPF1 conformation, resulting in less RNA binding (Chamieh et al. 2008). Unphosphorylated UPF1 interacts with SMG1 and eRF3, while phospho-UPF1 interacts with mRNA decay factors (Isken and Maquat 2008). The NMD pathway is further regulated by the phosphorylation and dephosphorylation cycle of UPF1, the latter step catalyzed by protein phosphatase 2A (PP2A) (Ohnishi et al. 2003).

In human cells, UPF2 and UPF3b stably interact and are required for phosphorylation of UPF1. Both are components of the exon-junction complex (EJC) (Baker and Parker 2004; Chamieh et al. 2008; Maquat 2004), which is deposited by the spliceosome 20-24 nt upstream of a splice site after an intron is removed, and recruit

UPF1 to this complex (Buchwald et al. 2010; Chamieh et al. 2008; Gehring et al. 2003; Kashima et al. 2006). The EJC, although not essential for mammalian NMD (Bühler et al. 2006), is postulated to be a modulator of this pathway (Amrani et al. 2006). The EJC provides a platform for interaction of the NMD core machinery (Le Hir et al. 2001), improves the translatability of transcripts, since translation and NMD are closely linked, and helps distinguish a nonsense stop codon from a normal stop codon. The proposed EJC model postulates that a PTC is recognized when an EJC complex is situated 50-55 nt downstream of a stop codon (Kashima et al. 2006; Le Hir et al. 2001; 2000; Maquat 2004; Shibuya et al. 2004; Sun and Maquat 2000; Tange et al. 2004). On the other hand, recognition of a PTC in the yeast NMD pathway has been described using the proposed faux 3′UTR model, wherein the stop codon is deemed abnormal because it occurs a long distance from the 3′ end, preventing the normal interaction between the terminating ribosome and the poly(A) binding protein (PABP) (Amrani et al. 2004). Instead, NMD factors associate with the terminating ribosome (Amrani et al. 2006; Brogna and Wen 2009). But UPF1's ability to sense the length of the 3'UTR is not limited to yeast cells. A study by J. Hogg and S. Goff showed UPF1-dependent sensing and degradation of mRNAs with long 3'UTRs (Hogg and Goff 2010). UPF1 increasingly associates with mRNAs containing longer 3'UTRs, especially transcripts that are NMD-sensitive (Hogg and Goff 2010). The commitment to undergo decay was found to occur independently from the UPF1-dependent sensing step (Hogg and Goff 2010). Also, insertion of retroviral sequences that promote translational read-through of stop codons decreased

UPF1 association with mRNAs, stabilizing the transcripts and uncoupling the sensing step from the initiation of decay (Hogg and Goff 2010).

After the NMD machinery identifies a stop codon as premature or aberrant, the NMD substrate is degraded by the mRNA turnover pathway (via decapping and/or deadenylation of the mRNA) or through endonucleolytic cleavage (Mühlemann and Lykke-Andersen 2010). NMD factors and substrates have been observed in P bodies (Durand et al. 2007; Sheth and Parker 2006), but there is no direct evidence that localization in these structures is a prerequisite for degradation. In fact, several groups failed to observe defects in both translation and mRNA turnover under conditions where formation of microscopically detectable P bodies was prevented (Eulalio et al. 2007; Stoecklin et al. 2006; Rehwinkel et al. 2005). NMD factors and substrates are only strongly observed in P bodies when the late steps in the NMD pathway are inhibited, such as inhibiting UPF1 ATPase activity or UPF1 dephosphorylation (Durand et al. 2007; Stoecklin et al. 2006; Stalder and Mühlemann 2009).

The UPF1 ATPase activity is essential for NMD (Bhattacharya et al. 2000; Czaplinski et al. 1995; Sun et al. 1998). The UPF1 mutant K498A, which lacks ATP binding and ATPase activity, has no NMD function (Chamieh et al. 2008). J. Lykke-Andersen and colleagues utilized this mutant to demonstrate that the ATPase-dependent function of UPF1 is also required in the disassembly of the NMD ribonucleoprotein complex after the mRNA undergoes degradation; otherwise, NMD factors accumulate in P bodies (Franks et al. 2010).

UPF1 is also engaged in the Staufen-mediated decay (SMD) pathway (see Figure 4.1B). Stau1 binds to a hairpin loop on the 3'UTR of some mRNAs and recruits UPF1 for the eventual degradation of these transcripts (Isken and Maquat 2008). SMD can be distinguished from NMD because it is EJC-independent (Kim et al. 2005; Meyer and Gavis 2005). Substrates described for SMD include PAX3 mRNA (Gong et al. 2009) and ADP-ribosylation factor 1 (Arf1) mRNA (Kim et al. 2005; 2007).

The CH motif of the UPF1 protein (see Figure 4.1C) serves as the binding site for UPF2 (Kadlec et al. 2006) and Stau1 (Gong et al. 2009), with mutually exclusive binding (see Figure 4.1C). Upon binding to UPF2, the CH domain adopts a conformation such that UPF1 switches from RNA clamping to RNA unwinding activity (Chakrabarti et al. 2011). Biochemical characterization of the UPF complex by H. Le Hir and colleagues also showed that addition of UPF2 decreases RNA binding and increases ATPase and ATP-dependent unwinding activity of UPF1. Since UPF2 mainly interfaces with the CH domain, this suggests that UPF2 binding to the CH domain activates the UPF1 helicase function (Chamieh et al. 2008). A cryo-EM study of the UPF1-UPF2-UPF3 complex suggests that UPF2 interaction sequesters the UPF1 CH domain, allowing the helicase region to remain accessible (Melero et al. 2012). The inhibitory effect of the CH domain is intramolecular, since the addition of 10-fold excess CH domain to UPF1 ΔCH has no effect (Chamieh et al. 2008).

Aside from NMD and SMD substrates, UPF1 is also involved in the degradation of a third class of mRNA. H. Kaygun and W. Marzluff have demonstrated that histone mRNA requires UPF1 for its regulated degradation upon DNA inhibition and exit from S

phase (Kaygun and Marzluff 2005). Histone mRNAs are remarkable such that they are not polyadenylated at the 3' end but rather possess a conserved stem loop structure (Dominski and Marzluff 1999). The stem loop binding protein (SBLP) binds to this RNA structure (Dominski et al. 1999) and recruits UPF1 (Kaygun and Marzluff 2005). This pathway is UPF2-independent but still requires UPF1's ATPase activity (Kaygun and Marzluff 2005). In the same study, ataxia telangiectasia and Rad3 related (ATR), a key regulator of the DNA damage checkpoint pathway, was also found to be required for histone mRNA degradation (Kaygun and Marzluff 2005). Presumably, ATR may be phosphorylating either UPF1 or SBLP to trigger the cascade of events leading to histone mRNA degradation. SMG1 requirement for UPF1 phosphorylation was not addressed in this study.

A fourth class of RNA is also impacted by UPF1. Telomere-repeat containing RNA (TERRA) is a noncoding RNA transcribed from telomeres (Azzalin et al. 2007; Schoeftner and Blasco 2008), which are DNA sequences found at the end of chromatin that progressively shorten with each cell division until they reach a critical length that signals the cells to undergo senescence. C. Azzalin and colleagues found that TERRA is negatively regulated by UPF1 and SMG1: depletion of UPF1 or SMG1 results in accumulation of TERRA at telomeres, although the half-life and total cellular levels of TERRA were unaffected (Azzalin et al. 2007). Also, depletion of UPF1 resulted in the loss of telomeric tracts (Azzalin et al. 2007). UPF2 seems to contribute minimally to this pathway (Azzalin et al. 2007). These preliminary findings suggest that UPF1 may play a role in displacing TERRA from telomeres. A newer study from R. Chawla et al.

demonstrated using chromatin immunoprecipitation experiments that a fraction of UPF1 is recruited in telomeres during S and G2/M phases in an ATR-dependent manner (Chawla et al. 2011). UPF1's ATPase function is needed for telomere stability, particularly in leading strand replication (Chawla et al. 2011). C. Azzalin and colleagues hypothesize that UPF1 helps maintain genomic stability by facilitating telomere replication and telomere length (Chawla et al. 2011).

A preliminary study by V. Narry Kim's group suggests a possible role for UPF1 in miRNA-mediated mRNA downregulation (Jin et al. 2009). UPF1 binds to RNA-induced silencing complex (RISC) proteins AGO1 and AGO2 (Jin et al. 2009). Also, UPF1 depletion decreases the binding of Hmga2 mRNA, a target of let-7 miRNA, onto RISC (Jin et al. 2009). In parallel experiments, overexpression of a UPF1 mutant lacking helicase activity increases the amount of bound Hmga2 mRNA to RISC (Jin et al. 2009), suggesting that UPF1 may play a role in the degradation of the miRNA target as well. V. Narry Kim's group have therefore proposed that, based on their data, UPF1 participates in RNA silencing by facilitating the binding of RISC to the target and by accelerating the decay of the mRNA (Jin et al. 2009).

UPF1 also plays an essential role in the cell, which is not necessarily NMD-related. UPF1 knockout mice do not survive beyond peri-implantation stage (3.5 days post-coitum) (Medghalchi et al. 2001). This is consistent with findings by C. Azzalin and J. Lingner, wherein UPF1-depleted cell lines underwent S phase arrest after one week, leading to a hypothesis that UPF1 may be playing a role during DNA replication and repair (Azzalin and Lingner 2006a). Another observation supporting this hypothesis is

that UPF1 physically interacts with the processive lagging strand DNA pol δ and the DNA dependent RNA polymerase II machinery (Carastro et al. 2002; Iborra et al. 2004; Azzalin and Lingner 2006a).

Like UPF1, UPF2 is required in embryonic development since UPF2 null embryos were lost by day 9.5 (Weischenfeldt et al. 2008). On the other hand, UPF2 conditional knockout mice have different phenotypes, depending on the tissue involved. Liver-specific UPF2 knockout in fetal mice leads to perinatal death (Thoren et al. 2010). Similarly, loss of UPF2 in adult livers of mice led to extensive liver damage (Thoren et al. 2010). However, UPF2 conditional knockout in the hematopoetic system of mice showed that differentiated cells, but not progenitor cells, tolerate UPF2 loss (Weischenfeldt et al. 2008).

UPF1 is a phosphoprotein, with three known kinases: SMG1, ATM, and ATR (Azzalin and Lingner 2006b; Brumbaugh et al. 2004; Yamashita et al.). Having different kinases might be a mechanism to regulate UPF1's varied roles in several pathways (Azzalin and Lingner 2006a). Phosphorylation sites on UPF1 are found in S/T and Q residues in the C-terminal end of the protein (see Figure 4.1C).

Given that UPF1 is an essential, multifunctional protein involved in several cellular pathways, we therefore sought to determine whether UPF1 is also required by HIV-1 in its viral life cycle. In this study, we observed that depletion of endogenous UPF1 or overexpression of nonfunctional UPF1 mutants in virus-producing cells decreases single-cycle infectivity. To characterize this UPF1 requirement by the virus, we assayed the effect of a dominant negative mutant on viral proteins and on the

incorporation of the viral genomic RNA into virions and found that these were unaffected. Lastly, we also measured the effect of the dominant negative mutant on the early steps of the life cycle, namely, viral entry, reverse transcription, and nuclear import. We found that viral entry is unaffected but reverse transcripts, and 2-LTR circles were decreased by the UPF1 dominant negative mutant. Our results, taken together, demonstrate that UPF1 is a host protein that plays an important role in an early stage of the HIV-1 life cycle.

C. Hypothesis:

UPF1 is a host factor that may be required for HIV-1 infectivity.

D. Results

1. **HIV-1 virions incorporate UPF1 and MOV10 in a nucleocapsid-dependent manner.**

We have identified UPF1, together with related protein MOV10, as a host protein packaged in HIV-1 virions by protein microsequencing (H. Göttlinger, unpublished data). To demonstrate incorporation of MOV10 into virions, we transfected 293T with HA-tagged MOV10 (HA-MOV10) together with wild-type proviral DNA (WT). The virions were purified through a sucrose cushion, and the virion lysates were resolved on an SDS-PAGE gel. As seen in Figure 4.2A (left lane), HA-MOV10 is detected in WT virions.

The viral nucleocapsid (NC) acts as the chaperone protein responsible for packaging the viral genome and other components of the viral core. To determine whether MOV10

Figure 4.2

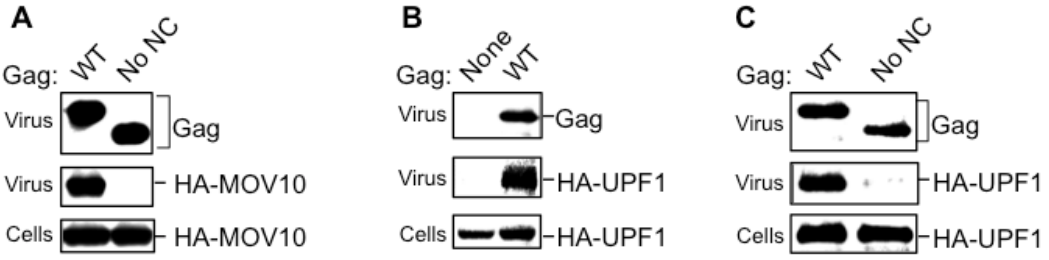
A
Gag: WT No NC
Virus
Gag
Virus
HA-MOV10
Cells
HA-MOV10
B
Gag: None WT
Virus
Gag
Virus
HA-UPF1
Cells
HA-UPF1
C
Gag: WT No NC
Virus
Gag
Virus
HA-UPF1
Cells
HA-UPF1

Figure 4.2 **HIV-1 virions encapsidate MOV10 and UPF1 in a nucleocapsid-dependent manner**. (A) 293T cells were transfected with either WT HIV-1 or HIV-1 lacking nucleocapsid (No NC) constructs plus HA-MOV10. Total cell lysates and purified virions were analyzed by Western blotting. (B) 293T cells were transfected with negative control (None) or WT HIV-1 construct (WT), together with HA-UPF1. Cell lysates and purified virions were analyzed with anti-CA serum for Gag and anti-HA antibody. (C) 293T cells were transfected with either WT HIV-1 or HIV-1 lacking nucleocapsid (No NC) constructs, and HA-UPF1. Total cell lysates and purified virions were analyzed by Western blotting as above.

requires the viral NC for incorporation into virions, we transfected a proviral construct with NC replaced by a leucine zipper (No NC) (Accola et al. 2000). Virion-like particles (VLPs) obtained from this sample did not contain detectable HA-MOV10 (Figure 4.2A, right lane), which suggests that MOV10 is dependent on NC for virion packaging. This corroborates the findings of Wang et al., wherein they show that MOV10 interacts with NC in an RNA-dependent manner using a GST pull-down experiment (Wang et al. 2010).

To confirm UPF1 incorporation into virions, we isolated virions produced in 293T cells co-transfected with HA-tagged UPF1 (HA-UPF1). Since the majority of UPF1 is in a complex with ribosomes (Atkin et al. 1995), which may co-sediment with virions through a sucrose cushion, we performed a second ultracentrifugation step utilizing an OptiPrep (60% iodixanol solution) step gradient to purify virions away from microvesicles (Dettenhofer and Yu 1999). After the sequential ultracentrifugation, we immunoblotted virion lysates for Gag and HA. Figure 4.2B shows the Gag and the HA signals for the wild-type virions and none for the negative control, indicating that UPF1 is specifically packaged into HIV-1 virions. To determine whether UPF1 requires the viral NC for incorporation into virions, we transfected 293T cells with the same proviral construct lacking NC used above. In Figure 4.2C, we show that HA-UPF1 is not incorporated into VLPs lacking NC (No NC), suggesting that UPF1 is packaged into virions in a NC-dependent manner. Therefore, both MOV10 and UPF1 are incorporated into HIV-1 virions through interactions with NC. However, it is unclear at this point if UPF1 interacts with the NC directly or in complex with RNA.

2. MOV10 and UPF1 have opposite effects on single-cycle HIV-1 infectivity.

To begin studying the effects of MOV10 and UPF1 on HIV-1 infectivity, we utilized a single cycle infectivity assay in which we provide viral Env *in trans* to obtain single-cycle virions and measure infectivity in GHOST CD4 CXCR4 cells. This reporter cell line expresses GFP under viral LTR control, with GFP+ signaling a successful infection. We co-transfected either HA-MOV10 or HA-UPF1 with the proviral constructs in 293T virus-producing cells. We then infected GHOST CD4 CXCR4 cells with equivalent amounts of virus as measured by p24. In Figure 4.3B, we show that MOV10 profoundly inhibits the single-cycle infectivity of HIV-1 when overexpressed in virus-producing cells, which is in agreement with previously published data by several groups (Arjan-Odedra et al. 2012; Burdick et al. 2010; Furtak et al. 2010; Wang et al. 2010). On the other hand, we saw that overexpression of UPF1 in virus-producing cells produced virions whose infectivity did not differ significantly from that of virions produced in the presence of an empty vector (Figure 4.3A). To further study the effect of MOV10 and UPF1 on HIV-1 infectivity, we constructed ATPase-deficient mutants for each helicase. In this case, $MOV10_{DE645AA}$ overexpression in virus-producing cells lost its restrictive effect (Figure 4.3C) while $UPF1_{DE636AA}$ overexpression decreased the infectivity of HIV-1 virions by ~20-fold (Figure 4.3A). This suggests that ATPase-deficient UPF1 has a dominant negative effect on the single-cycle infectivity of HIV-1. In contrast, MOV10's inhibition of HIV-1 infectivity is dependent on its ATPase activity.

Figure 4.3

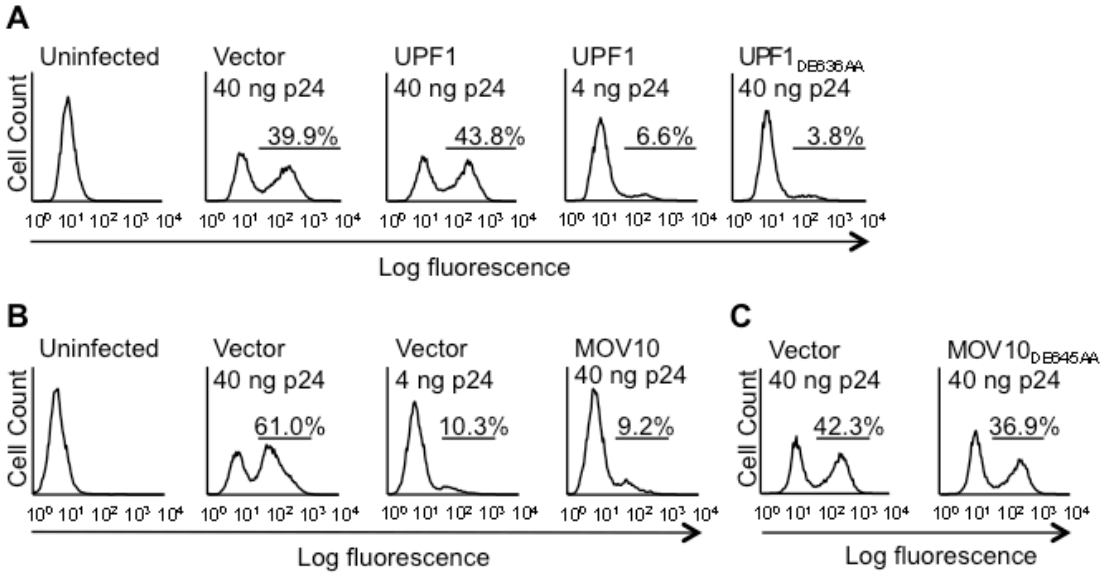
A
Uninfected
Vector
40 ng p24
39.9%
UPF1
40 ng p24
43.8%
UPF1
4 ng p24
6.6%
UPF1DEB36AA
40 ng p24
3.8%
Cell Count
Log fluorescence
B
Uninfected
Vector
40 ng p24
61.0%
Vector
4 ng p24
10.3%
MOV10
40 ng p24
9.2%
Cell Count
Log fluorescence
C
Vector
40 ng p24
42.3%
MOV10DEB45AA
40 ng p24
36.9%
Cell Count
Log fluorescence

Figure 4.3 **Opposite effects of overexpression of UPF1 and MOV10 wild-type protein and ATPase mutants on HIV-1 single cycle infectivity**. (A) 293T cells were transfected with proviral constructs to produce single cycle virions and co-transfected with empty vector, HA-UPF1, or corresponding ATPase mutant HA-UPF1$_{DE636AA}$. Virus supernatant equivalent to indicated inoculum were used to infect GHOST CD4 CXCR4 indicator cells. Infected cells were harvested and analyzed by FACS for LTR-driven GFP expression at 2 days p.i. (B) Virus supernatants were prepared as above, this time co-transfected with HA-MOV10. (C) Virus supernatants were prepared as above, co-transfected with either empty vector or MOV10 ATPase mutant HA-MOV10$_{DE645AA}$.

3. Point mutations in UPF1 catalytic domain motifs cause dominant negative effects on HIV-1 single cycle infectivity.

To further assess the role of the helicase domain of UPF1 in the HIV-1 life cycle, we constructed additional point mutations in HA-UPF1 to inactivate specific functions of the UPF1 catalytic domain (Bhattacharya et al. 2000; Cheng et al. 2007; Czaplinski et al. 1995; Weng et al. 1996; Chen et al. 2012): HA-UPF1$_{DE636AA}$ and HA-UPF1$_{Q665A}$, which both lose ATPase activity (Cheng et al. 2007); HA-UPF1$_{R703A}$ and HA-UPF1$_{K498A}$, which both lose ATP binding and ATPase activity (Cheng et al. 2007; Czaplinski et al. 1995); and HA-UPF1$_{R865A}$, which prevents P body accumulation in the yeast homolog (Cheng et al. 2007), suggesting loss of RNA binding, in addition to loss of ATP binding and ATPase activities (summary in Table 4.1). These mutants were overexpressed individually in virus-producing 293T cells (Figure 4.4A), and single-cycle virions equivalent to 40 ng p24 were assayed for infectivity in GHOST CD4 CXCR4 cells. All mutant proteins were expressed at similar levels (Figure 4.4A). Figure 4.4B shows that overexpression of almost all mutants in virus-producing cells decreases single cycle virus infectivity, compared to wild-type HA-UPF1 or empty vector. In independent experiments by E. Popova from our lab, the HA-UPF1$_{DE636AA}$ mutant decreased infectivity by as much as 20-fold (Figure 4.3A). In my experiments, the HA-UPF1$_{R865A}$ mutant causes the greatest decrease in infectivity (~10-fold, Figure 4.4B). HA-UPF1$_{Q665A}$ only had a mild effect (decreased by ~1.3-fold). Residue Q665, an uncharged amino acid, has only a minor effect when mutated to alanine, suggesting the importance of the other charged residues in maintaining the UPF1 function we are investigating. These results

Figure 4.4

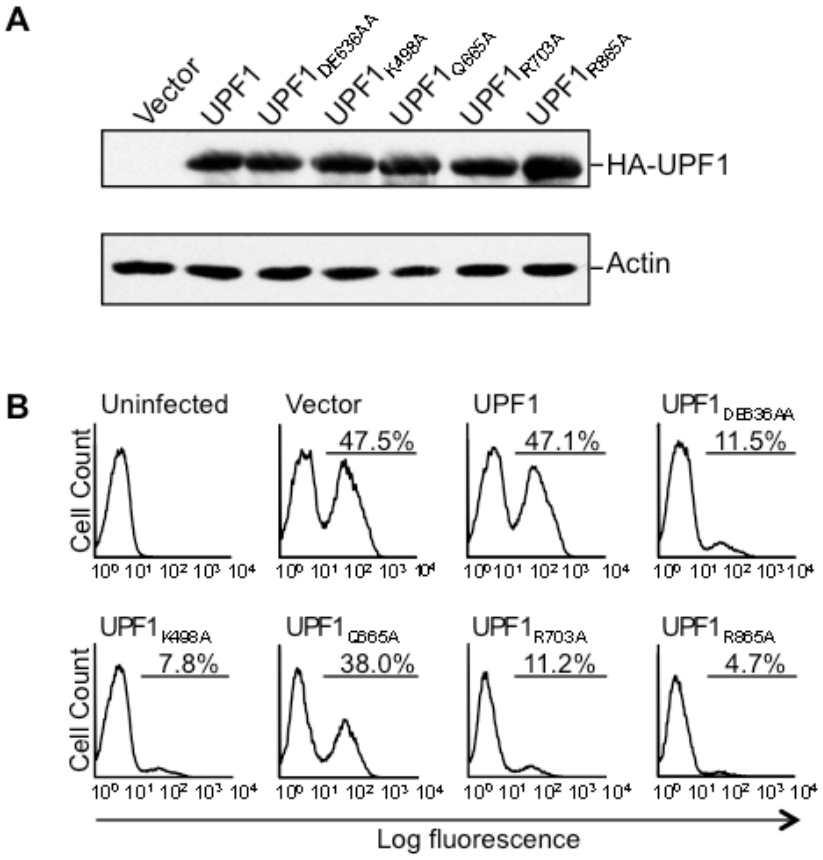
A
Vector
UPF1
UPF1DE636AA
UPF1K498A
UPF1Q665A
UPF1R703A
UPF1R865A
HA-UPF1
Actin
B
Uninfected
Vector
UPF1
UPF1DE636AA
47.5%
47.1%
11.5%
UPF1K498A
UPF1Q665A
UPF1R703A
UPF1R865A
7.8%
38.0%
11.2%
4.7%
Cell Count
Log fluorescence

Figure 4.4 **Overexpression of UPF1 catalytic domain mutants decreases HIV-1 single cycle infectivity. (**A) Total cell lysates of 293T transiently transfected with 2 μg pNL4-3 env-, 1 μg SRαNL4-3 env, and 0.2 μg HA-UPF1 or mutant and immunoblotted with anti-HA and anti-actin antibody demonstrates relative protein expression of UPF1 catalytic domain mutants. (B) FACS analysis for single-cycle infectivity assay performed on GHOST CD4 CXCR4 2 days p.i. with single-cycle virions produced in the presence of overexpressed UPF1 constructs.

Table 4.1

UPF1 Mutants	Phenotype	Literature
K498A (motif I)	•Inhibits ATP hydrolysis •Inhibits ATP binding •Intact RNA binding •Induces P body accumulation (yeast)	Czaplinski 1995 Weng 1996 Cheng 2007 Franks 2010
DE636AA (motif II)	•Inhibits ATP hydrolysis •Intact ATP binding •Intact RNA binding (increased 25%) •Induces P body accumulation (yeast)	Bhattacharya 2000 Weng 1996 Cheng 2007 Franks 2010
Q665A (motif III)	•Inhibits ATP hydrolysis •Intact ATP binding •Intact RNA binding (increased 10%) •Induces P body accumulation (yeast)	Cheng 2007
R703A (motif IV)	•Inhibits ATP hydrolysis •Inhibits ATP binding •Intact RNA binding •Induces P body accumulation (yeast)	Cheng 2007
R865A (motif VI)	•Inhibits ATP hydrolysis •Inhibits ATP binding •No RNA binding •Does not induce P body accumulation (yeast)	Cheng 2007

demonstrate that UPF1 catalytic domain mutants have a dominant negative effect on HIV-1 single cycle infectivity.

4. HIV-1 single cycle infectivity involves endogenous UPF1 but not UPF2.

To determine whether UPF1 is required by HIV-1, we depleted endogenous UPF1 via the transient transfection of siRNA into virus-producing 293T cells (Figure 4.5A, left panel) and assayed for the single-cycle infectivities of the virions. When assaying for infectivity, we performed infections of GHOST CD4 CXCR4 indicator cells, which express GFP upon infection with HIV-1. The cells were infected using equivalent amounts of virus as measured by p24 and examined for GFP expression using FACS (Figure 4.5B). Here, we clearly see that HIV-1 single cycle infectivity is reduced to almost background levels upon knockdown of endogenous UPF1 in virus-producing cells.

In parallel experiments, we also measured single-cycle infectivities in TZMbl indicator cells, which display β-galactosidase activity after successful infection. Similar to the GHOST cell infectivity assay, the TZMbl assay showed decreased infectivity of virions produced in the absence of UPF1 (Appendix 4.3A).

To test whether this effect on infectivity is specific only to virus produced in 293T cells, we also depleted endogenous UPF1 in HeLa cells producing single-cycle virions lacking Vpr-, which mitigates the cytopathic effect of the NL4-3 virus (Vpr+) on HeLa cells. We observed that virions produced in HeLa cells with UPF1 knockdown also had decreased infectivity (Appendix 4.3B), suggesting that this involvement of UPF1 in HIV-

Figure 4.5

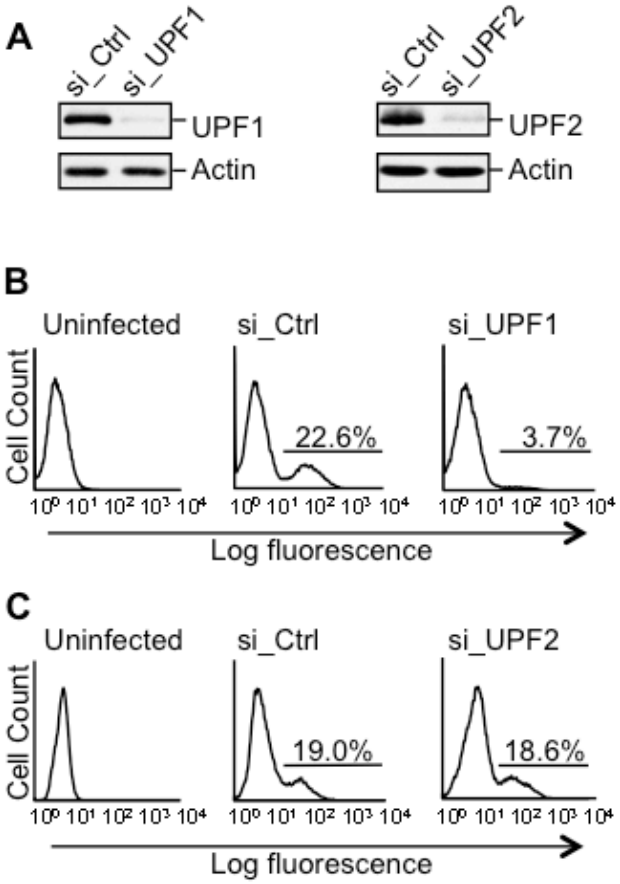
A
si_Ctrl
si_UPF1
UPF1
Actin
si_Ctrl
si_UPF2
UPF2
Actin
B
Uninfected
si_Ctrl
si_UPF1
Cell Count
22.6%
3.7%
Log fluorescence
C
Uninfected
si_Ctrl
si_UPF2
Cell Count
19.0%
18.6%
Log fluorescence

Figure 4.5 **HIV-1 single cycle infectivity involves endogenous UPF1 but not UPF2 in virus-producing cells.** 293T cells were transfected with the indicated siRNA, 0.76 μg pNL4-3 env-, and 0.38 μg SRαNL4-3 env and washed the next day. Two days post-transfection, virus supernatant was harvested and quantified by p24 ELISA prior to infection of GHOST CD4 CXCR4 cells with equivalent amounts of virus particles. Infected target cells were fixed and analyzed by FACS 2 days p.i. (A) Left panel, immunoblot of total cell lysates of virus-producing 293T cells to assay depletion of UPF1; right panel, immunoblot of total cell lysates of virus-producing 293T UPF2 to assay for depletion of UPF2. (B) FACS analysis for single-cycle infectivity assay performed on GHOST CD4 CXCR4 for virions produced when UPF1 is depleted. (C) As above, FACS analysis for single-cycle infectivity assay for virions produced when UPF2 is depleted.

1 infectivity is not limited to virions produced in the 293T cell line.

To determine if the NMD pathway is involved, we also depleted endogenous levels of the UPF1-binding partner, UPF2, in a similar experiment (Figure 4.5A, right panel), but we did not observe any changes in the infectivity of HIV-1 virions (Figure 4.5C). This indicates that the role of UPF1 in HIV-1 infectivity does not involve UPF2.

5. $UPF1_{R865A}$ mutant does not affect viral protein expression and packaging.

To find out whether UPF1 is required for viral protein expression and incorporation, we studied the effect of the dominant negative $UPF1_{R865A}$ mutant on the major viral polyprotein products: Gag, Gag-Pol, and Env. For Gag, we looked at Pr55, p41, p25, and p24 levels, because decreased levels in the viral protease-processed Gag proteins (p25/p24) and increased levels in unprocessed Gag (Pr55) or partially processed Gag (p41) would indicate a processing defect, resulting in immature virions that are less infectious. Looking at cellular levels of Gag (Figure 4.6A, left panel), we observe that the only effect of $UPF1_{R865A}$ is a slight decrease in cell-associated p24/p25 levels but without any significant accumulation in Pr55 or p41. Likewise, the virion lysate (Figure 4.6A, right panel) also shows only a slight decrease in p24 levels.

Additionally, assaying for particle production by p24 ELISA shows a slight decrease (~30%) when overexpressing HA-$UPF1_{R865A}$ in virus-producing cells (Figure 4.6B). However, particle production after UPF1 depletion is not severely affected (Figure 4.6D). This may indicate that the decreased p25/p24 seen with $UPF1_{R865A}$ transfection

Figure 4.6

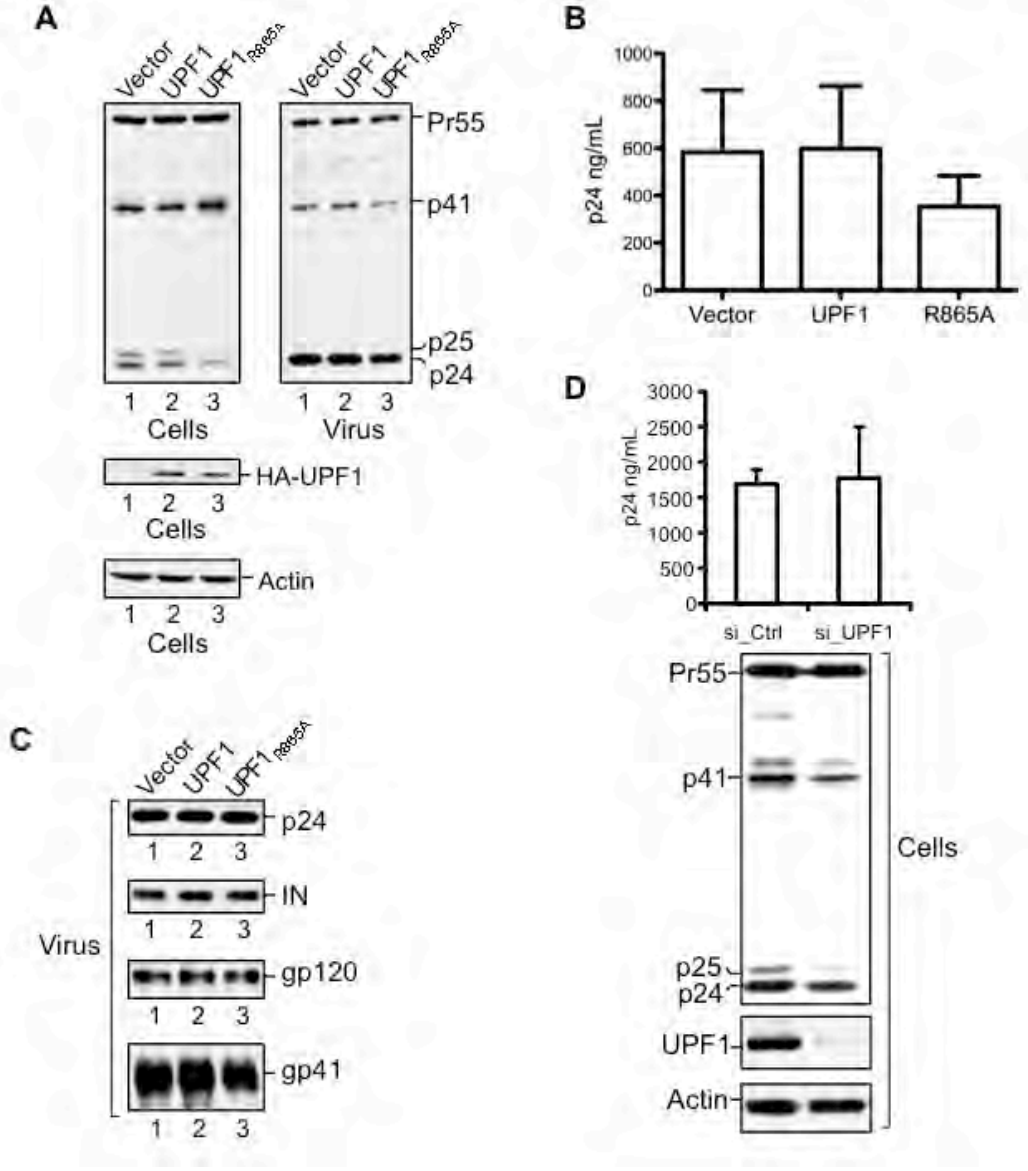
A
Vector
UPF1
UPF1R865A
Pr55
p41
p25
p24
1 2 3
Cells
Virus
HA-UPF1
Actin
B
p24 ng/mL
1000
800
600
400
200
0
Vector
UPF1
R865A
C
p24
IN
gp120
gp41
Virus
D
3000
2500
2000
1500
1000
500
si_Ctrl
si_UPF1
Pr55
p41
p25
p24
UPF1
Actin
Cells

Figure 4.6 **Effect of UPF1 on virus production, viral protein expression and viral incorporation**. (A) 293T cells were transiently transfected with proviral DNA and HA-UPF1 or mutant $UPF1_{R865A}$. Purified virions and total cell lysates were analyzed by Western blotting with anti-CA serum, anti-HA and anti-actin antibodies. (B) Virus production in the presence of empty vector, HA-UPF1, or mutant $UPF1_{R865A}$ was measured by p24 ELISA. (C) 293T cells were transfected as above and virions were purified after adjusting for CA content, as assayed on p24 ELISA. Immunoblotting for integrase (read-out for Gag-Pol), gp120, and gp41 were performed. (D) Virus production after UPF1 depletion in virus-producing cells, as assayed by p24 ELISA. Corresponding cell lysates were immunoblotted for Gag, UPF1, and actin.

may be an artefact due to exogenous protein overexpression.

To determine if UPF1 affects the packaging of other translated viral proteins, we assayed for integrase (IN, as a read-out for Gag-Pol), gp120, and gp41 in virions normalized for the amount of viral particles. In Figure 4.6C, we show that there is no appreciable difference in IN, gp120, and gp41 levels upon overexpression of HA-$UPF1_{R865A}$, compared to wild-type HA-UPF1 or empty vector. These results suggest that $UPF1_{R865A}$ does not significantly affect viral protein expression and packaging into virions.

6. $UPF1_{R865A}$ mutant does not affect viral genomic RNA integrity or packaging into virions.

Since UPF1 is an RNA binding protein and $UPF1_{R865A}$ potentially loses its capacity to bind RNA (Cheng et al. 2007), we wanted to determine whether overexpression of HA-$UPF1_{R865A}$ would affect genomic RNA incorporation in the virions. To study this, we co-expressed HA-UPF1 or HA- $UPF1_{R865A}$ and proviral DNA in 293T cells, collected viral supernatants and purified virions through a sucrose cushion (Figure 4.7B). We extracted viral RNA, reverse transcribed this, then assayed the viral cDNA using Sybr Green quantitative PCR with primers targeting only the full-length viral RNA (i.e. genomic) and not the 4kb or 2 kb viral RNAs (spliced). These primers can differentiate the genomic RNA since they target the location of the major splice donor site, which is intact in full-

Figure 4.7

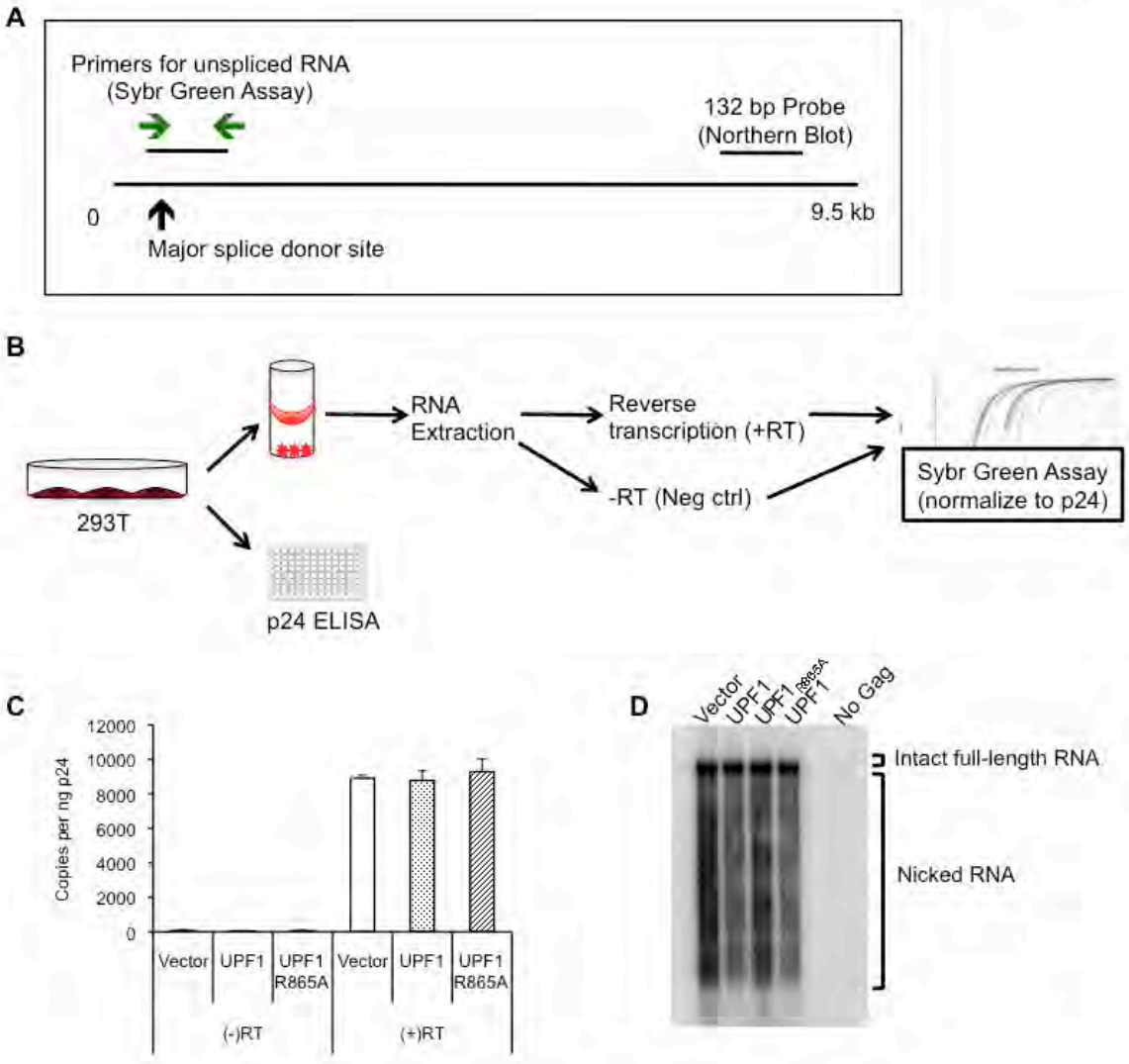
A
Primers for unspliced RNA
(Sybr Green Assay)
132 bp Probe
(Northern Blot)
0
9.5 kb
Major splice donor site
B
293T
RNA
Extraction
Reverse
transcription (+RT)
-RT (Neg ctrl)
Sybr Green Assay
(normalize to p24)
p24 ELISA
C
Copies per ng p24
12000
10000
8000
6000
4000
2000
0
Vector
UPF1
UPF1
R865A
Vector
UPF1
UPF1
R865A
(-)RT
(+)RT
D
Vector
UPF1
UPF1 R865A
UPF1
No Gag
Intact full-length RNA
Nicked RNA

Figure 4.7 **UPF1$_{R865A}$ does not affect viral genomic RNA incorporation or integrity.** 293T were transfected with proviral DNA and 0.2 μg wild-type HA-UPF1 or mutant HA-UPF1$_{R865A}$. The same volume of virus supernatant were purified, RNA was extracted from virions, reverse transcribed, and assayed by Sybr Green using primers specific for full-length, genomic viral RNA. Copy numbers were normalized by viral particle amount (p24).

length viral RNA (Figure 4.7A). As negative controls, we utilized RNA samples that were not reverse transcribed (-RT, Figure 4.7C), and these were run alongside our +RT samples during quantitative PCR. We also used a Gag stop construct (Gag is not translated due to a PTC engineered into the construct), and this negative control consistently had a signal 2 logs below our +RT samples. After normalizing for particle production, we observed that there is no difference in the amount of genomic RNA packaged in the viral particles (Figure 4.7C, average of 3 biological replicates).

Virion-associated retroviral genomes may contain nicks (Coffin 1979), and it is possible that UPF1 may be contributing towards maintaining HIV-1 genome integrity within virions. To address this, our collaborators (Christian Roy and Ogooluwa Ojelabi from Melissa Moore's group) performed Northern blots to assay for the integrity of virion-associated viral RNA (see probe target site, Figure 4.7A). In Figure 4.7D, we demonstrate that overexpression of UPF1 results in slightly less nicked RNA, as shown by a slight decrease in the smear. However, the profile of intact and nicked RNA in the empty vector and HA-UPF1$_{R865A}$ samples did not differ. Thus, UPF1$_{R865A}$ has no effect on viral genomic RNA integrity or incorporation into nascent virions.

7. **UPF1$_{R865A}$ mutant does not affect viral entry into target cells.**

Since the late steps of the HIV-1 life cycle were unaffected by UPF1$_{R865A}$, we then wanted to study its effects on the early steps of the life cycle. To assay for viral entry, we utilized a modified BLaM-Vpr assay (described in (Cavrois et al. 2002; Brandano and Stevenson 2012)). The reporter construct BLaM-Vpr expresses a fusion protein that

Figure 4.8

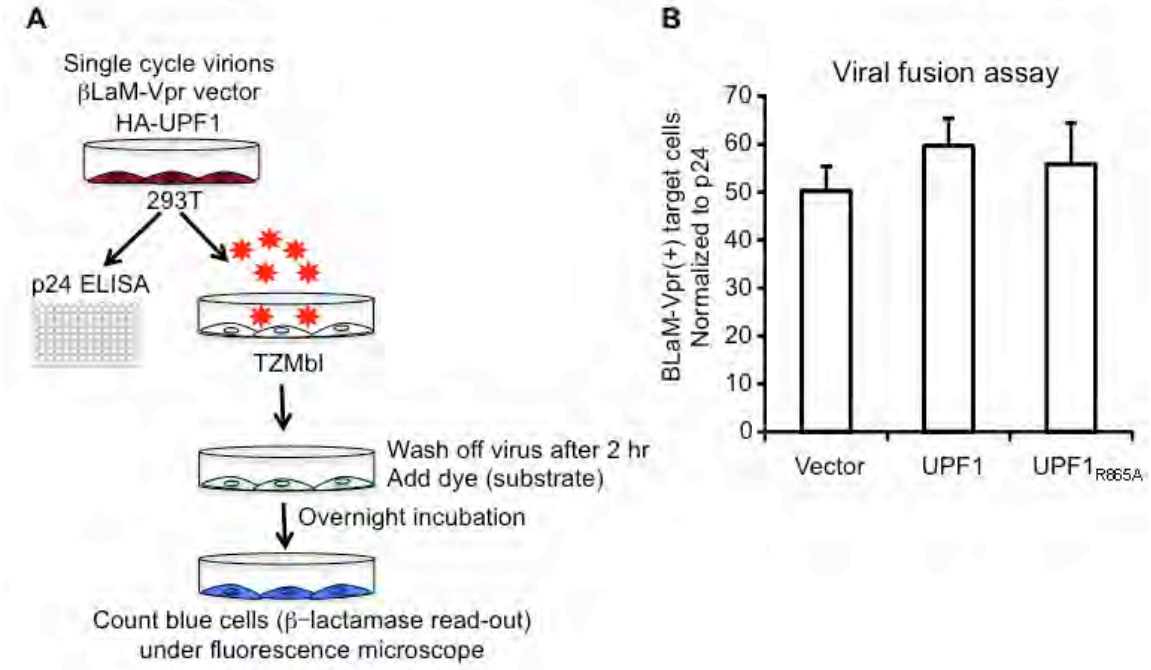
A
Single cycle virions
βLaM-Vpr vector
HA-UPF1
293T
p24 ELISA
TZMbl
Wash off virus after 2 hr
Add dye (substrate)
Overnight incubation
Count blue cells (β−lactamase read-out)
under fluorescence microscope
B
Viral fusion assay
BLaM-Vpr(+) target cells
Normalized to p24
70
60
50
40
30
20
10
0
Vector
UPF1
UPF1R865A

Figure 4.8 **UPF1$_{R865A}$ mutant does not affect viral entry.** (A) Workflow for the viral fusion assay. (B) Viral entry is unaffected by HA-UPF1$_{R865A}$, as demonstrated by the BLaM-Vpr fusion assay.

contains the β-lactamase gene, which provides a read-out for viral entry upon addition of the cell-permeable dye substrate CCF4 to infected cells. The reporter gene construct also encodes for Vpr, which targets the recombinant fusion protein into newly-assembled virions. Virus stocks were prepared from 293T cells transiently transfected with either HA-UPF1 or HA-UPF1$_{R865A}$ (Figure 4.8A). After a 2-hour infection, the virus supernatants were washed away and replaced by the dye substrate. Infected cells were counted under fluorescence microscopy and values were normalized to p24 content. As seen in Figure 4.7B, there was no significant difference in the number of viral fusion events.

8. UPF1$_{R865A}$ decreases viral reverse transcriptase products in target cells.

We proceeded to investigate the early, post-entry events occurring in the infected target cells. To accomplish this, we adopted a PCR-based approach (Mbisa et al. 2009) with primer sets designed to assay certain steps such as early reverse transcription (RT), late RT, and nuclear transport. The latter step is measured by quantifying the episomal forms of the provirus in the nucleus known as 2-LTR circles (Mbisa et al. 2009; Sharkey et al. 2000). The primers for the early RT step correspond to the vDNA in Figure 1.3A, while the late RT step is measured with primers specific to the U5-PBS-psi region in Figure 1.3F. The psi region, which corresponds to the packaging signal in the viral RNA genome, is found near the 3' end of the primer-binding site (PBS). We co-transfected either HA-UPF1 or HA- UPF1$_{R865A}$ with proviral DNA in virus-producing 293T cells, harvested the virus supernatant, and infected GHOST CD4 CXCR4 target cells with

Figure 4.9

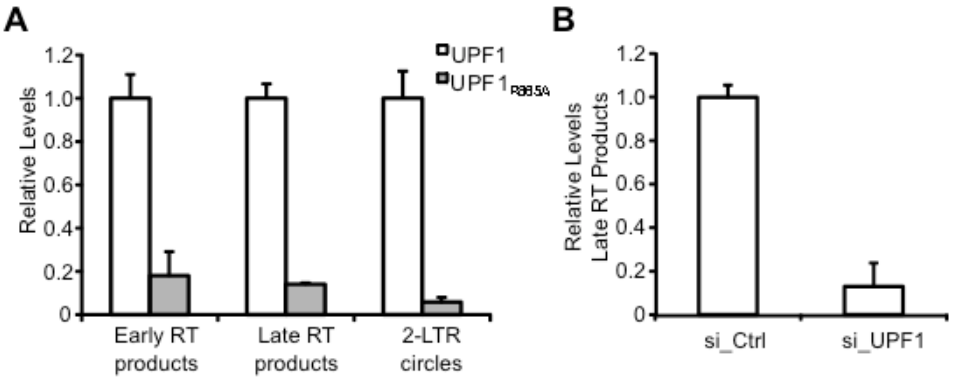
A
B
UPF1
Relative Levels
1.2
1.0
0.8
0.6
0.4
0.2
0
Early RT products
Late RT products
2-LTR circles
Relative Levels Late RT Products
si_Ctrl
si_UPF1

Figure 4.9 **UPF1 from virus-producing cells is required at an early, post-entry step of the HIV-1 life cycle.** (A) The overexpression of HA-UPF1$_{R865A}$ in virus-producing cells decreases RT products and 2-LTR circles in infected target cells. (B) UPF1 depletion in virus-producing cells causes decreased viral late RT products in target cells.

supernatants normalized to p24 content. For early and late RT assays, we treated the supernatant with DNase prior to infection to remove any plasmid contamination. We also included “no envelope control” samples, which we considered our background signal and these values were subtracted from those obtained with infected samples. With qPCR, we found that target cells infected with viruses produced in the presence of HA- $UPF1_{R865A}$ had significantly decreased early and late reverse transcripts and, consequently, 2-LTR circles (Figure 4.9A) compared to cells infected with virus produced in the presence of wild-type HA-UPF1. These observations suggested that functional UPF1 is required at a post-entry step, and to confirm this notion, we also examined single-cycle virions produced from UPF1-depleted 293T cells. Cells infected with these virions were likewise assayed for late RT products. Although the depletion of UPF1 had no effect on HIV-1 particle production, the infectivity of these particles was severely compromised. Figure 4.9B shows that late reverse transcriptase products were decreased to ~13% of control levels in cells infected with virus harvested from UPF1-depleted cells. Taken together, our results indicate that UPF1 is required at an early, post-entry event in the HIV-1 life cycle.

E. Discussion

1. Helicases in HIV-1

Several helicases have already been implicated in the HIV-1 life cycle (Chen et al. 2012). A microarray analysis of CD4+ T cell lines showed that 34% of host cell genes upregulated due to HIV-1 infection were RNA helicases (van 't Wout et al. 2003).

Independent genome-wide screens of HeLa and 293T cell lines for HIV-1-associated cellular factors yielded 12 different RNA helicases, overlapping only with DDX3X helicase ((Brass et al. 2008; König et al. 2008; Zhou et al. 2008), summarized in (Chen et al. 2012)). An example of a helicase that contributes to HIV-1 replication is RNA Helicase A (RHA), which may be important during viral assembly, especially in shaping the Gag ribonucleoprotein complex (Bolinger et al. 2010; Chen et al. 2012). RHA interacts with Gag in a nucleocapsid-dependent manner and this interaction is diminished by RNase A treatment, implying an RNA-dependent interaction (Roy et al. 2006). RHA also binds full-length viral RNA, with 2 RHA molecules packaged per viral particle (Roy et al. 2006; Sharma and Boris-Lawrie 2012). Depletion of RHA leads to a defect in reverse transcription (Roy et al. 2006) and to diminished infectivity in primary lymphocytes (Bolinger et al. 2010), but with no noticeable decrease in the packaging or dimerization of genomic RNA in virions (Roy et al. 2006).

It has been reported that the helicase DDX24 is also required for the packaging of HIV-1 genomic RNA into virions, particularly for viral RNA exported from the nucleus in a Rev-dependent manner (Ma et al. 2008).

In a study by another group, the RNA helicase RH116 was found in a screen for host genes downregulated by the anti-HIV-1 drug Murabutide (Cocude et al. 2003). Overexpression of RH116 led to ~30-fold increase in HIV-1 replication, as measured by p24 assay, and a 3-fold increase in viral transcription (Cocude et al. 2003). This implies that RH116 contributes to regulating HIV-1 replication. In the same study, the authors reported that RH116 shares 99.5% amino acid sequence identity to melanoma

differentiation-associated gene-5 (MDA5) (Cocude et al. 2003), which is a member of the retinoic acid-inducible gene (RIG)-I-like receptor family. MDA5 detects long dsRNA (e.g. polyinosinic polycytidylic acid, poly I:C) and is required for inducing the interferon response against RNA viruses (Kato et al. 2006).

DDX3, another RNA helicase, has been shown to be upregulated in Tat-expressing cells and to shuttle between the nucleus and cytoplasm in association with CRM1 (Yedavalli et al. 2004). DDX3 may be involved in the viral RNA export pathway for unspliced and partially spliced viral transcripts facilitated by Rev and CRM1 (Yedavalli et al. 2004).

Inhibitors targeting helicases involved in HIV-1 replication to control infection are being explored as an alternative therapy to HAART, since cellular factors do not mutate as quickly as viral proteins. The first DDX3 helicase inhibitor has been reported by M. Radi and colleagues (Radi et al. 2012).

2. Opposite effects of MOV10 and UPF1

MOV10, a putative helicase, has been demonstrated to inhibit HIV-1 replication when overexpressed in virus-producing cells (Arjan-Odedra et al. 2012; Furtak et al. 2010; Burdick et al. 2010; Wang et al. 2010), but has no appreciable effect on HIV-1 production and infectivity when endogenous MOV10 is depleted (Burdick et al. 2010; Arjan-Odedra et al. 2012).

In this study, we have shown opposite effects on HIV-1 infectivity by two related helicases, MOV10 and UPF1, both of which are encapsidated into virions. The

overexpression of MOV10 in virus-producing cells reduces viral infectivity (Figure 4.3B) while overexpression of UPF1 in virus-producing cells has no effect (Figure 4.3A). However, overexpression of ATPase-deficient UPF1 causes decreased single cycle infectivity (Figure 4.3A) while ATPase-deficient MOV10 has no effect (Figure 4.3C). Furthermore, we have demonstrated that both MOV10 and UPF1 are incorporated into HIV-1 virions in a nucleocapsid-dependent manner (Figure 4.2). Our data suggest that the incorporation of MOV10 and UPF1 into virions and their effect on infectivity may be related. This will be further discussed in the section relating to future directions.

3. UPF1 depletion

Given that UPF1 is an essential protein, we have depleted UPF1 in cell lines for relatively short periods of time (assaying 1 or 2 days post-transfection) to determine the requirement of endogenous UPF1 on HIV-1 infectivity. Single-cycle infectivity assays demonstrated that HIV-1 virions produced in cells depleted of UPF1 have diminished infectivity (Figure 4.5B, Appendix 4.3A, and Appendix 4.3B). We used both GHOST CD4 CXCR4 cells (assaying for GFP expression by FACS: Figure 4.5B) and TZMbl cells (assaying for β-galactosidase activity: Appendix 4.3A, Appendix 4.3B) to confirm this observation. We also utilized 293T cells and HeLa cells as virus-producing cell lines. In our hands, endogenous UPF1 is depleted by one day post-transfection of siRNA (Appendix 4.1C). In a study by A. Mouland and colleagues, they have seen depletion of endogenous UPF1 as early as 6 hours after transfection (Ajamian et al. 2008).

It remains to be seen what the effect of endogenous UPF1 depletion is in infected primary cells producing fully replication-competent virus. Neither siRNA transfection using Lipofectamine 2000 nor Amaxa nucleofection worked consistently for UPF1 depletion in peripheral blood lymphocytes (PBLs, see Appendix 4.2). Differences in donor characteristics may also be causing the experimental variability for UPF1 depletion in PBLs, since one batch (i.e. cells from one donor) would have some UPF1 depletion 5 days post-nucleofection (Appendix 4.2B) while another batch of PBLs would have no knockdown seen by immunoblotting at similar time points (Appendix 4.2C). UPF1 protein expression in cell lines (HeLa, HEK293) is comparable to peripheral blood mononuclear cells (PBMCs, which is comprised of PBLs, macrophages and monocytes), since both exhibit strong antibody staining, as reported in the Human Protein Atlas (www.proteinatlas.org). We have not yet compared UPF1 expression in PBLs to cell lines directly.

Currently, we are optimizing conditions for UPF1 depletion in PBLs using an inducible shRNA against UPF1. After selecting for transduced PBLs, we have to maintain them in culture for five days or more to obtain sufficient amounts of virions in the supernatant, which will eventually be used for an infectivity assay. We are concerned about prolonged UPF1 depletion since this has been shown to cause non-apoptotic cell death in HeLa cells by 4-7 days, as reported by C. Azzalin and J. Lingner (Azzalin and Lingner 2006a).

We attempted UPF1 depletion in target cells, but the siRNA transfection was poorly tolerated by the TZMbl cells, which are HeLa derived. Although the preliminary

experiment showed that the β-galactosidase read-out from the UPF1- depleted infected cells was not very different from si_Control-transfected cells (Appendix 4.3D), further work needs to be done to optimize the experimental conditions.

4. Depletion of UPF1 binding partners

We have also depleted UPF2, the UPF1-interacting adaptor protein, to determine whether the NMD pathway is involved in the UPF1 requirement by HIV-1. However, we did not detect any differences in infectivity following UPF2 knockdown in virus-producing cells (Figure 4.5C, Appendix 4.3B), suggesting that the role of UPF1 in HIV-1 infectivity does not involve UPF2-dependent NMD. However, we cannot rule out the UPF2-independent branch of NMD. A. Kulozik and colleagues have described this alternative NMD pathway that is UPF2-independent but UPF3-dependent (Gehring et al. 2003).

In vertebrates, there are 2 paralogs of UPF3: UPF3A (on chromosome 13) and UPF3B (or UPF3x, located on the x chromosome), with the latter being a stronger NMD activator (Lykke-Andersen et al. 2000). Depletion of UPF3A has no effect on UPF3B but depletion of UPF3B results in increased UPF3A protein levels (Chan et al. 2009). UPF3A, like UPF3B, binds UPF2 and this interaction also triggers NMD. Experiments to determine whether UPF3-dependent NMD is involved in this UPF1 requirement by HIV-1, therefore, would require concomitant UPF3A and UPF3B depletion in virus-producing cells. These experiments have not yet been done by our group.

We have not looked at depletion of Stau1, another binding partner of UPF1, to rule out the involvement of the SMD pathway. L. Abrahamyan and colleagues have studied Stau1-depleted virions (Abrahamyan et al. 2010), which showed increased UPF1 packaging into virions and decreased viral infectivity. Since depletion of UPF1 and depletion of Stau1 both result in decreased viral infectivity, it would be interesting to explore whether both proteins function in the same pathway to facilitate HIV-1 infection. Also, it would be worthwhile to look at the stoichiometry of both Stau1 and UPF1 in the virions, since upsetting the balance of both proteins (i.e. depleting Stau1 results in increased UPF1 encapsidation) seems to negatively affect HIV-1. It is unknown whether UPF1 depletion would result in increased Stau1 packaging in virions.

5. UPF1 mutant studies

To characterize which step of the virus life cycle is affected by UPF1, we utilized UPF1 helicase mutants that exert a dominant negative effect on viral infectivity (Figure 4.4). Overexpression of dominant negative $UPF1_{R865A}$ did not result in any defects in the incorporation and processing of viral proteins (Figure 4.6), or in the genomic viral RNA packaging (Figure 4.7C) and genomic viral RNA integrity (Figure 4.7D). This suggests that UPF1 might not directly interact with the HIV-1 virion-associated genomic RNA. While UPF1 is incorporated into virions in a NC-dependent manner, it remains to be seen whether UPF1 associates with the HIV-1 NC through RNA-dependent interactions.

Overexpression of $UPF1_{R865A}$ in virus-producing cells did not seem to affect viral entry either, as measured by a viral fusion assay (Figure 4.8). However, $UPF1_{R865A}$

overexpression in virus-producing cells severely impaired reverse transcription by incoming virions in newly-infected target cells (Figure 4.9A). Similarly, depletion of endogenous UPF1 in virus-producing cells also caused a decrease in late reverse transcription products in newly-infected cells (Figure 4.9B). This implies a block at an early, post-entry step in the viral life cycle when UPF1 is absent or nonfunctional in virus-producing cells, which presumably causes decreased encapsidation of wild-type UPF1 in virions.

Since $UPF1_{R865A}$ affects viral post-entry events as early as at the beginning of reverse transcription (Figure 4.9A), it would be interesting to find out how UPF1 contributes towards the virus infection at this point. The requirement of UPF1 in the virus-producing cells and its subsequent incorporation into nascent virions hints at a function wherein this host protein is in complex with viral components. A. Hulme and colleagues have reported that reverse transcription inhibitor Nevirapine delays uncoating, implying that a block or delay in reverse transcription affects the kinetics of viral uncoating (Hulme et al. 2011). As discussed in the Introduction chapter, N. Arhel proposed three current models for uncoating (Arhel 2010) and all of these depend on the uncoating of the viral core in a timely manner that is coordinated with reverse transcription and nuclear import of the proviral DNA; otherwise, it would lead to unsuccessful infection. Since uncoating is basically the disassembly of the viral capsid from the fullerene, multimeric viral core to CA monomers and the unpacking of the viral ribonucleoprotein complex, consisting of the two copies of viral RNA genome and associated proteins, it is worthwhile to explore whether this process is similar to the

disassembly of the NMD complex, with its requirement for the UPF1 ATPase activity (Franks et al. 2010).

Prior to characterizing the effect of $UPF1_{R865A}$, we also looked at the effect of $UPF1_{DE636AA}$. While performing these assays with $UPF1_{DE636AA}$, we found that the sequence of our $UPF1_{DE636AA}$ construct had additional mutations as follows: T496A, I377T, and E532G. We re-cloned the DE636AA construct and tested its effect on single-cycle infectivity, which was similar to the original mutant construct $UPF1_{DE636AA}$* (DE636AA/T496A/I377T/E532G, from hereon designated with an asterisk). We have included in the Appendix the earlier work we did characterizing the effect of $UPF1_{DE636AA}$* on HIV-1 (Appendix 4.5, 4.6). We found that overexpression of $UPF1_{DE636AA}$* in virus-producing cells does not affect Gag processing (i.e. no accumulation of unprocessed or partially processed Gag, Appendix 4.5A), incorporation of Gag-Pol, Env (Appendix 4.5C), and incorporation of genomic viral RNA (Appendix 4.5D). There is an observable decrease in p25 and p24, both in PR+ (has viral protease, Appendix 4.5A) and PR- (lacks viral protease, Appendix 4.5B) viral constructs but with no accumulation of unprocessed or partially processed Gag, which we interpret as unaffected Gag processing. We also looked at the effect of $UPF1_{DE636AA}$* overexpression in virus-producing cells on early, post-entry events in newly infected HeLa CD4 ΔCT target cells using VSV-G-pseudotyped virions. Interestingly, there is no effect at the early reverse transcription step but the block is apparent from the intermediate reverse transcription step onwards (Appendix 4.6D). In contrast, the $UPF1_{R865A}$ block is apparent in the early reverse transcription step. Why would these two mutants manifest blocks at

different steps? Is it due to the inherent characteristics (e.g. lack of function; also due to additional mutations of $UPF1_{DE636AA}$*) of each mutant? Or is it due to technical differences in how these two batches of assays were performed? For the $UPF1_{DE636AA}$* virions, we pseudotyped with VSV-G while we were using HeLa CD4 ΔCT as target cells, since we had not yet optimized conditions for using GHOST CD4 CXCR4 as target cells. For the $UPF1_{R865A}$ experiments, we provided HIV-1 NL4-3 Env *in trans* and used the latter cell type for target cells. It is possible that the kinetics of viral entry may differ between VSV-G-pseudotyped virions and virions complemented with authentic HIV-1 Env. However, J. Thomas et al. have reported that after initiation of reverse transcription, efficiencies are not affected by mode of entry (Thomas et al. 2007).

Both APOBEC3G and HIV-1 mRNP complexes have been reported to shuttle in different cytoplasmic foci involved in RNA metabolism such as P bodies, Staufen granules, and stress granules (Gallo 2003; Gallois-Montbrun et al. 2007; Kozak et al. 2006; Wichroski et al. 2006). It is notable in this regard that the overexpression of some UPF1 dominant-negative mutants results in the accumulation of NMD complexes in P bodies (Franks et al. 2010; Cheng et al. 2010). However, $UPF1_{R865A}$ does not display this phenotype (Cheng et al. 2007), indicating that the inhibitory effects of dominant-negative UPF1 mutants on HIV-1 infectivity are unrelated to their effects on P body accumulation.

6. Future directions and working hypothesis

Although RHA belongs to helicase superfamily SF2, there are similarities between the observations seen by previous groups after RHA depletion and the effects of

UPF1 depletion or of the overexpression of a dominant negative UPF1 mutant. In each case, genomic viral RNA encapsidation is unaffected but the infectivity of HIV-1 virions is nevertheless impaired, probably due to defects at the level of reverse transcription. It would be interesting to explore whether RHA and UPF1 perform redundant or complementary functions in the HIV-1 life cycle. Virion-associated RHA has been estimated to be 2 molecules per viral particle, as assayed by quantitative immunoblotting (Sharma and Boris-Lawrie 2012). With our current experimental conditions, we are unable to detect endogenous UPF1 in purified viral particles by immunoblotting, probably due to the limited sensitivity of the antibody and purity of our viral preparations (Sharma and Boris-Lawrie 2012). Alternatively, purified virions can be analyzed by mass spectrometry to determine the stoichiometry of virion-associated UPF1 and MOV10.

We have presented data on two related helicases, UPF1 and MOV10, which manifest opposite effects on HIV-1 infectivity. We would like to propose that: 1) UPF1 is crucial to the HIV-1 life cycle and 2) MOV10 restriction is due to its ability to displace UPF1 in virions. In other words, MOV10 overexpression in virus-producing cells results in increased encapsidation of MOV10 in virions, crowding out UPF1 and consequently, impairing infectivity. Similarly, the overexpression of dominant-negative UPF1 mutants limits the pool of functional UPF1 that can be packaged into virions. This model would predict that the depletion of UPF1 results in increased MOV10 incorporation? We can test this hypothesis by assaying for virion-associated UPF1 and MOV10 in the conditions shown in Figure 4.10. For instance, the overexpression of UPF1 may result in increased

packaging of UPF1 in virions. However, since UPF1 is required by HIV-1 during the next round of infection, this is not detrimental to the virus (Figure 4.10, upper left panel). On the other hand, when MOV10 is overexpressed in virus-producing cells, more MOV10 is packaged in virions, resulting in the elimination of UPF1 incorporation (Figure 4.10, upper right panel). This, however, would result in noninfectious virions due to the lack of UPF1. We would like to propose assaying virions after UPF1 depletion (Figure 4.10, middle panel) and after UPF1 mutant overexpression (Figure 4.10, lower panel) to determine which predicted outcome is correct, as illustrated by the viral cores in the diagram.

Why does the MOV10 ATPase-deficient mutant have no effect on infectivity? Either the MOV10 mutant is not packaged as efficiently as the wild-type MOV10 or our displacement hypothesis is wrong and the underlying mechanism is not due to whether there is enough UPF1 in the virions.

To pinpoint the mechanism of action of UPF1 in the post-entry step of the viral cycle, we would also like to propose measuring the kinetics of the post-entry steps (uncoating and stability of the reverse transcription complex (RTC)) using an assay developed by V. Arfi and colleagues (V. Arfi, et al. J Virol 2009). In addition, an *in situ* uncoating assay (A. Hulme, et. al. PNAS 2011) would reveal whether UPF1 is required at this particular step. It is possible that UPF1 is incorporated with the RTC in the viral core, assisting in the uncoating and/or reverse transcription of the viral genome by performing a translocase function, such as removing associated viral or cellular proteins from the viral genome to allow reverse transcription to proceed.

UPF1 is probably not in an activated state when incorporated into virions (i.e. RNA-bound state of S. Chakrabarti et al.'s model of UPF1 activation (Chakrabarti et al. 2011)). Which binding partner activates UPF1 in the context of HIV-1? UPF2 depletion does not affect infectivity, suggesting that UPF2 is not involved in this pathway. There is some evidence from A. Mouland's group suggesting that Stau1 may possibly play this role. Stau1 depletion leads to increased UPF1 encapsidation but decreased infectivity (Abrahamyan et al. 2010). It is possible that despite the increased amount of virion-associated UPF1, this protein may be inactive due to lack of Stau1, contributing to the decreased viral infectivity. Further experiments need to be done to confirm this.

Figure 4.10

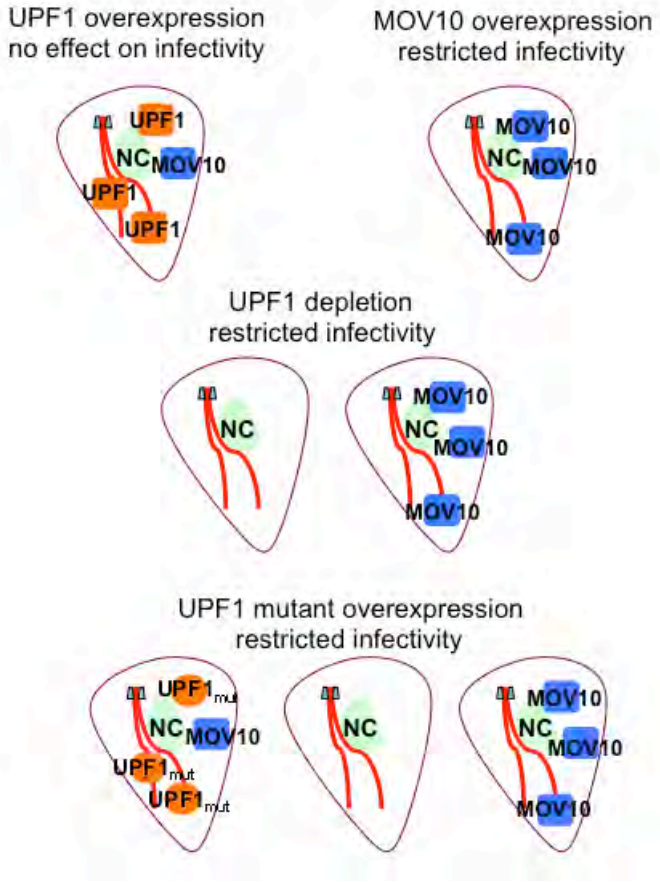
UPF1 overexpression
no effect on infectivity
UPF1
NC
MOV10
UPF1
UPF1
MOV10 overexpression
restricted infectivity
MOV10
NC
MOV10
MOV10
UPF1 depletion
restricted infectivity
NC
MOV10
NC
MOV10
MOV10
UPF1 mutant overexpression
restricted infectivity
UPF1mut
NC
MOV10
UPF1mut
UPF1mut
NC
MOV10
NC
MOV10
MOV10

Figure 4.10 **Proposed hypothesis for future experiments.** UPF1 overexpression does not have a deleterious effect on infectivity, which indicates that cellular UPF1 levels do not affect assembly of virions or increased UPF1 packaging into virions does not affect infectivity, provided that binding partner Stau1 is not depleted (upper left panel). MOV10 overexpression on the other hand, may increase packaging of MOV10 in virions, which may displace UPF1 (upper right panel). UPF1 depletion is detrimental to the virus, probably either due to lack of packaged UPF1 or increased packaging of MOV10 (middle panel). Overexpression of a dominant negative UPF1 may increase packaging of this nonfunctional protein, or may block packaging of any UPF1 or over-packaging of MOV10 (lower panel).

Appendix for Chapter IV

Appendix 4.1

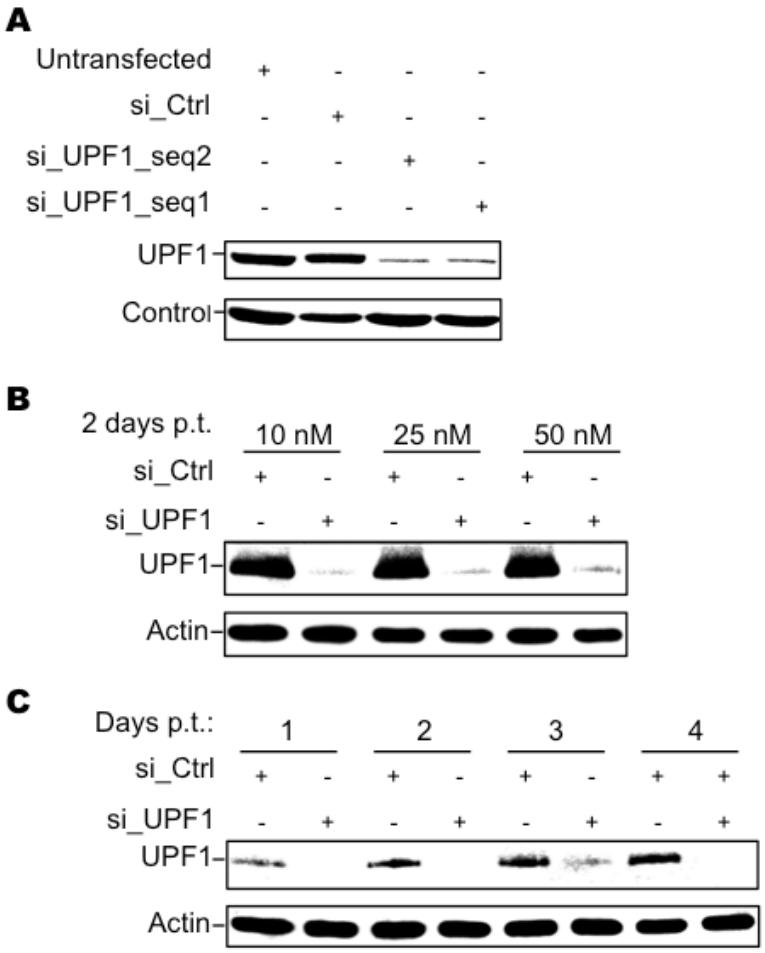
A
Untransfected
si_Ctrl
si_UPF1_seq2
si_UPF1_seq1
UPF1
Control
B
2 days p.t.
10 nM
25 nM
50 nM
si_Ctrl
si_UPF1
UPF1
Actin
C
Days p.t.:
1
2
3
4
si_Ctrl
si_UPF1
UPF1
Actin

Appendix 4.1 **Depletion of UPF1 in cell lines.** (A) Lipofectamine 2000 transfection of 293T cells with two different siRNAs targeting UPF1 results in depletion of endogenous UPF1 levels. (B) Optimization of UPF1 siRNA concentration transfected in HeLa cells. (C) Time-course assay of UPF1 depletion by siRNA transfection in HeLa cells.

Appendix 4.2

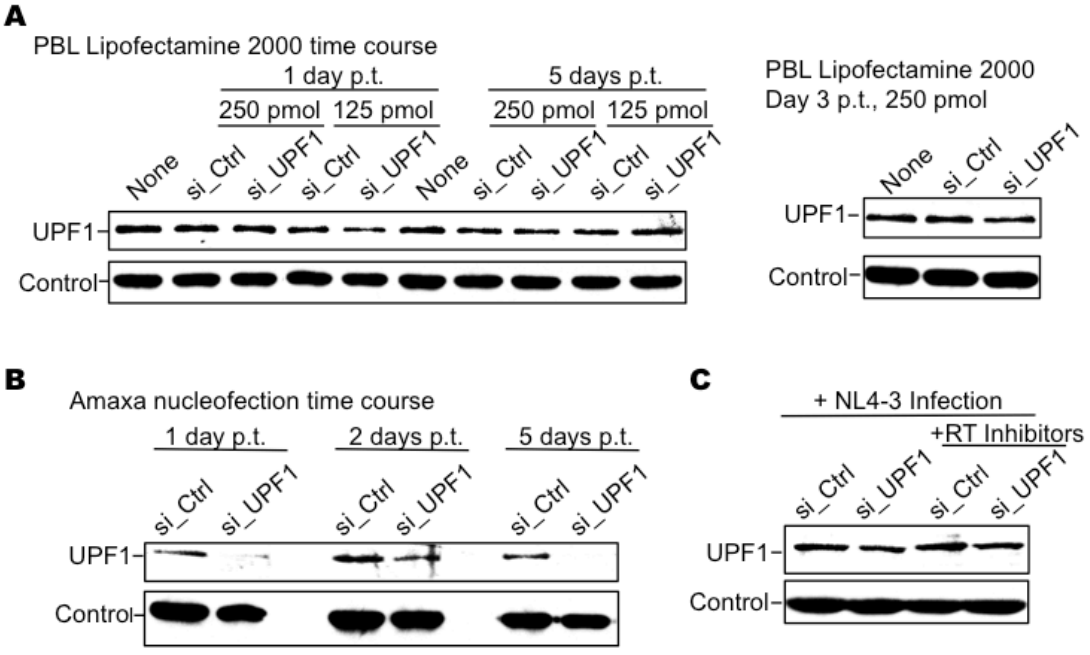
A
PBL Lipofectamine 2000 time course
1 day p.t.
5 days p.t.
250 pmol
125 pmol
250 pmol
125 pmol
None
si_Ctrl
si_UPF1
si_Ctrl
si_UPF1
None
si_Ctrl
si_UPF1
si_Ctrl
si_UPF1
UPF1
Control
PBL Lipofectamine 2000
Day 3 p.t., 250 pmol
None
si_Ctrl
si_UPF1
UPF1
Control
B
Amaxa nucleofection time course
1 day p.t.
2 days p.t.
5 days p.t.
si_Ctrl
si_UPF1
si_Ctrl
si_UPF1
si_Ctrl
si_UPF1
UPF1
Control
C
+ NL4-3 Infection
+RT Inhibitors
si_Ctrl
si_UPF1
si_Ctrl
si_UPF1
UPF1
Control

Appendix 4.2 **Depletion of UPF1 in primary cells.** (A) Lipofectamine 2000 transfection of siRNAs against UPF1 in activated peripheral blood lymphocytes (PBLs) does not deplete endogenous protein levels. (B) Time-course assay for Amaxa nucleofection of si_UPF1. (C) Amaxa nucleofection and NL4-3 infection of PBLs.

Appendix 4.3

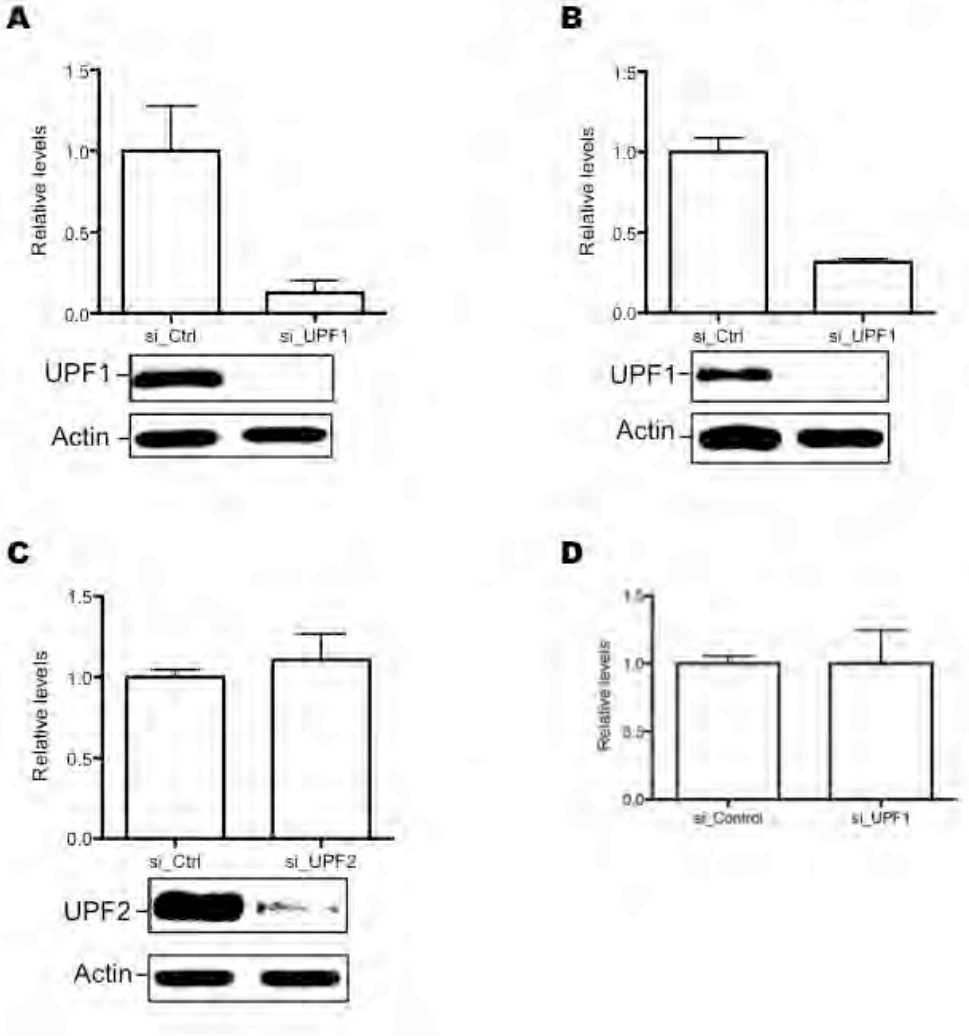
A
Relative levels
1.5
1.0
0.5
0.0
si_Ctrl
si_UPF1
UPF1
Actin
B
Relative levels
1.5
1.0
0.5
0.0
si_Ctrl
si_UPF1
UPF1
Actin
C
Relative levels
1.5
1.0
0.5
0.0
si_Ctrl
si_UPF2
UPF2
Actin
D
Relative levels
1.0
0.5
0.0
si_Control
si_UPF1

Appendix 4.3 **β-galactosidase assay for TZMbl indicator cells to demonstrate single cycle infectivity of HIV-1.** (A) UPF1 depletion in 293T virus-producing cells decrease single cycle infectivity of NL4-3 virus in TZMbl. (B) UPF1 depletion in HeLa virus-producing cells decreases single cycle infectivity of NL4-3 Vpr- virus. (C) UPF2 depletion in 293T virus-producing cells does not affect single cycle infectivity. (D) UPF1 depletion of TZMbl target cells did not affect single cycle infectivity.

Appendix 4.4

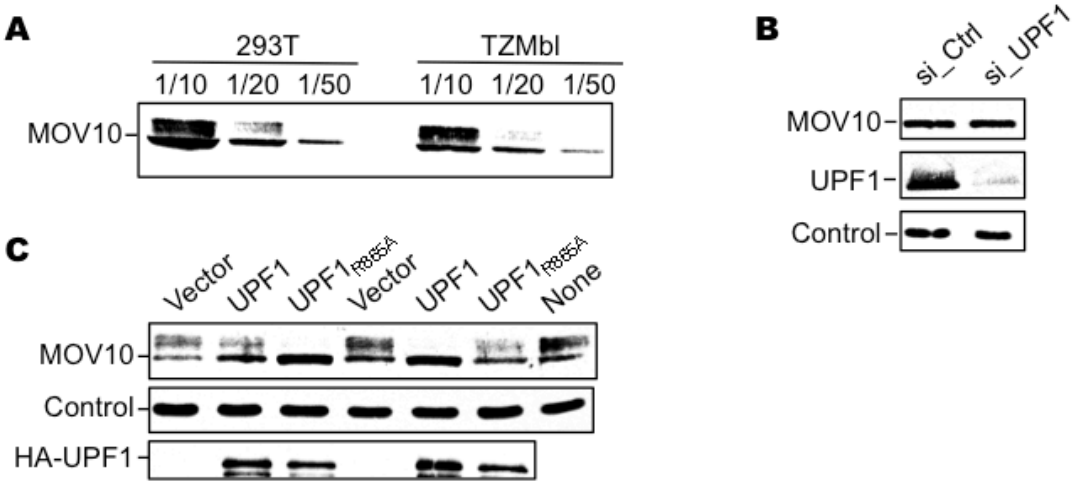
A
293T
TZMbl
1/10 1/20 1/50
1/10 1/20 1/50
MOV10
B
si_Ctrl
si_UPF1
MOV10
UPF1
Control
C
Vector
UPF1
UPF1R855A
Vector
UPF1
UPF1R855A
None
MOV10
Control
HA-UPF1

Appendix 4.4 **Endogenous MOV10 levels.** (A) Endogenous MOV10 levels in untransfected 293T and TZMbl cell lines. (B) Endogenous MOV10 levels are unaffected by UPF1 depletion in 293T cells. (C) Endogenous MOV10 levels with overexpression of UPF1 wild-type and $UPF1_{R865A}$ mutant proteins.

Appendix 4.5

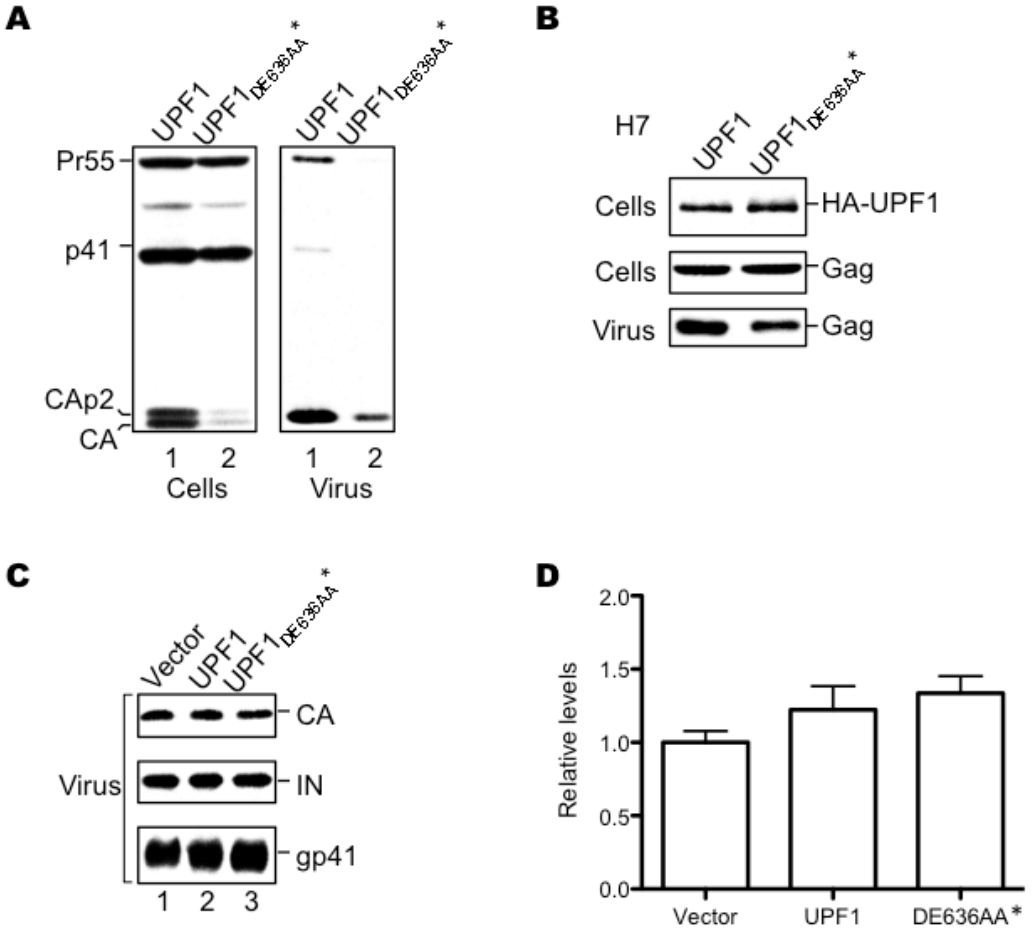
A
UPF1
UPF1DE636AA*
UPF1
UPF1DE636AA*
Pr55
p41
CAp2
CA
1 2
Cells
1 2
Virus
B
H7
UPF1
UPF1DE636AA*
Cells
HA-UPF1
Cells
Gag
Virus
Gag
C
Vector
UPF1
UPF1DE636AA*
Virus
CA
IN
gp41
1 2 3
D
Relative levels
2.0
1.5
1.0
0.5
0.0
Vector
UPF1
DE636AA*

Appendix 4.5 **Biochemical characterization of HIV-1 virions produced with the overexpression of UPF1$_{DE636AA}$*.** (A) Gag processing is unaffected by overexpression of UPF1$_{DE636AA}$* but p25/p24 levels are decreased. (B) Overexpression of UPF1$_{DE636AA}$* results in slight defect of viral release of protease-deficient virions. (C) Incorporation of Gag-Pol (assayed by integrase, IN) and Env (assayed by gp41) are unaffected by overexpression of UPF1$_{DE636AA}$*. (D) Levels of virion-associated genomic RNA are unaffected by overexpression of UPF1$_{DE636AA}$* in virus-producing cells.

Appendix 4.6

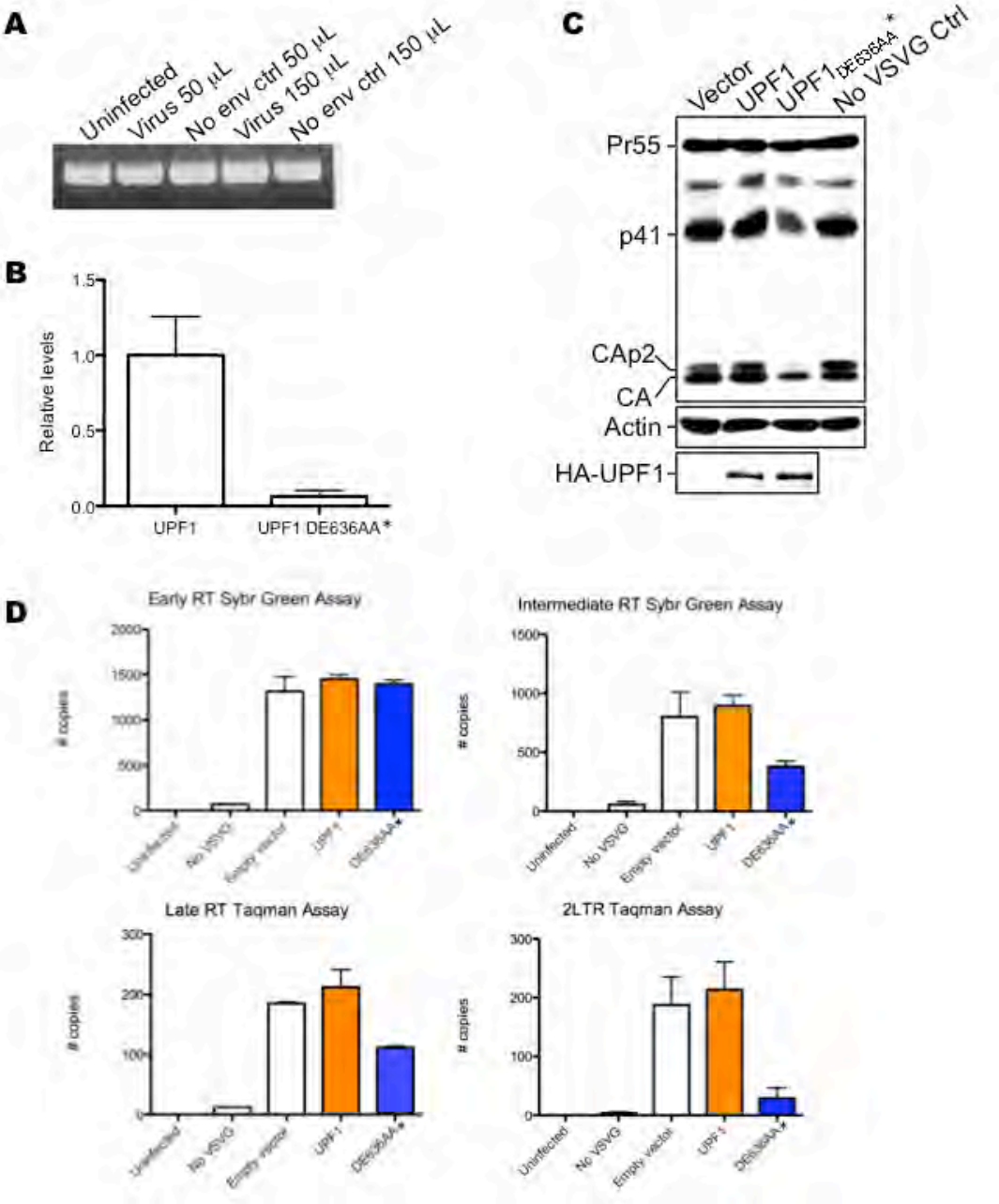
A
Uninfected
Virus 50 µL
No env ctrl 50 µL
Virus 150 µL
No env ctrl 150 µL
B
Relative levels
1.5
1.0
0.5
0.0
UPF1
UPF1 DE636AA*
C
Vector
UPF1
UPF1DE636AA*
No VSVG Ctrl
Pr55
p41
CAp2
CA
Actin
HA-UPF1
D
Early RT Sybr Green Assay
Intermediate RT Sybr Green Assay
Late RT Taqman Assay
2LTR Taqman Assay
copies
Uninfected
No VSVG
Empty vector
UPF1
DE636AA*

Appendix 4.6 **VSV-G-pseudotyped NL4-3 virions produced with the overexpression of UPF1$_{DE636AA}$*.** (A) Uninfected TZMbl cells contain the HIV-1 LTR and are inappropriate target cells for the 2-LTR assay. (B) Decreased single cycle infectivity of VSV-G-pseudotyped virions produced in the presence of UPF1$_{DE636AA}$*. (C) Slight decrease in p25/p24 upon overexpression of UPF1$_{DE636AA}$ upon co-transfection of VSV-G construct. (D) Assay for early, post-entry events using HeLa CD4 ΔCT cell line as target cells upon overexpression of UPF1$_{DE636AA}$*.

Appendix 4.7

A

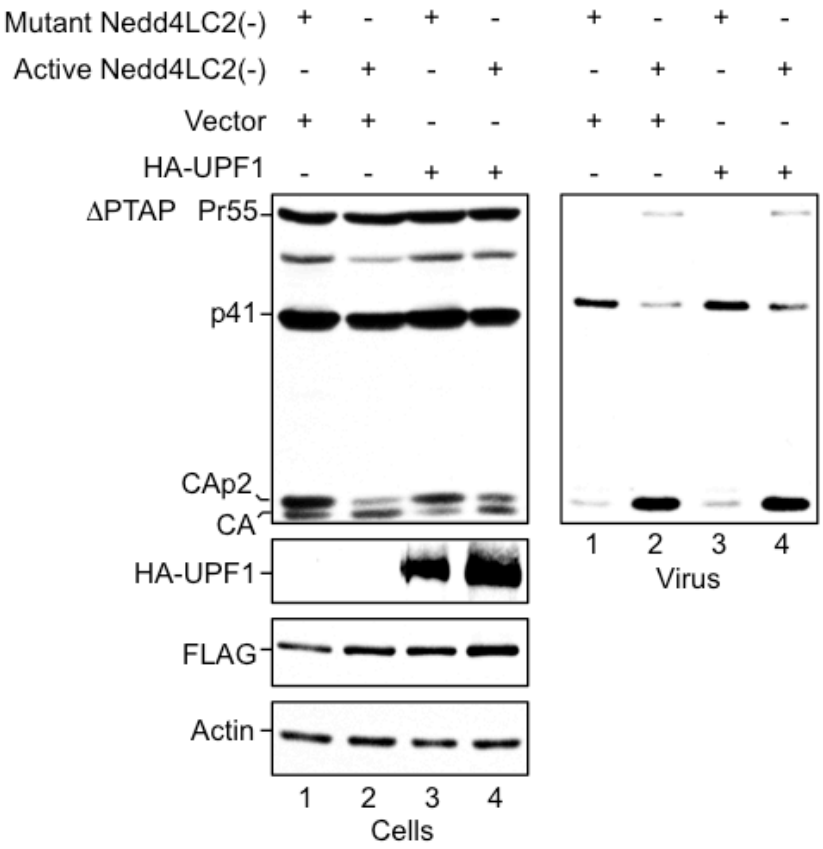

Appendix 4.7

B

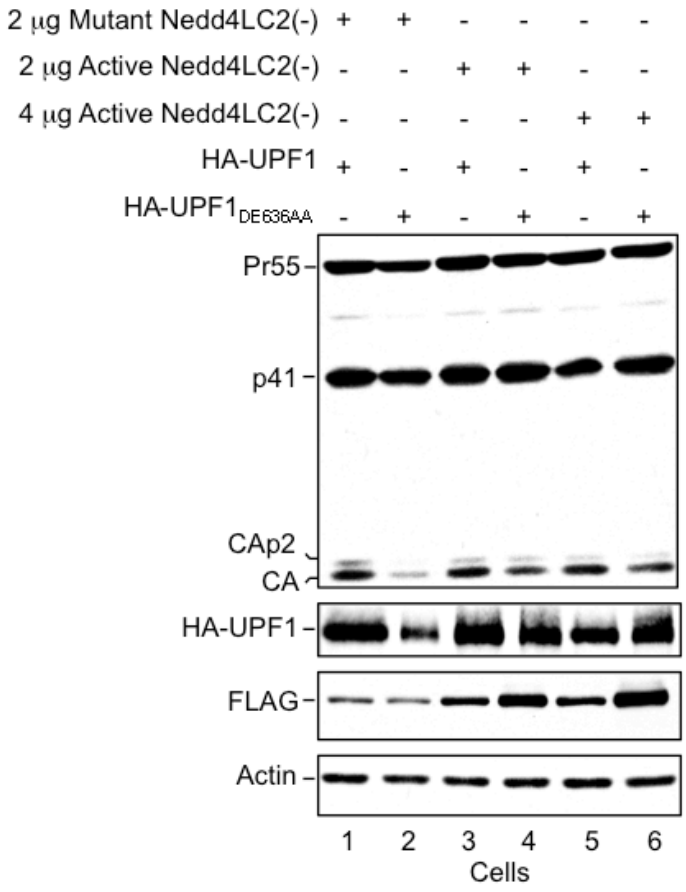

Appendix 4.7 **Overexpression of active Nedd4LC2(-) rescues the decrease in p25/p24 in virus-producing cells when UPF1$_{DE636AA}$* is co-expressed.** (A) Virions lacking the DTAP motif exhibit a block in Gag processing manifested as decreased p24 protein levels and accumulation of p25 proteins. This late block is rescued by overexpression of active Nedd4LC2(-), as seen in lanes 2 and 4, left and right panels. (B) Co-expression of UPF1$_{DE636AA}$* results in decreased Gag p25 and p24 protein levels (lane 2), which is rescued by overexpression of active Nedd4LC2(-), lanes 4 and 6.

Chapter V: References

Abdool Karim SS. 2012. An AIDS-Free Generation? *Science* **337**: 133–133.

Abrahamyan LG, Chatel-Chaix L, Ajamian L, Milev MP, Monette A, Clément J-F, Song R, Lehmann M, DesGroseillers L, Laughrea M, et al. 2010. Novel Staufen1 ribonucleoproteins prevent formation of stress granules but favour encapsidation of HIV-1 genomic RNA. *J Cell Sci* **123**: 369–383.

Accola MA, Strack B, Göttlinger HG. 2000. Efficient particle production by minimal Gag constructs which retain the carboxy-terminal domain of human immunodeficiency virus type 1 capsid-p2 and a late assembly domain. *J Virol* **74**: 5395–5402.

Adams J, Patel N, Mankaryous N, Tadros M, Miller CD. 2010. Nonnucleoside reverse transcriptase inhibitor resistance and the role of the second-generation agents. *Ann Pharmacother* **44**: 157–165.

Ajamian L, Abrahamyan L, Milev M, Ivanov PV, Kulozik AE, Gehring NH, Mouland AJ. 2008. Unexpected roles for UPF1 in HIV-1 RNA metabolism and translation. *RNA* **14**: 914–927.

Amrani N, Ganesan R, Kervestin S, Mangus DA, Ghosh S, Jacobson A. 2004. A faux 3'-UTR promotes aberrant termination and triggers nonsense-mediated mRNA decay. *Nature* **432**: 112–118.

Amrani N, Sachs MS, Jacobson A. 2006. Early nonsense: mRNA decay solves a translational problem. *Nat Rev Mol Cell Biol* **7**: 415–425.

Andreadis S, Lavery T, Davis HE, Le Doux JM, Yarmush ML, Morgan JR. 2000. Toward a more accurate quantitation of the activity of recombinant retroviruses: alternatives to titer and multiplicity of infection. *J Virol* **74**: 3431–3439.

Arfi V, Lienard J, Nguyen X-N, Berger G, Rigal D, Darlix J-L, Cimarelli A. 2009. Characterization of the behavior of functional viral genomes during the early steps of human immunodeficiency virus type 1 infection. *J Virol* **83**: 7524–7535.

Arhel N. 2010. Revisiting HIV-1 uncoating. *Retrovirology* **7**: 96.

Arhel N, Genovesio A, Kim K-A, Miko S, Perret E, Olivo-Marin J-C, Shorte S, Charneau P. 2006. Quantitative four-dimensional tracking of cytoplasmic and nuclear HIV-1 complexes. *Nat Methods* **3**: 817–824.

Arhel NJ, Souquere-Besse S, Munier S, Souque P, Guadagnini S, Rutherford S, Prévost M-C, Allen TD, Charneau P. 2007. HIV-1 DNA Flap formation promotes uncoating

of the pre-integration complex at the nuclear pore. *EMBO J* **26**: 3025–3037.

Ariumi Y, Turelli P, Masutani M, Trono D. 2005. DNA damage sensors ATM, ATR, DNA-PKcs, and PARP-1 are dispensable for human immunodeficiency virus type 1 integration. *J Virol* **79**: 2973–2978.

Arjan-Odedra S, Swanson CM, Sherer NM, Wolinsky SM, Malim MH. 2012. Endogenous MOV10 inhibits the retrotransposition of endogenous retroelements but not the replication of exogenous retroviruses. *Retrovirology* **9**: 53.

Ashkenazi A, Wexler-Cohen Y, Shai Y. 2011. Multifaceted action of Fuzeon as virus-cell membrane fusion inhibitor. *Biochim Biophys Acta* **1808**: 2352–2358.

Atkin AL, Altamura N, Leeds P, Culbertson MR. 1995. The majority of yeast UPF1 co-localizes with polyribosomes in the cytoplasm. *Mol Biol Cell* **6**: 611–625.

Azzalin CM, Lingner J. 2006a. The double life of UPF1 in RNA and DNA stability pathways. *Cell Cycle* **5**: 1496–1498.

Azzalin CM, Lingner J. 2006b. The human RNA surveillance factor UPF1 is required for S phase progression and genome stability. *Curr Biol* **16**: 433–439.

Azzalin CM, Reichenbach P, Khoriauli L, Giulotto E, Lingner J. 2007. Telomeric repeat containing RNA and RNA surveillance factors at mammalian chromosome ends. *Science* **318**: 798–801.

Baeten JM, Donnell D, Ndase P, Mugo NR, Campbell JD, Wangisi J, Tappero JW, Bukusi EA, Cohen CR, Katabira E, et al. 2012. Antiretroviral prophylaxis for HIV prevention in heterosexual men and women. *N Engl J Med* **367**: 399–410.

Baker KE, Parker R. 2004. Nonsense-mediated mRNA decay: terminating erroneous gene expression. *Curr Opin Cell Biol* **16**: 293–299.

Barré-Sinoussi F, Chermann JC, Rey F, Nugeyre MT, Chamaret S, Gruest J, Dauguet C, Axler-Blin C, Vézinet-Brun F, Rouzioux C, et al. 1983. Isolation of a T-lymphotropic retrovirus from a patient at risk for acquired immune deficiency syndrome (AIDS). *Science* **220**: 868–871.

Baumert TF, Rösler C, Malim MH, Weizsäcker von F. 2007. Hepatitis B virus DNA is subject to extensive editing by the human deaminase APOBEC3C. *Hepatology* **46**: 682–689.

Berger G, Durand S, Fargier G, Nguyen X-N, Cordeil S, Bouaziz S, Muriaux D, Darlix J-L, Cimarelli A. 2011. APOBEC3A is a specific inhibitor of the early phases of HIV-1 infection in myeloid cells. *PLoS Pathog* **7**: e1002221.

Bess JW, Gorelick RJ, Bosche WJ, Henderson LE, Arthur LO. 1997. Microvesicles are a source of contaminating cellular proteins found in purified HIV-1 preparations. *Virology* **230**: 134–144.

Bess JW, Powell PJ, Issaq HJ, Schumack LJ, Grimes MK, Henderson LE, Arthur LO. 1992. Tightly bound zinc in human immunodeficiency virus type 1, human T-cell leukemia virus type I, and other retroviruses. *J Virol* **66**: 840–847.

Bhattacharya A, Czaplinski K, Trifillis P, He F, Jacobson A, Peltz SW. 2000. Characterization of the biochemical properties of the human Upf1 gene product that is involved in nonsense-mediated mRNA decay. *RNA* **6**: 1226–1235.

Bishop KN, Holmes RK, Malim MH. 2006. Antiviral potency of APOBEC proteins does not correlate with cytidine deamination. *J Virol* **80**: 8450–8458.

Bishop KN, Holmes RK, Sheehy AM, Malim MH. 2004. APOBEC-mediated editing of viral RNA. *Science* **305**: 645.

Bogerd HP, Doehle BP, Wiegand HL, Cullen BR. 2004. A single amino acid difference in the host APOBEC3G protein controls the primate species specificity of HIV type 1 virion infectivity factor. *Proc Natl Acad Sci USA* **101**: 3770–3774.

Bolinger C, Sharma A, Singh D, Yu L, Boris-Lawrie K. 2010. RNA helicase A modulates translation of HIV-1 and infectivity of progeny virions. *Nucleic Acids Res* **38**: 1686–1696.

Bonvin M, Achermann F, Greeve I, Stroka D, Keogh A, Inderbitzin D, Candinas D, Sommer P, Wain-Hobson S, Vartanian J-P, et al. 2006. Interferon-inducible expression of APOBEC3 editing enzymes in human hepatocytes and inhibition of hepatitis B virus replication. *Hepatology* **43**: 1364–1374.

Braaten D, Franke EK, Luban J. 1996. Cyclophilin A is required for an early step in the life cycle of human immunodeficiency virus type 1 before the initiation of reverse transcription. *J Virol* **70**: 3551–3560.

Brandano L, Stevenson M. 2012. A highly conserved residue in the C-terminal helix of HIV-1 matrix is required for envelope incorporation into virus particles. *J Virol* **86**: 2347–2359.

Brass AL, Dykxhoorn DM, Benita Y, Yan N, Engelman A, Xavier RJ, Lieberman J, Elledge SJ. 2008. Identification of host proteins required for HIV infection through a functional genomic screen. *Science* **319**: 921–926.

Breslow JL. 1988. Apolipoprotein genetic variation and human disease. *Physiol Rev* **68**: 85–132.

Briggs JAG, Simon MN, Gross I, Kräusslich H-G, Fuller SD, Vogt VM, Johnson MC. 2004. The stoichiometry of Gag protein in HIV-1. *Nat Struct Mol Biol* **11**: 672–675.

Brogna S, Wen J. 2009. Nonsense-mediated mRNA decay (NMD) mechanisms. *Nat Struct Mol Biol* **16**: 107–113.

Brumbaugh KM, Otterness DM, Geisen C, Oliveira V, Brognard J, Li X, Lejeune F, Tibbetts RS, Maquat LE, Abraham RT. 2004. The mRNA surveillance protein hSMG-1 functions in genotoxic stress response pathways in mammalian cells. *Mol Cell* **14**: 585–598.

Buchwald G, Ebert J, Basquin C, Sauliere J, Jayachandran U, Bono F, Le Hir H, Conti E. 2010. Insights into the recruitment of the NMD machinery from the crystal structure of a core EJC-UPF3b complex. *Proc Natl Acad Sci USA* **107**: 10050–10055.

Buckman JS, Bosche WJ, Gorelick RJ. 2003. Human immunodeficiency virus type 1 nucleocapsid zn(2+) fingers are required for efficient reverse transcription, initial integration processes, and protection of newly synthesized viral DNA. *J Virol* **77**: 1469–1480.

Burdick R, Smith JL, Chaipan C, Friew Y, Chen J, Venkatachari NJ, Delviks-Frankenberry KA, Hu W-S, Pathak VK. 2010. P body-associated protein Mov10 inhibits HIV-1 replication at multiple stages. *J Virol* **84**: 10241–10253.

Burton DR, Desrosiers RC, Johnson PR, Koff WC. 2004. An AIDS vaccine: no time to give up. *Lancet* **364**: 1938.

Butler SL, Johnson EP, Bushman FD. 2002. Human immunodeficiency virus cDNA metabolism: notable stability of two-long terminal repeat circles. *J Virol* **76**: 3739–3747.

Butsch M, Boris-Lawrie K. 2002. Destiny of unspliced retroviral RNA: ribosome and/or virion? *J Virol* **76**: 3089–3094.

Bühler M, Steiner S, Mohn F, Paillusson A, Mühlemann O. 2006. EJC-independent degradation of nonsense immunoglobulin-mu mRNA depends on 3' UTR length. *Nat Struct Mol Biol* **13**: 462–464.

Carastro LM, Tan C-K, Selg M, Jäck H-M, So AG, Downey KM. 2002. Identification of delta helicase as the bovine homolog of HUPF1: demonstration of an interaction with the third subunit of DNA polymerase delta. *Nucleic Acids Res* **30**: 2232–2243.

Catanzaro AT, Koup RA, Roederer M, Bailer RT, Enama ME, Moodie Z, Gu L, Martin JE, Novik L, Chakrabarti BK, et al. 2006. Phase 1 safety and immunogenicity evaluation of a multiclade HIV-1 candidate vaccine delivered by a replication-

defective recombinant adenovirus vector. *J Infect Dis* **194**: 1638–1649.

Cavrois M, de Noronha C, Greene WC. 2002. A sensitive and specific enzyme-based assay detecting HIV-1 virion fusion in primary T lymphocytes. *Nat Biotechnol* **20**: 1151–1154.

CDC. 1982a. Current Trends Update on Acquired Immune Deficiency Syndrome (AIDS). *Morbidity and Mortality Weekly Reports* **31**: 507–508.

CDC. 1982b. Epidemiologic Notes and Reports Pneumocystis carinii Pneumonia among Persons with Hemophilia A. *Morbidity and Mortality Weekly Reports* **31**: 356–367.

CDC. 1981a. Follow-up on Kaposi's Sarcoma and Pneumocystis Pneumonia. *Morbidity and Mortality Weekly Reports* **30**: 409–410.

CDC. 1981b. Kaposi's Sarcoma and Pneumocystis Pneumonia Among Heterosexual Men - New York and California. *Morbidity and Mortality Weekly Reports* **30**: 305–308.

Chakrabarti S, Jayachandran U, Bonneau F, Fiorini F, Basquin C, Domcke S, Le Hir H, Conti E. 2011. Molecular mechanisms for the RNA-dependent ATPase activity of Upf1 and its regulation by Upf2. *Mol Cell* **41**: 693–703.

Chamieh H, Ballut L, Bonneau F, Le Hir H. 2008. NMD factors UPF2 and UPF3 bridge UPF1 to the exon junction complex and stimulate its RNA helicase activity. *Nat Struct Mol Biol* **15**: 85–93.

Chan W-K, Bhalla AD, Le Hir H, Nguyen LS, Huang L, Gécz J, Wilkinson MF. 2009. A UPF3-mediated regulatory switch that maintains RNA surveillance. *Nat Struct Mol Biol* **16**: 747–753.

Chappelle R. 2012. FDA approves first over-the-counter home-use rapid HIV test. *fdagov*.

Chawla R, Redon S, Raftopoulou C, Wischnewski H, Gagos S, Azzalin CM. 2011. Human UPF1 interacts with TPP1 and telomerase and sustains telomere leading-strand replication. *EMBO J* **30**: 4047–4058.

Chen C-Y, Liu X, Boris-Lawrie K, Sharma A, Jeang K-T. 2012. Cellular RNA helicases and HIV-1: Insights from genome-wide, proteomic, and molecular studies. *Virus Res*.

Chen H, Lilley CE, Yu Q, Lee DV, Chou J, Narvaiza I, Landau NR, Weitzman MD. 2006. APOBEC3A is a potent inhibitor of adeno-associated virus and retrotransposons. *Curr Biol* **16**: 480–485.

Chen K-M, Harjes E, Gross PJ, Fahmy A, Lu Y, Shindo K, Harris RS, Matsuo H. 2008. Structure of the DNA deaminase domain of the HIV-1 restriction factor APOBEC3G.

Nature **452**: 116–119.

Cheng Z, Morisawa G, Song H. 2010. Biochemical characterization of human Upf1 helicase. *Methods Mol Biol* **587**: 327–338.

Cheng Z, Muhlrad D, Lim MK, Parker R, Song H. 2007. Structural and functional insights into the human Upf1 helicase core. *EMBO J* **26**: 253–264.

Cherepanov P, Devroe E, Silver PA, Engelman A. 2004. Identification of an evolutionarily conserved domain in human lens epithelium-derived growth factor/transcriptional co-activator p75 (LEDGF/p75) that binds HIV-1 integrase. *J Biol Chem* **279**: 48883–48892.

Chertova E, Chertov O, Coren LV, Roser JD, Trubey CM, Bess JW, Sowder RC, Barsov E, Hood BL, Fisher RJ, et al. 2006. Proteomic and biochemical analysis of purified human immunodeficiency virus type 1 produced from infected monocyte-derived macrophages. *J Virol* **80**: 9039–9052.

Chiu Y-L, Greene WC. 2008. The APOBEC3 cytidine deaminases: an innate defensive network opposing exogenous retroviruses and endogenous retroelements. *Annu Rev Immunol* **26**: 317–353.

Chiu Y-L, Soros VB, Kreisberg JF, Stopak K, Yonemoto W, Greene WC. 2005. Cellular APOBEC3G restricts HIV-1 infection in resting CD4+ T cells. *Nature* **435**: 108–114.

Chiu Y-L, Soros VB, Kreisberg JF, Stopak K, Yonemoto W, Greene WC. 2010. Cellular APOBEC3G restricts HIV-1 infection in resting CD4+ T cells. *Nature* **466**: 276–276.

Chiu Y-L, Witkowska HE, Hall SC, Santiago M, Soros VB, Esnault C, Heidmann T, Greene WC. 2006. High-molecular-mass APOBEC3G complexes restrict Alu retrotransposition. *Proc Natl Acad Sci USA* **103**: 15588–15593.

Christ F, Thys W, De Rijck J, Gijsbers R, Albanese A, Arosio D, Emiliani S, Rain J-C, Benarous R, Cereseto A, et al. 2008. Transportin-SR2 imports HIV into the nucleus. *Curr Biol* **18**: 1192–1202.

Chu C-Y, Rana TM. 2006. Translation repression in human cells by microRNA-induced gene silencing requires RCK/p54. *PLoS Biol* **4**: e210.

Cihlar T, Ray AS. 2010. Nucleoside and nucleotide HIV reverse transcriptase inhibitors: 25 years after zidovudine. *Antiviral Res* **85**: 39–58.

Ciuffi A, Llano M, Poeschla E, Hoffmann C, Leipzig J, Shinn P, Ecker JR, Bushman F. 2005. A role for LEDGF/p75 in targeting HIV DNA integration. *Nat Med* **11**: 1287–1289.

Clapham PR, Weiss RA. 1997. Immunodeficiency viruses. Spoilt for choice of co-receptors. *Nature* **388**: 230–231.

Cocohoba J, Dong B. 2008. Raltegravir: The First HIV Integrase Inhibitor. *Clinical Therapeutics* **30**: 95–105.

Cocude C, Truong M-J, Billaut-Mulot O, Delsart V, Darcissac E, Capron A, Mouton Y, Bahr GM. 2003. A novel cellular RNA helicase, RH116, differentially regulates cell growth, programmed cell death and human immunodeficiency virus type 1 replication. *J Gen Virol* **84**: 3215–3225.

Coffin JM. 1979. Structure, replication, and recombination of retrovirus genomes: some unifying hypotheses. *J Gen Virol* **42**: 1–26.

Coffin JM, Hughes SH, Varmus HE, Coffin JM, Hughes SH, Varmus HE. 1997. *The Interactions of Retroviruses and their Hosts*. Cold Spring Harbor Laboratory Press, Cold Spring Harbor (NY).

Cohen J. 2007. AIDS research. Did Merck's failed HIV vaccine cause harm? *Science* **318**: 1048-1049.

Cohen J. 2009. HIV/AIDS research. Beyond Thailand: making sense of a qualified AIDS vaccine "success". *Science* **326**: 652-653.

Cohen J. 2010. New HIV Infections Drop, But Treatment Demands Rise. *Science* **330**: 1301.

Cohen J. 2011. The emerging race to cure HIV infections. *Science* **332**: 784-789.

Cohen J, Enserink M. 2008. Nobel Prize in Physiology or Medicine. HIV, HPV researchers honored, but one scientist is left out. *Science* **332**: 174-175.

Cougot N, Babajko S, Séraphin B. 2004. Cytoplasmic foci are sites of mRNA decay in human cells. *J Cell Biol* **165**: 1171–1173.

Czaplinski K, Ruiz-Echevarria MJ, Paushkin SV, Han X, Weng Y, Perlick HA, Dietz HC, Ter-Avanesyan MD, Peltz SW. 1998. The surveillance complex interacts with the translation release factors to enhance termination and degrade aberrant mRNAs. *Genes Dev* **12**: 1665–1677.

Czaplinski K, Weng Y, Hagan KW, Peltz SW. 1995. Purification and characterization of the Upf1 protein: a factor involved in translation and mRNA degradation. *RNA* **1**: 610–623.

Daecke J, Fackler OT, Dittmar MT, Kräusslich H-G. 2005. Involvement of clathrin-mediated endocytosis in human immunodeficiency virus type 1 entry. *J Virol* **79**:

1581–1594.

Dalgleish AG, Beverley PCL, Clapham PR, Crawford DH, Greaves MF, Weiss RA. 1984. The CD4 (T4) antigen is an essential component of the receptor for the AIDS retrovirus. *Nature* **312**: 763–767.

Dang Y, Wang X, Esselman WJ, Zheng Y-H. 2006. Identification of APOBEC3DE as another antiretroviral factor from the human APOBEC family. *J Virol* **80**: 10522–10533.

Daniel R, Katz RA, Skalka AM. 1999. A role for DNA-PK in retroviral DNA integration. *Science* **284**: 644–647.

Dehart JL, Andersen JL, Zimmerman ES, Ardon O, An DS, Blackett J, Kim B, Planelles V. 2005. The ataxia telangiectasia-mutated and Rad3-related protein is dispensable for retroviral integration. *J Virol* **79**: 1389–1396.

Deng H, Liu R, Ellmeier W, Choe S, Unutmaz D, Burkhart M, Di Marzio P, Marmon S, Sutton RE, Hill CM, et al. 1996. Identification of a major co-receptor for primary isolates of HIV-1. *Nature* **381**: 661–666.

Dettenhofer M, Yu XF. 1999. Highly purified human immunodeficiency virus type 1 reveals a virtual absence of Vif in virions. *J Virol* **73**: 1460–1467.

Diaz-Griffero F. 2012. The Role of TNPO3 in HIV-1 Replication. *Mol Biol Int* **2012**: 868597.

Dimitrov DS, Willey RL, Sato H, Chang LJ, Blumenthal R, Martin MA. 1993. Quantitation of human immunodeficiency virus type 1 infection kinetics. *J Virol* **67**: 2182–2190.

Doehle BP, Schäfer A, Cullen BR. 2005a. Human APOBEC3B is a potent inhibitor of HIV-1 infectivity and is resistant to HIV-1 Vif. *Virology* **339**: 281–288.

Doehle BP, Schäfer A, Wiegand HL, Bogerd HP, Cullen BR. 2005b. Differential sensitivity of murine leukemia virus to APOBEC3-mediated inhibition is governed by virion exclusion. *J Virol* **79**: 8201–8207.

Dominski Z, Marzluff WF. 1999. Formation of the 3' end of histone mRNA. *Gene* **239**: 1–14.

Dominski Z, Zheng LX, Sanchez R, Marzluff WF. 1999. Stem-loop binding protein facilitates 3'-end formation by stabilizing U7 snRNP binding to histone pre-mRNA. *Mol Cell Biol* **19**: 3561–3570.

Dragic T, Litwin V, Allaway GP, Martin SR, Huang Y, Nagashima KA, Cayanan C,

Maddon PJ, Koup RA, Moore JP, et al. 1996. HIV-1 entry into CD4+ cells is mediated by the chemokine receptor CC-CKR-5. *Nature* **381**: 667–673.

Durand S, Cougot N, Mahuteau-Betzer F, Nguyen C-H, Grierson DS, Bertrand E, Tazi J, Lejeune F. 2007. Inhibition of nonsense-mediated mRNA decay (NMD) by a new chemical molecule reveals the dynamic of NMD factors in P-bodies. *J Cell Biol* **178**: 1145–1160.

Dutko JA, Schäfer A, Kenny AE, Cullen BR, Curcio MJ. 2005. Inhibition of a yeast LTR retrotransposon by human APOBEC3 cytidine deaminases. *Curr Biol* **15**: 661–666.

Ejima T, Hirota M, Mizukami T, Otsuka M, Fujita M. 2011. An anti-HIV-1 compound that increases steady-state expression of apoplipoprotein B mRNA-editing enzyme-catalytic polypeptide-like 3G. *Int J Mol Med* **28**: 613–616.

Emerman M, Malim MH. 1998. HIV-1 regulatory/accessory genes: keys to unraveling viral and host cell biology. *Science* **280**: 1880–1884.

Emiliani S, Mousnier A, Busschots K, Maroun M, Van Maele B, Tempé D, Vandekerckhove L, Moisant F, Ben-Slama L, Witvrouw M, et al. 2005. Integrase mutants defective for interaction with LEDGF/p75 are impaired in chromosome tethering and HIV-1 replication. *J Biol Chem* **280**: 25517–25523.

Esnault C, Heidmann O, Delebecque F, Dewannieux M, Ribet D, Hance AJ, Heidmann T, Schwartz O. 2005. APOBEC3G cytidine deaminase inhibits retrotransposition of endogenous retroviruses. *Nature* **433**: 430–433.

Estébanez M, Arribas JR. 2012. Protease inhibitor monotherapy: what is its role? *Curr HIV/AIDS Rep* **9**: 179–185.

Eulalio A, Behm-Ansmant I, Izaurralde E. 2007. P bodies: at the crossroads of post-transcriptional pathways. *Nat Rev Mol Cell Biol* **8**: 9–22.

Fairman-Williams ME, Guenther U-P, Jankowsky E. 2010. SF1 and SF2 helicases: family matters. *Curr Opin Struct Biol* **20**: 313–324.

Fassati A, Goff SP. 2001. Characterization of intracellular reverse transcription complexes of human immunodeficiency virus type 1. *J Virol* **75**: 3626–3635.

Feng Y, Broder CC, Kennedy PE, Berger EA. 1996. HIV-1 entry cofactor: functional cDNA cloning of a seven-transmembrane, G protein-coupled receptor. *Science* **272**: 872–877.

Flexner C. 2007. HIV drug development: the next 25 years. *Nat Rev Drug Discov* **6**: 959–966.

Forshey BM, Aiken C. 2003. Disassembly of human immunodeficiency virus type 1 cores in vitro reveals association of Nef with the subviral ribonucleoprotein complex. *J Virol* **77**: 4409–4414.

Franke EK, Yuan HE, Luban J. 1994. Specific incorporation of cyclophilin A into HIV-1 virions. *Nature* **372**: 359–362.

Frankel AD, Young JA. 1998. HIV-1: fifteen proteins and an RNA. *Annu Rev Biochem* **67**: 1–25.

Franks TM, Singh G, Lykke-Andersen J. 2010. Upf1 ATPase-dependent mRNP disassembly is required for completion of nonsense- mediated mRNA decay. *Cell* **143**: 938–950.

Freed EO. 1998. HIV-1 gag proteins: diverse functions in the virus life cycle. *Virology* **251**: 1–15.

Furtak V, Mulky A, Rawlings SA, Kozhaya L, Lee K, Kewalramani VN, Unutmaz D. 2010. Perturbation of the P-body component Mov10 inhibits HIV-1 infectivity. *PLoS ONE* **5**: e9081.

Gaddis NC, Sheehy AM, Ahmad KM, Swanson CM, Bishop KN, Beer BE, Marx PA, Gao F, Bibollet-Ruche F, Hahn BH, et al. 2004. Further investigation of simian immunodeficiency virus Vif function in human cells. *J Virol* **78**: 12041–12046.

Gallo R. 2003. The Discovery of HIV as the Cause of AIDS. *N Engl J Med* **349**: 2283-2285.

Gallo RC, Montagnier L. 1987. The chronology of AIDS research. *Nature* **326**: 435–436.

Gallois-Montbrun S, Kramer B, Swanson CM, Byers H, Lynham S, Ward M, Malim MH. 2007. Antiviral protein APOBEC3G localizes to ribonucleoprotein complexes found in P bodies and stress granules. *J Virol* **81**: 2165–2178.

Gandhi SK, Siliciano JD, Bailey JR, Siliciano RF, Blankson JN. 2008. Role of APOBEC3G/F-mediated hypermutation in the control of human immunodeficiency virus type 1 in elite suppressors. *J Virol* **82**: 3125–3130.

Gao K, Gorelick RJ, Johnson DG, Bushman F. 2003. Cofactors for human immunodeficiency virus type 1 cDNA integration in vitro. *J Virol* **77**: 1598–1603.

Garrus JE, Schwedler von UK, Pornillos OW, Morham SG, Zavitz KH, Wang HE, Wettstein DA, Stray KM, Côté M, Rich RL, et al. 2001. Tsg101 and the vacuolar protein sorting pathway are essential for HIV-1 budding. *Cell* **107**: 55–65.

Gehring NH, Neu-Yilik G, Schell T, Hentze MW, Kulozik AE. 2003. Y14 and hUpf3b

form an NMD-activating complex. *Mol Cell* **11**: 939–949.

Gluschankof P, Mondor I, Gelderblom HR, Sattentau QJ. 1997. Cell membrane vesicles are a major contaminant of gradient-enriched human immunodeficiency virus type-1 preparations. *Virology* **230**: 125–133.

Goff SP. 2007. Host factors exploited by retroviruses. *Nat Rev Microbiol* **5**: 253–263.

Goila-Gaur R, Khan MA, Miyagi E, Strebel K. 2009. Differential sensitivity of "old" versus “new” APOBEC3G to human immunodeficiency virus type 1 vif. *J Virol* **83**: 1156–1160.

Gong C, Kim YK, Woeller CF, Tang Y, Maquat LE. 2009. SMD and NMD are competitive pathways that contribute to myogenesis: effects on PAX3 and myogenin mRNAs. *Genes Dev* **23**: 54–66.

Göttlinger HG, Dorfman T, Sodroski JG, Haseltine WA. 1991. Effect of mutations affecting the p6 gag protein on human immunodeficiency virus particle release. *Proc Natl Acad Sci USA* **88**: 3195–3199.

Graham BS, Koup RA, Roederer M, Bailer RT, Enama ME, Moodie Z, Martin JE, McCluskey MM, Chakrabarti BK, Lamoreaux L, et al. 2006. Phase 1 safety and immunogenicity evaluation of a multiclade HIV-1 DNA candidate vaccine. *J Infect Dis* **194**: 1650–1660.

Grant RM, LaMa J, Anderson PL, McMahan V, Liu A, Vargas L, Goicochea P, Casapia M, Guanira-Carranza JV, Ramirez-Cardich ME, et al. 2010. Preexposure Chemoprophylaxis for HIV Prevention in Men Who Have Sex with Men. *N Engl J Med* **363**: 2587–2599.

Gurer C, Cimarelli A, Luban J. 2002. Specific incorporation of heat shock protein 70 family members into primate lentiviral virions. *J Virol* **76**: 4666–4670.

Harris RS, Bishop KN, Sheehy AM, Craig HM, Petersen-Mahrt SK, Watt IN, Neuberger MS, Malim MH. 2003. DNA Deamination Mediates Innate Immunity to Retroviral Infection. *Cell* **113**: 803–809.

Hatziioannou T, Perez-Caballero D, Cowan S, Bieniasz PD. 2005. Cyclophilin interactions with incoming human immunodeficiency virus type 1 capsids with opposing effects on infectivity in human cells. *J Virol* **79**: 176–183.

Hatziioannou T, Perez-Caballero D, Yang A, Cowan S, Bieniasz PD. 2004. Retrovirus resistance factors Ref1 and Lv1 are species-specific variants of TRIM5alpha. *Proc Natl Acad Sci USA* **101**: 10774–10779.

He F, Brown AH, Jacobson A. 1997. Upf1p, Nmd2p, and Upf3p are interacting components of the yeast nonsense-mediated mRNA decay pathway. *Mol Cell Biol* **17**: 1580–1594.

Hogg JR, Goff SP. 2010. Upf1 senses 3'UTR length to potentiate mRNA decay. *Cell* **143**: 379–389.

Holden LG, Prochnow C, Chang YP, Bransteitter R, Chelico L, Sen U, Stevens RC, Goodman MF, Chen XS. 2008. Crystal structure of the anti-viral APOBEC3G catalytic domain and functional implications. *Nature* **456**: 121–124.

Holmes RK, Malim MH, Bishop KN. 2007. APOBEC-mediated viral restriction: not simply editing? *Trends Biochem Sci* **32**: 118–128.

Hopkins AL, Groom CR. 2002. The druggable genome. *Nat Rev Drug Discov* **1**: 727–730.

Hulme AE, Perez O, Hope TJ. 2011. Complementary assays reveal a relationship between HIV-1 uncoating and reverse transcription. *Proc Natl Acad Sci USA* **108**: 9975–9980.

Huthoff H, Malim MH. 2007. Identification of amino acid residues in APOBEC3G required for regulation by human immunodeficiency virus type 1 Vif and Virion encapsidation. *J Virol* **81**: 3807–3815.

Iborra FJ, Escargueil AE, Kwek KY, Akoulitchev A, Cook PR. 2004. Molecular cross-talk between the transcription, translation, and nonsense-mediated decay machineries. *J Cell Sci* **117**: 899–906.

Isken O, Maquat LE. 2008. The multiple lives of NMD factors: balancing roles in gene and genome regulation. *Nat Rev Genet* **9**: 699–712.

Ivanov PV, Gehring NH, Kunz JB, Hentze MW, Kulozik AE. 2008. Interactions between UPF1, eRFs, PABP and the exon junction complex suggest an integrated model for mammalian NMD pathways. *EMBO J* **27**: 736–747.

Iwatani Y, Takeuchi H, Strebel K, Levin JG. 2006. Biochemical activities of highly purified, catalytically active human APOBEC3G: correlation with antiviral effect. *J Virol* **80**: 5992–6002.

Jaenisch R, Jähner D, Nobis P, Simon I, Löhler J, Harbers K, Grotkopp D. 1981. Chromosomal position and activation of retroviral genomes inserted into the germ line of mice. *Cell* **24**: 519–529.

Janini M, Rogers M, Birx DR, McCutchan FE. 2001. Human immunodeficiency virus

type 1 DNA sequences genetically damaged by hypermutation are often abundant in patient peripheral blood mononuclear cells and may be generated during near-simultaneous infection and activation of CD4(+) T cells. *J Virol* **75**: 7973–7986.

Jankowsky E, Gross CH, Shuman S, Pyle AM. 2001. Active disruption of an RNA-protein interaction by a DExH/D RNA helicase. *Science* **291**: 121–125.

Jarmuz A, Chester A, Bayliss J, Gisbourne J, Dunham I, Scott J, Navaratnam N. 2002. An anthropoid-specific locus of orphan C to U RNA-editing enzymes on chromosome 22. *Genomics* **79**: 285–296.

Jefferson E. 2012. FDA approves first drug for reducing the risk of sexually acquired HIV infection. *FDA*.

Jin H, Suh MR, Han J, Yeom K-H, Lee Y, Heo I, Ha M, Hyun S, Kim VN. 2009. Human UPF1 participates in small RNA-induced mRNA downregulation. *Mol Cell Biol* **29**: 5789–5799.

Johnson DF, Poksay KS, Innerarity TL. 1993. The mechanism for apo-B mRNA editing is deamination. *Biochem Biophys Res Commun* **195**: 1204–1210.

Jouvenet N, Neil SJD, Zhadina M, Zang T, Kratovac Z, Lee Y, McNatt M, Hatziioannou T, Bieniasz PD. 2009. Broad-spectrum inhibition of retroviral and filoviral particle release by tetherin. *J Virol* **83**: 1837–1844.

Kadlec J, Guilligay D, Ravelli RB, Cusack S. 2006. Crystal structure of the UPF2-interacting domain of nonsense-mediated mRNA decay factor UPF1. *RNA* **12**: 1817–1824.

Kamata M, Nagaoka Y, Chen ISY. 2009. Reassessing the role of APOBEC3G in human immunodeficiency virus type 1 infection of quiescent CD4+ T-cells. *PLoS Pathog* **5**: e1000342.

Kao S, Khan MA, Miyagi E, Plishka R, Buckler-White A, Strebel K. 2003. The human immunodeficiency virus type 1 Vif protein reduces intracellular expression and inhibits packaging of APOBEC3G (CEM15), a cellular inhibitor of virus infectivity. *J Virol* **77**: 11398–11407.

Kashima I, Yamashita A, Izumi N, Kataoka N, Morishita R, Hoshino S, Ohno M, Dreyfuss G, Ohno S. 2006. Binding of a novel SMG-1-Upf1-eRF1-eRF3 complex (SURF) to the exon junction complex triggers Upf1 phosphorylation and nonsense-mediated mRNA decay. *Genes Dev* **20**: 355–367.

Kato H, Takeuchi O, Sato S, Yoneyama M, Yamamoto M, Matsui K, Uematsu S, Jung A, Kawai T, Ishii KJ, et al. 2006. Differential roles of MDA5 and RIG-I helicases in the

recognition of RNA viruses. *Nature* **441**: 101–105.

Kaygun H, Marzluff WF. 2005. Regulated degradation of replication-dependent histone mRNAs requires both ATR and Upf1. *Nat Struct Mol Biol* **12**: 794–800.

Kedersha N, Anderson P. 2007. Mammalian Stress Granules and Processing Bodies. *Meth Enzymol* **431**: 61–81.

Kedersha N, Stoecklin G, Ayodele M, Yacono P, Lykke-Andersen J, Fritzler MJ, Scheuner D, Kaufman RJ, Golan DE, Anderson P. 2005. Stress granules and processing bodies are dynamically linked sites of mRNP remodeling. *J Cell Biol* **169**: 871–884.

Khurana S, Krementsov DN, de Parseval A, Elder JH, Foti M, Thali M. 2007. Human immunodeficiency virus type 1 and influenza virus exit via different membrane microdomains. *J Virol* **81**: 12630–12640.

Kilby JM, Hopkins S, Venetta TM, DiMassimo B, Cloud GA, Lee JY, Alldredge L, Hunter E, Lambert D, Bolognesi D, et al. 1998. Potent suppression of HIV-1 replication in humans by T-20, a peptide inhibitor of gp41-mediated virus entry. *Nat Med* **4**: 1302–1307.

Kim SY, Byrn R, Groopman J, Baltimore D. 1989. Temporal aspects of DNA and RNA synthesis during human immunodeficiency virus infection: evidence for differential gene expression. *J Virol* **63**: 3708–3713.

Kim YK, Furic L, DesGroseillers L, Maquat LE. 2005. Mammalian Staufen1 recruits Upf1 to specific mRNA 3'UTRs so as to elicit mRNA decay. *Cell* **120**: 195–208.

Kim YK, Furic L, Parisien M, Major F, DesGroseillers L, Maquat LE. 2007. Staufen1 regulates diverse classes of mammalian transcripts. *EMBO J* **26**: 2670–2681.

Kimpton J, Emerman M. 1992. Detection of replication-competent and pseudotyped human immunodeficiency virus with a sensitive cell line on the basis of activation of an integrated beta-galactosidase gene. *J Virol* **66**: 2232–2239.

Koonin EV. 1992. A new group of putative RNA helicases. *Trends Biochem Sci* **17**: 495–497.

Kourteva Y, De Pasquale M, Allos T, McMunn C, D'Aquila RT. 2012. APOBEC3G expression and hypermutation are inversely associated with human immunodeficiency virus type 1 (HIV-1) burden in vivo. *Virology* **430**: 1–9.

Kozak SL, Marin M, Rose KM, Bystrom C, Kabat D. 2006. The anti-HIV-1 editing enzyme APOBEC3G binds HIV-1 RNA and messenger RNAs that shuttle between

polysomes and stress granules. *J Biol Chem* **281**: 29105–29119.

Köck J, Blum HE. 2008. Hypermutation of hepatitis B virus genomes by APOBEC3G, APOBEC3C and APOBEC3H. *J Gen Virol* **89**: 1184–1191.

König R, Zhou Y, Elleder D, Diamond TL, Bonamy GMC, Irelan JT, Chiang C-Y, Tu BP, De Jesus PD, Lilley CE, et al. 2008. Global analysis of host-pathogen interactions that regulate early-stage HIV-1 replication. *Cell* **135**: 49–60.

Krishnan L, Matreyek KA, Oztop I, Lee K, Tipper CH, Li X, Dar MJ, Kewalramani VN, Engelman A. 2010. The requirement for cellular transportin 3 (TNPO3 or TRN-SR2) during infection maps to human immunodeficiency virus type 1 capsid and not integrase. *J Virol* **84**: 397–406.

Kupzig S, Korolchuk V, Rollason R, Sugden A, Wilde A, Banting G. 2003. Bst-2/HM1.24 is a raft-associated apical membrane protein with an unusual topology. *Traffic* **4**: 694–709.

Layne SP, Merges MJ, Dembo M, Spouge JL, Conley SR, Moore JP, Raina JL, Renz H, Gelderblom HR, Narat PL. 1992. Factors underlying spontaneous inactivation and susceptibility to neutralization of human immunodeficiency virus. *Virology* **189**: 695–714.

Le Hir H, Gatfield D, Izaurralde E, Moore MJ. 2001. The exon-exon junction complex provides a binding platform for factors involved in mRNA export and nonsense-mediated mRNA decay. *EMBO J* **20**: 4987–4997.

Le Hir H, Moore MJ, Maquat LE. 2000. Pre-mRNA splicing alters mRNP composition: evidence for stable association of proteins at exon-exon junctions. *Genes Dev* **14**: 1098–1108.

Lee K, Ambrose Z, Martin TD, Oztop I, Mulky A, Julias JG, Vandegraaff N, Baumann JG, Wang R, Yuen W, et al. 2010. Flexible use of nuclear import pathways by HIV-1. *Cell Host Microbe* **7**: 221–233.

Leeds P, Wood JM, Lee BS, Culbertson MR. 1992. Gene products that promote mRNA turnover in Saccharomyces cerevisiae. *Mol Cell Biol* **12**: 2165–2177.

Lenz G, Staudt LM. 2010. Aggressive lymphomas. *N Engl J Med* **362**: 1417–1429.

Liu R, Paxton WA, Choe S, Ceradini D, Martin SR, Horuk R, MacDonald ME, Stuhlmann H, Koup RA, Landau NR. 1996. Homozygous defect in HIV-1 coreceptor accounts for resistance of some multiply-exposed individuals to HIV-1 infection. *Cell* **86**: 367–377.

Llano M, Delgado S, Vanegas M, Poeschla EM. 2004. Lens epithelium-derived growth factor/p75 prevents proteasomal degradation of HIV-1 integrase. *J Biol Chem* **279**: 55570–55577.

Llano M, Saenz DT, Meehan A, Wongthida P, Peretz M, Walker WH, Teo W, Poeschla EM. 2006. An essential role for LEDGF/p75 in HIV integration. *Science* **314**: 461–464.

Luban J, Bossolt KL, Franke EK, Kalpana GV, Goff SP. 1993. Human immunodeficiency virus type 1 Gag protein binds to cyclophilins A and B. *Cell* **73**: 1067–1078.

Lykke-Andersen J, Shu MD, Steitz JA. 2000. Human Upf proteins target an mRNA for nonsense-mediated decay when bound downstream of a termination codon. *Cell* **103**: 1121–1131.

Ma J, Rong L, Zhou Y, Roy BB, Lu J, Abrahamyan L, Mouland AJ, Pan Q, Liang C. 2008. The requirement of the DEAD-box protein DDX24 for the packaging of human immunodeficiency virus type 1 RNA. *Virology* **375**: 253–264.

Madani N, Kabat D. 1998. An endogenous inhibitor of human immunodeficiency virus in human lymphocytes is overcome by the viral Vif protein. *J Virol* **72**: 10251–10255.

Maderazo AB, He F, Mangus DA, Jacobson A. 2000. Upf1p control of nonsense mRNA translation is regulated by Nmd2p and Upf3p. *Mol Cell Biol* **20**: 4591–4603.

Malim MH, Bieniasz PD. 2012. HIV Restriction Factors and Mechanisms of Evasion. *Cold Spring Harb Perspect Med* **2**: a006940.

Mangeat B, Turelli P, Caron G, Friedli M, Perrin L, Trono D. 2003. Broad antiretroviral defence by human APOBEC3G through lethal editing of nascent reverse transcripts. *Nature* **424**: 99–103.

Mangeat B, Turelli P, Liao S, Trono D. 2004. A single amino acid determinant governs the species-specific sensitivity of APOBEC3G to Vif action. *J Biol Chem* **279**: 14481–14483.

Maquat LE. 2004. Nonsense-mediated mRNA decay: splicing, translation and mRNP dynamics. *Nat Rev Mol Cell Biol* **5**: 89–99.

Mariani R, Chen D, Schröfelbauer B, Navarro F, König R, Bollman B, Münk C, Nymark-McMahon H, Landau NR. 2003. Species-specific exclusion of APOBEC3G from HIV-1 virions by Vif. *Cell* **114**: 21–31.

Marin M, Rose KM, Kozak SL, Kabat D. 2003. HIV-1 Vif protein binds the editing

enzyme APOBEC3G and induces its degradation. *Nat Med* **9**: 1398–1403.

Marozsan AJ, Fraundorf E, Abraha A, Baird H, Moore D, Troyer R, Nankja I, Arts EJ. 2004. Relationships between infectious titer, capsid protein levels, and reverse transcriptase activities of diverse human immunodeficiency virus type 1 isolates. *J Virol* **78**: 11130–11141.

Martin KL, Johnson M, D'Aquila RT. 2011. APOBEC3G complexes decrease human immunodeficiency virus type 1 production. *J Virol* **85**: 9314–9326.

Martin-Serrano J, Neil SJD. 2011. Host factors involved in retroviral budding and release. *Nat Rev Microbiol* **9**: 519–531.

Martin-Serrano J, Zang T, Bieniasz PD. 2001. HIV-1 and Ebola virus encode small peptide motifs that recruit Tsg101 to sites of particle assembly to facilitate egress. *Nat Med* **7**: 1313–1319.

Mbisa JL, Barr R, Thomas JA, Vandegraaff N, Dorweiler IJ, Svarovskaia ES, Brown WL, Mansky LM, Gorelick RJ, Harris RS, et al. 2007. Human immunodeficiency virus type 1 cDNAs produced in the presence of APOBEC3G exhibit defects in plus-strand DNA transfer and integration. *J Virol* **81**: 7099–7110.

Mbisa JL, Delviks-Frankenberry KA, Thomas JA, Gorelick RJ, Pathak VK. 2009. Real-time PCR analysis of HIV-1 replication post-entry events. *Methods Mol Biol* **485**: 55–72.

McDonald D, Vodicka MA, Lucero G, Svitkina TM, Borisy GG, Emerman M, Hope TJ. Visualization of the intracellular behavior of HIV in living cells.

Medghalchi SM, Frischmeyer PA, Mendell JT, Kelly AG, Lawler AM, Dietz HC. 2001. Rent1, a trans-effector of nonsense-mediated mRNA decay, is essential for mammalian embryonic viability. *Hum Mol Genet* **10**: 99–105.

Mehle A, Goncalves J, Santa-Marta M, McPike M, Gabuzda D. 2004a. Phosphorylation of a novel SOCS-box regulates assembly of the HIV-1 Vif-Cul5 complex that promotes APOBEC3G degradation. *Genes Dev* **18**: 2861–2866.

Mehle A, Strack B, Ancuta P, Zhang C, McPike M, Gabuzda D. 2004b. Vif overcomes the innate antiviral activity of APOBEC3G by promoting its degradation in the ubiquitin-proteasome pathway. *J Biol Chem* **279**: 7792–7798.

Meister G, Landthaler M, Peters L, Chen PY, Urlaub H, Lührmann R, Tuschl T. 2005. Identification of novel argonaute-associated proteins. *Curr Biol* **15**: 2149–2155.

Melero R, Buchwald G, Castaño R, Raabe M, Gil D, Lázaro M, Urlaub H, Conti E,

Llorca O. 2012. The cryo-EM structure of the UPF-EJC complex shows UPF1 poised toward the RNA 3' end. *Nat Struct Mol Biol* **19**: 498–505– S1–2.

Mendell JT, Sharifi NA, Meyers JL, Martinez-Murillo F, Dietz HC. 2004. Nonsense surveillance regulates expression of diverse classes of mammalian transcripts and mutes genomic noise. *Nat Genet* **36**: 1073–1078.

Mercenne G, Bernacchi S, Richer D, Bec G, Henriet S, Paillart J-C, Marquet R. 2010. HIV-1 Vif binds to APOBEC3G mRNA and inhibits its translation. *Nucleic Acids Res* **38**: 633–646.

Meyer EL, Gavis ER. 2005. Staufen does double duty. *Nature structural & molecular biology*, April.

Miller MD, Farnet CM, Bushman FD. 1997. Human immunodeficiency virus type 1 preintegration complexes: studies of organization and composition. *J Virol* **71**: 5382–5390.

Miyauchi K, Kim Y, Latinovic O, Morozov V, Melikyan GB. 2009. HIV enters cells via endocytosis and dynamin-dependent fusion with endosomes. *Cell* **137**: 433–444.

Mooslehner K, Müller U, Karls U, Hamann L, Harbers K. 1991. Structure and expression of a gene encoding a putative GTP-binding protein identified by provirus integration in a transgenic mouse strain. *Mol Cell Biol* **11**: 886–893.

Mouland AJ, Mercier J, Luo M, Bernier L, DesGroseillers L, Cohen EA. 2000. The double-stranded RNA-binding protein Staufen is incorporated in human immunodeficiency virus type 1: evidence for a role in genomic RNA encapsidation. *J Virol* **74**: 5441–5451.

Muriaux D, Mirro J, Harvin D, Rein A. 2001. RNA is a structural element in retrovirus particles. *Proc Natl Acad Sci USA* **98**: 5246–5251.

Mühlemann O, Lykke-Andersen J. 2010. How and where are nonsense mRNAs degraded in mammalian cells? *RNA Biol* **7**: 28–32.

Müller B, Tessmer U, Schubert U, Kräusslich HG. 2000. Human immunodeficiency virus type 1 Vpr protein is incorporated into the virion in significantly smaller amounts than gag and is phosphorylated in infected cells. *J Virol* **74**: 9727–9731.

Nathans R, Cao H, Sharova N, Ali A, Sharkey M, Stranska R, Stevenson M, Rana TM. 2008. Small-molecule inhibition of HIV-1 Vif. *Nat Biotechnol* **26**: 1187–1192.

Nathans R, Chu C-Y, Serquina AK, Lu C-C, Cao H, Rana TM. 2009. Cellular microRNA and P bodies modulate host-HIV-1 interactions. *Mol Cell* **34**: 696–709.

Navaratnam N, Bhattacharya S, Fujino T, Patel D, Jarmuz AL, Scott J. 1995. Evolutionary origins of apoB mRNA editing: catalysis by a cytidine deaminase that has acquired a novel RNA-binding motif at its active site. *Cell* **81**: 187–195.

Navaratnam N, Morrison JR, Bhattacharya S, Patel D, Funahashi T, Giannoni F, Teng BB, Davidson NO, Scott J. 1993. The p27 catalytic subunit of the apolipoprotein B mRNA editing enzyme is a cytidine deaminase. *J Biol Chem* **268**: 20709–20712.

Navarro F, Bollman B, Chen H, König R, Yu Q, Chiles K, Landau NR. 2005. Complementary function of the two catalytic domains of APOBEC3G. *Virology* **333**: 374–386.

Neil SJD, Eastman SW, Jouvenet N, Bieniasz PD. 2006. HIV-1 Vpu promotes release and prevents endocytosis of nascent retrovirus particles from the plasma membrane. *PLoS Pathog* **2**: e39.

Neil SJD, Sandrin V, Sundquist WI, Bieniasz PD. 2007. An interferon-alpha-induced tethering mechanism inhibits HIV-1 and Ebola virus particle release but is counteracted by the HIV-1 Vpu protein. *Cell Host Microbe* **2**: 193–203.

Neil SJD, Zang T, Bieniasz PD. 2008. Tetherin inhibits retrovirus release and is antagonized by HIV-1 Vpu. *Nature* **451**: 425–430.

Newman ENC, Holmes RK, Craig HM, Klein KC, Lingappa JR, Malim MH, Sheehy AM. 2005. Antiviral function of APOBEC3G can be dissociated from cytidine deaminase activity. *Curr Biol* **15**: 166–170.

Nicholson P, Yepiskoposyan H, Metze S, Zamudio Orozco R, Kleinschmidt N, Mühlemann O. 2009. Nonsense-mediated mRNA decay in human cells: mechanistic insights, functions beyond quality control and the double-life of NMD factors. *Cell Mol Life Sci* **67**: 677–700.

Noguchi C, Hiraga N, Mori N, Tsuge M, Imamura M, Takahashi S, Fujimoto Y, Ochi H, Abe H, Maekawa T, et al. 2007. Dual effect of APOBEC3G on Hepatitis B virus. *J Gen Virol* **88**: 432–440.

Nydegger S, Khurana S, Krementsov DN, Foti M, Thali M. 2006. Mapping of tetraspanin-enriched microdomains that can function as gateways for HIV-1. *J Cell Biol* **173**: 795–807.

O'Doherty U, Swiggard WJ, Malim MH. 2000. Human immunodeficiency virus type 1 spinoculation enhances infection through virus binding. *J Virol* **74**: 10074–10080.

Ohnishi T, Yamashita A, Kashima I, Schell T, Anders KR, Grimson A, Hachiya T, Hentze MW, Anderson P, Ohno S. 2003. Phosphorylation of hUPF1 induces

formation of mRNA surveillance complexes containing hSMG-5 and hSMG-7. *Mol Cell* **12**: 1187–1200.

Okazaki I-M, Kinoshita K, Muramatsu M, Yoshikawa K, Honjo T. 2002. The AID enzyme induces class switch recombination in fibroblasts. *Nature* **416**: 340–345.

Olivieri D, Sykora MM, Sachidanandam R, Mechtler K, Brennecke J. 2010. An in vivo RNAi assay identifies major genetic and cellular requirements for primary piRNA biogenesis in Drosophila. *EMBO J* **29**: 3301–3317.

Opi S, Takeuchi H, Kao S, Khan MA, Miyagi E, Goila-Gaur R, Iwatani Y, Levin JG, Strebel K. 2006. Monomeric APOBEC3G is catalytically active and has antiviral activity. *J Virol* **80**: 4673–4682.

Ott DE. 2008. Cellular proteins detected in HIV-1. *Rev Med Virol* **18**: 159–175.

Ott DE. 2002. Potential roles of cellular proteins in HIV-1. *Rev Med Virol* **12**: 359–374.

Pace C, Keller J, Nolan D, James I, Gaudieri S, Moore C, Mallal S. 2006. Population level analysis of human immunodeficiency virus type 1 hypermutation and its relationship with APOBEC3G and vif genetic variation. *J Virol* **80**: 9259–9269.

Parent LJ, Bennett RP, Craven RC, Nelle TD, Krishna NK, Bowzard JB, Wilson CB, Puffer BA, Montelaro RC, Wills JW. 1995. Positionally independent and exchangeable late budding functions of the Rous sarcoma virus and human immunodeficiency virus Gag proteins. *J Virol* **69**: 5455–5460.

Perez-Caballero D, Zang T, Ebrahimi A, McNatt MW, Gregory DA, Johnson MC, Bieniasz PD. 2009. Tetherin inhibits HIV-1 release by directly tethering virions to cells. *Cell* **139**: 499–511.

Pertel T, Hausmann S, Morger D, Züger S, Guerra J, Lascano J, Reinhard C, Santoni FA, Uchil PD, Chatel L, et al. 2011. TRIM5 is an innate immune sensor for the retrovirus capsid lattice. *Nature* **472**: 361–365.

Petersen-Mahrt SK, Harris RS, Neuberger MS. 2002. AID mutates E. coli suggesting a DNA deamination mechanism for antibody diversification. *Nature* **418**: 99–103.

Piatak M, Saag MS, Yang LC, Clark SJ, Kappes JC, Luk KC, Hahn BH, Shaw GM, Lifson JD. 1993. High levels of HIV-1 in plasma during all stages of infection determined by competitive PCR. *Science* **259**: 1749–1754.

Pierson TC, Kieffer TL, Ruff CT, Buck C, Gange SJ, Siliciano RF. 2002. Intrinsic stability of episomal circles formed during human immunodeficiency virus type 1 replication. *J Virol* **76**: 4138–4144.

Pitisuttithum P, Rerks-Ngarm S, Bussaratid V, Dhitavat J, Maekanantawat W, Pungpak S, Suntharasamai P, Vanijanonta S, Nitayapan S, Kaewkungwal J, et al. 2011. Safety and reactogenicity of canarypox ALVAC-HIV (vCP1521) and HIV-1 gp120 AIDSVAX B/E vaccination in an efficacy trial in Thailand. *PLoS ONE* **6**: e27837.

Poiesz BJ, Ruscetti FW, Gazdar AF, Bunn PA, Minna JD, Gallo RC. 1980. Detection and isolation of type C retrovirus particles from fresh and cultured lymphocytes of a patient with cutaneous T-cell lymphoma. *Proc Natl Acad Sci USA* **77**: 7415–7419.

Pommier Y, Johnson AA, Marchand C. 2005. Integrase inhibitors to treat HIV/AIDS. *Nat Rev Drug Discov* **4**: 236–248.

Popova E, Popov S, Göttlinger HG. 2010. Human immunodeficiency virus type 1 nucleocapsid p1 confers ESCRT pathway dependence. *J Virol* **84**: 6590–6597.

Popovic M, Sarngadharan MG, Read E, Gallo RC. 1984. Detection, isolation, and continuous production of cytopathic retroviruses (HTLV-III) from patients with AIDS and pre-AIDS. *Science* **224**: 497–500.

Qian X, Balestra ME, Yamanaka S, Borén J, Lee I, Innerarity TL. 1998. Low expression of the apolipoprotein B mRNA-editing transgene in mice reduces LDL levels but does not cause liver dysplasia or tumors. *Arterioscler Thromb Vasc Biol* **18**: 1013–1020.

Quashie PK, Sloan RD, Wainberg MA. 2012. Novel therapeutic strategies targeting HIV integrase. *BMC Med* **10**: 34.

Radi M, Falchi F, Garbelli A, Samuele A, Bernardo V, Paolucci S, Baldanti F, Schenone S, Manetti F, Maga G, et al. 2012. Discovery of the first small molecule inhibitor of human DDX3 specifically designed to target the RNA binding site: Towards the next generation HIV-1 inhibitors. *Bioorg Med Chem Lett* **22**: 2094–2098.

Rehwinkel J, Behm-Ansmant I, Gatfield D, Izaurralde E. 2005. A crucial role for GW182 and the DCP1:DCP2 decapping complex in miRNA-mediated gene silencing. *RNA* **11**: 1640–1647.

Robertson D. 2003. US FDA approves new class of HIV therapeutics. *Nature biotechnology*, May.

Robinson HL, Weinhold KJ. 2006. Phase 1 clinical trials of the National Institutes of Health Vaccine Research Center HIV/AIDS candidate vaccines. *J Infect Dis* **194**: 1625–1627.

Rose KM, Marin M, Kozak SL, Kabat D. 2004. Transcriptional regulation of APOBEC3G, a cytidine deaminase that hypermutates human immunodeficiency

virus. *J Biol Chem* **279**: 41744–41749.

Roy BB, Hu J, Guo X, Russell RS, Guo F, Kleiman L, Liang C. 2006. Association of RNA helicase a with human immunodeficiency virus type 1 particles. *J Biol Chem* **281**: 12625–12635.

Rösler C, Köck J, Kann M, Malim MH, Blum HE, Baumert TF, Weizsäcker von F. 2005. APOBEC-mediated interference with hepadnavirus production. *Hepatology* **42**: 301–309.

Samson M, Libert F, Doranz BJ, Rucker J, Liesnard C, Farber CM, Saragosti S, Lapoumeroulie C, Cognaux J, Forceille C, et al. 1996. Resistance to HIV-1 infection in caucasian individuals bearing mutant alleles of the CCR-5 chemokine receptor gene. *Nature* **382**: 722–725.

Santoni de Sio FR, Trono D. 2009. APOBEC3G-depleted resting CD4+ T cells remain refractory to HIV1 infection. *PLoS ONE* **4**: e6571.

Saphire ACS, Gallay PA, Bark SJ. 2006. Proteomic analysis of human immunodeficiency virus using liquid chromatography/tandem mass spectrometry effectively distinguishes specific incorporated host proteins. *J Proteome Res* **5**: 530–538.

Sattentau QJ, Moore JP. 1991. Conformational changes induced in the human immunodeficiency virus envelope glycoprotein by soluble CD4 binding. *J Exp Med* **174**: 407–415.

Sayah DM, Sokolskaja E, Berthoux L, Luban J. 2004. Cyclophilin A retrotransposition into TRIM5 explains owl monkey resistance to HIV-1. *Nature* **430**: 569–573.

Schoeftner S, Blasco MA. 2008. Developmentally regulated transcription of mammalian telomeres by DNA-dependent RNA polymerase II. *Nat Cell Biol* **10**: 228–236.

Schröfelbauer B, Chen D, Landau NR. 2004. A single amino acid of APOBEC3G controls its species-specific interaction with virion infectivity factor (Vif). *Proc Natl Acad Sci USA* **101**: 3927–3932.

Schumacher AJ, Nissley DV, Harris RS. 2005. APOBEC3G hypermutates genomic DNA and inhibits Ty1 retrotransposition in yeast. *Proc Natl Acad Sci USA* **102**: 9854–9859.

Sekaly R-P. 2008. The failed HIV Merck vaccine study: a step back or a launching point for future vaccine development? *J Exp Med* **205**: 7–12.

Serin G, Gersappe A, Black JD, Aronoff R, Maquat LE. 2001. Identification and characterization of human orthologues to Saccharomyces cerevisiae Upf2 protein and

Upf3 protein (Caenorhabditis elegans SMG-4). *Mol Cell Biol* **21**: 209–223.

Sharkey ME, Teo I, Greenough T, Sharova N, Luzuriaga K, Sullivan JL, Bucy RP, Kostrikis LG, Haase A, Veryard C, et al. 2000. Persistence of episomal HIV-1 infection intermediates in patients on highly active anti-retroviral therapy. *Nat Med* **6**: 76–81.

Sharma A, Boris-Lawrie K. 2012. Determination of host RNA helicases activity in viral replication. *Meth Enzymol* **511**: 405–435.

Sheehy AM, Gaddis NC, Choi JD, Malim MH. 2002. Isolation of a human gene that inhibits HIV-1 infection and is suppressed by the viral Vif protein. *Nature* **418**: 646–650.

Sheehy AM, Gaddis NC, Malim MH. 2003. The antiretroviral enzyme APOBEC3G is degraded by the proteasome in response to HIV-1 Vif. *Nat Med* **9**: 1404–1407.

Sheth U, Parker R. 2006. Targeting of aberrant mRNAs to cytoplasmic processing bodies. *Cell* **125**: 1095–1109.

Shibuya T, Tange TØ, Sonenberg N, Moore MJ. 2004. eIF4AIII binds spliced mRNA in the exon junction complex and is essential for nonsense-mediated decay. *Nat Struct Mol Biol* **11**: 346–351.

Shindo K, Takaori-Kondo A, Kobayashi M, Abudu A, Fukunaga K, Uchiyama T. 2003. The enzymatic activity of CEM15/Apobec-3G is essential for the regulation of the infectivity of HIV-1 virion but not a sole determinant of its antiviral activity. *J Biol Chem* **278**: 44412–44416.

Simon JH, Gaddis NC, Fouchier RA, Malim MH. 1998. Evidence for a newly discovered cellular anti-HIV-1 phenotype. *Nat Med* **4**: 1397–1400.

Singh G, Lykke-Andersen J. 2003. New insights into the formation of active nonsense-mediated decay complexes. *Trends Biochem Sci* **28**: 464–466.

Singleton MR, Dillingham MS, Wigley DB. 2007. Structure and mechanism of helicases and nucleic acid translocases. *Annu Rev Biochem* **76**: 23–50.

Smith JA, Daniel R. 2006. Following the path of the virus: the exploitation of host DNA repair mechanisms by retroviruses. *ACS Chem Biol* **1**: 217–226.

Sokolskaja E, Sayah DM, Luban J. 2004. Target cell cyclophilin A modulates human immunodeficiency virus type 1 infectivity. *J Virol* **78**: 12800–12808.

Soros VB, Yonemoto W, Greene WC. 2007. Newly synthesized APOBEC3G is incorporated into HIV virions, inhibited by HIV RNA, and subsequently activated by

RNase H. *PLoS Pathog* **3**: e15.

Sowden M, Hamm JK, Smith HC. 1996. Overexpression of APOBEC-1 results in mooring sequence-dependent promiscuous RNA editing. *J Biol Chem* **271**: 3011–3017.

Sowden MP, Ballatori N, Jensen KL de M, Reed LH, Smith HC. 2002. The editosome for cytidine to uridine mRNA editing has a native complexity of 27S: identification of intracellular domains containing active and inactive editing factors. *J Cell Sci* **115**: 1027–1039.

Stalder L, Mühlemann O. 2009. Processing bodies are not required for mammalian nonsense-mediated mRNA decay. *RNA* **15**: 1265–1273.

Stoecklin G, Mayo T, Anderson P. 2006. ARE-mRNA degradation requires the 5“-3” decay pathway. *EMBO Rep* **7**: 72–77.

Stopak K, de Noronha C, Yonemoto W, Greene WC. 2003. HIV-1 Vif blocks the antiviral activity of APOBEC3G by impairing both its translation and intracellular stability. *Mol Cell* **12**: 591–601.

Strack B, Calistri A, Accola MA, Palu G, Göttlinger HG. 2000. A role for ubiquitin ligase recruitment in retrovirus release. *Proc Natl Acad Sci USA* **97**: 13063–13068.

Strebel K, Luban J, Jeang K-T. 2009. Human cellular restriction factors that target HIV-1 replication. *BMC Med* **7**: 48.

Stremlau M, Owens CM, Perron MJ, Kiessling M, Autissier P, Sodroski J. 2004. The cytoplasmic body component TRIM5alpha restricts HIV-1 infection in Old World monkeys. *Nature* **427**: 848–853.

Sun X, Maquat LE. 2000. mRNA surveillance in mammalian cells: the relationship between introns and translation termination. *RNA* **6**: 1–8.

Sun X, Perlick HA, Dietz HC, Maquat LE. 1998. A mutated human homologue to yeast Upf1 protein has a dominant-negative effect on the decay of nonsense-containing mRNAs in mammalian cells. *Proc Natl Acad Sci USA* **95**: 10009–10014.

Suspène R, Rusniok C, Vartanian J-P, Wain-Hobson S. 2006. Twin gradients in APOBEC3 edited HIV-1 DNA reflect the dynamics of lentiviral replication. *Nucleic Acids Res* **34**: 4677–4684.

Swanson CM, Puffer BA, Ahmad KM, Doms RW, Malim MH. 2004. Retroviral mRNA nuclear export elements regulate protein function and virion assembly. *EMBO J* **23**: 2632–2640.

Tange TØ, Nott A, Moore MJ. 2004. The ever-increasing complexities of the exon junction complex. *Curr Opin Cell Biol* **16**: 279–284.

Tejerina F, Bernaldo de Quirós JCL. 2011. Protease inhibitors as preferred initial regimen for antiretroviral-naive HIV patients. *AIDS Rev* **13**: 227–233.

Teng B, Burant CF, Davidson NO. 1993. Molecular cloning of an apolipoprotein B messenger RNA editing protein. *Science* **260**: 1816–1819.

Thali M, Bukovsky A, Kondo E, Rosenwirth B, Walsh CT, Sodroski J, Göttlinger HG. 1994. Functional association of cyclophilin A with HIV-1 virions. *Nature* **372**: 363–365.

Thomas JA, Ott DE, Gorelick RJ. 2007. Efficiency of human immunodeficiency virus type 1 postentry infection processes: evidence against disproportionate numbers of defective virions. *J Virol* **81**: 4367–4370.

Thoren LA, Nørgaard GA, Weischenfeldt J, Waage J, Jakobsen JS, Damgaard I, Bergström FC, Blom AM, Borup R, Bisgaard HC, et al. 2010. UPF2 is a critical regulator of liver development, function and regeneration. *PLoS ONE* **5**: e11650.

Tomari Y, Du T, Haley B, Schwarz DS, Bennett R, Cook HA, Koppetsch BS, Theurkauf WE, Zamore PD. 2004. RISC assembly defects in the Drosophila RNAi mutant armitage. *Cell* **116**: 831–841.

Ugolini S, Moulard M, Mondor I, Barois N, Demandolx D, Hoxie J, Brelot A, Alizon M, Davoust J, Sattentau QJ. 1997. HIV-1 gp120 induces an association between CD4 and the chemokine receptor CXCR4. *J Immunol* **159**: 3000–3008.

Vahlne A. 2009. A historical reflection on the discovery of human retroviruses. *Retrovirology* **6**: 40.

van 't Wout AB, Lehrman GK, Mikheeva SA, O'Keeffe GC, Katze MG, Bumgarner RE, Geiss GK, Mullins JI. 2003. Cellular gene expression upon human immunodeficiency virus type 1 infection of CD4(+)-T-cell lines. *J Virol* **77**: 1392–1402.

van Damme L, Corneli A, Ahmed K, Agot K, Lombaard J, Kapiga S, Malahleha M, Owino F, Manongi R, Onyango J, et al. 2012. Preexposure Prophylaxis for HIV Infection among African Women. *N Engl J Med* **367**: 411-422.

Van Damme N, Goff D, Katsura C, Jorgenson RL, Mitchell R, Johnson MC, Stephens EB, Guatelli J. 2008. The interferon-induced protein BST-2 restricts HIV-1 release and is downregulated from the cell surface by the viral Vpu protein. *Cell Host Microbe* **3**: 245–252.

Varthakavi V, Smith RM, Bour SP, Strebel K, Spearman P. 2003. Viral protein U counteracts a human host cell restriction that inhibits HIV-1 particle production. *Proc Natl Acad Sci USA* **100**: 15154–15159.

VerPlank L, Bouamr F, LaGrassa TJ, Agresta B, Kikonyogo A, Leis J, Carter CA. 2001. Tsg101, a homologue of ubiquitin-conjugating (E2) enzymes, binds the L domain in HIV type 1 Pr55(Gag). *Proc Natl Acad Sci USA* **98**: 7724–7729.

Vogt V. 1997. *Retroviral Virions and Genomes*. eds. J.M. Coffin, S.H. Hughes, and H.E. Varmus. Cold Spring Harbor Laboratory Press, Cold Spring Harbor (NY).

Wainberg Z, Oliveira M, Lerner S, Tao Y, Brenner BG. 1997. Modulation of stress protein (hsp27 and hsp70) expression in CD4+ lymphocytic cells following acute infection with human immunodeficiency virus type-1. *Virology* **233**: 364–373.

Wang X, Han Y, Dang Y, Fu W, Zhou T, Ptak RG, Zheng Y-H. 2010. Moloney leukemia virus 10 (MOV10) protein inhibits retrovirus replication. *J Biol Chem* **285**: 14346–14355.

Wedekind JE, Dance GSC, Sowden MP, Smith HC. 2003. Messenger RNA editing in mammals: new members of the APOBEC family seeking roles in the family business. *Trends Genet* **19**: 207–216.

Weischenfeldt J, Damgaard I, Bryder D, Theilgaard-Mönch K, Thoren LA, Nielsen FC, Jacobsen SEW, Nerlov C, Porse BT. 2008. NMD is essential for hematopoietic stem and progenitor cells and for eliminating by-products of programmed DNA rearrangements. *Genes Dev* **22**: 1381–1396.

Weiss ER, Göttlinger H. 2011. The role of cellular factors in promoting HIV budding. *J Mol Biol* **410**: 525–533.

Welker R, Hohenberg H, Tessmer U, Huckhagel C, Kräusslich HG. 2000. Biochemical and structural analysis of isolated mature cores of human immunodeficiency virus type 1. *J Virol* **74**: 1168–1177.

Weng Y, Czaplinski K, Peltz SW. 1998. ATP is a cofactor of the Upf1 protein that modulates its translation termination and RNA binding activities. *RNA* **4**: 205–214.

Weng Y, Czaplinski K, Peltz SW. 1996. Genetic and biochemical characterization of mutations in the ATPase and helicase regions of the Upf1 protein. *Mol Cell Biol* **16**: 5477–5490.

Wichroski MJ, Robb GB, Rana TM. 2006. Human retroviral host restriction factors APOBEC3G and APOBEC3F localize to mRNA processing bodies. *PLoS Pathog* **2**: e41.

Wollert T, Hurley JH. 2010. Molecular mechanism of multivesicular body biogenesis by ESCRT complexes. *Nature* **464**: 864–869.

Writing Committee for the CASCADE Collaboration. 2011. Timing of HAART initiation and clinical outcomes in human immunodeficiency virus type 1 seroconverters. *Arch Intern Med* **171**: 1560–1569.

Yamashita A, Kashima I, Ohno S. Role of SMG-1-mediated Phosphorylation of Upf1 in NMD - Madame Curie Bioscience Database - NCBI Bookshelf. *Madame Curie Bioscience Database - NCBI Bookshelf*.

Yang X, Gabuzda D. 1998. Mitogen-activated protein kinase phosphorylates and regulates the HIV-1 Vif protein. *J Biol Chem* **273**: 29879–29887.

Yang Y, Yang Y, Smith HC. 1997. Multiple protein domains determine the cell type-specific nuclear distribution of the catalytic subunit required for apolipoprotein B mRNA editing. *Proc Natl Acad Sci USA* **94**: 13075–13080.

Yankulov K, Bentley D. 1998. Transcriptional control: Tat cofactors and transcriptional elongation. *Curr Biol* **8**: R447–9.

Yedavalli VSRK, Neuveut C, Chi Y-H, Kleiman L, Jeang K-T. 2004. Requirement of DDX3 DEAD box RNA helicase for HIV-1 Rev-RRE export function. *Cell* **119**: 381–392.

Yoshikawa K, Okazaki I-M, Eto T, Kinoshita K, Muramatsu M, Nagaoka H, Honjo T. 2002. AID enzyme-induced hypermutation in an actively transcribed gene in fibroblasts. *Science* **296**: 2033–2036.

Yu Q, Chen D, König R, Mariani R, Unutmaz D, Landau NR. 2004a. APOBEC3B and APOBEC3C are potent inhibitors of simian immunodeficiency virus replication. *J Biol Chem* **279**: 53379–53386.

Yu Q, König R, Pillai S, Chiles K, Kearney M, Palmer S, Richman D, Coffin JM, Landau NR. 2004b. Single-strand specificity of APOBEC3G accounts for minus-strand deamination of the HIV genome. *Nat Struct Mol Biol* **11**: 435–442.

Zennou V, Petit C, Guetard D, Nerhbass U, Montagnier L, Charneau P. 2000. HIV-1 genome nuclear import is mediated by a central DNA flap. *Cell* **101**: 173–185.

Zhang H, Yang B, Pomerantz RJ, Zhang C, Arunachalam SC, Gao L. 2003. The cytidine deaminase CEM15 induces hypermutation in newly synthesized HIV-1 DNA. *Nature* **424**: 94–98.

Zhang K-L, Mangeat B, Ortiz M, Zoete V, Trono D, Telenti A, Michielin O. 2007.

Model structure of human APOBEC3G. *PLoS ONE* **2**: e378.

Zhou H, Xu M, Huang Q, Gates AT, Zhang XD, Castle JC, Stec E, Ferrer M, Strulovici B, Hazuda DJ, et al. 2008. Genome-Scale RNAi Screen for Host Factors Required for HIV Replication. *Cell Host Microbe* **4**: 495–504.

Zhu P, Chertova E, Bess J, Lifson JD, Arthur LO, Liu J, Taylor KA, Roux KH. 2003. Electron tomography analysis of envelope glycoprotein trimers on HIV and simian immunodeficiency virus virions. *Proc Natl Acad Sci USA* **100**: 15812–15817.